Summer 2024

Analytical Methods for Monitoring Traumatic Brain Injury Biomarkers/treatment and Pharmaceutical Residual Solvents

Olajide Philip Adetunji
Missouri University of Science and Technology

Department: Chemistry

ANALYTICAL METHODS FOR MONITORING TRAUMATIC BRAIN INJURY BIOMARKERS/TREATMENT AND PHARMACEUTICAL RESIDUAL SOLVENTS

by

OLAJIDE PHILIP ADETUNJI

A DISSERTATION

Presented to the Graduate Faculty of the

MISSOURI UNIVERSITY OF SCIENCE AND TECHNOLOGY

In Partial Fulfillment of the Requirements for the Degree

DOCTOR OF PHILOSOPHY

in

CHEMISTRY

2024

Approved by:

Paul Nam, Advisor
Honglan Shi
V. Prakash Reddy
Philip Whitefield
Yue-Wern Huang

PUBLICATION DISSERTATION OPTION

This dissertation consists of the following three articles, formatted in the style used by the Missouri University of Science and Technology:

Paper I, found on pages 56–95, has been submitted to *Analytical and Bioanalytical Chemistry (ABC) journal*.

Paper II, found on pages 96–130, has been submitted to *CURRENT TOPICS IN BIOCHEMICAL RESEARCH*.

Paper III, found on pages 131–149, has been submitted to the *Journal of Pharmaceutical and Biomedical analysis*.

ABSTRACT

The development of highly sensitive and efficient analytical methods utilizing advanced instrumentation is necessary to help improve disease diagnosis and therapeutics. A major neuro-consequence of traumatic brain injury (TBI) is oxidative stress from the generation of reactive oxygen species and the depletion of antioxidant defenses. Alteration in concentrations of certain small molecules also occurs with the disease progression and can help understand TBI pathophysiology. Two analytical methods employing liquid chromatography with tandem mass spectrometry (LC-MS/MS) were developed and validated to monitor the potential small-molecule TBI biomarkers at sub-ppb levels. Subsequently, the neuroprotective effect of an antioxidant prodrug, *N*-acetylcysteine amide (NACA), was evaluated in rat models that were exposed to the blast-induced TBI from open-field blasts simulating what military personnel are regularly exposed to in combat. The benefit of antioxidant pretreatment was indicated by the significantly lower levels of biomarkers detected in rat urine, plasma, and brain tissue.

Pharmaceutical manufacturers utilize solvents at different stages of production. Some of these harmful solvent residues can be retained in the final products and need to be monitored to meet regulatory requirements. A novel method for the rapid analysis of residual solvents in pharmaceutical products was developed by employing a compact and portable gas chromatography with a photoionization detector (GC-PID). The method detection limits for selected residual solvents in over-the-counter drugs were significantly lower than the compliance concentration limits. The validation of the new method yielded excellent accuracy, precision, and linear response.

ACKNOWLEDGMENTS

"Success is a journey, not a destination". My time at Missouri University of Science and Technology has helped me grow in every aspect of my life, and this was made possible by the support and guidance of many wonderful individuals. I would like to express my gratitude to my advisor, Dr. Paul Nam, for his mentorship, feedback, and willingness to share his knowledge and expertise to help me succeed in my research.

Also, I would like to thank my committee members, Drs. Honglan Shi, Reddy V. Prakash, Philip Whitefield, and Huang Yue-Wern for their support and contribution with their broad range of expertise in different areas of science. I am grateful to Dr. Nuran Ercal for her invaluable advice and suggestions all through these years. My heartfelt gratitude goes to Drs. Jiandong Wu and Annalise Pfaff for the time they spent answering my numerous questions and contributing to some of our works. To my colleagues, friends, and the Departmental staff of Chemistry, I am grateful for your contributions to my success. I would also like to show appreciation to the funding agencies, Leonard Wood Institute (US Army Research Laboratory) and Nanova Environmental.

Lastly, I want to express my love and profound gratitude to my Parents (Soji and Iyabo), siblings (Adeola, Sola, Yemi, and Damola), and every single one of my loved ones (Bolu, Raheemat, and Adashi) whose support has inspired and encouraged me. Particularly, I would like to thank my mother for showing me that love is king, and my father for teaching me grit and to be dauntless and to never give up on my dreams. Above all, all thanks, glory, and honor go to God Almighty for his mercies endureth forever.

"No matter where you go, there you are". – Terry Bone.

TABLE OF CONTENTS

Page

LIST OF ILLUSTRATIONS

SECTION Page

LIST OF TABLES

1. INTRODUCTION

1.1. BACKGROUND

Analytical method development and utilization help understand disease pathology for diagnostics and therapeutic purposes. Additionally, it can be useful in monitoring harmful substances used in manufacturing in a quality control manner, such as the monitoring of residual solvents, a by-product from the manufacturing process of drug products. This research explored the use of analytical methods for pathophysiological understanding of traumatic brain injury (TBI) for diagnostic biomarkers and antioxidant therapy evaluation. It also uses sensitive analytical methods developed on miniaturized instrumentation to monitor residual solvents in pharmaceutical products.

1.2. TRAUMATIC BRAIN INJURY (TBI)

TBI, a significant public health concern affecting an estimated population of 1.7 million people yearly in the United States alone [1], is prevalent among athletes, civilians, and military personnel [1–5]. Reintegration of the latter group into the civilian population is often difficult as a consequence of the burden rendered by TBI. The Global financial consequence of TBI is estimated to be around $US400 billion annually owing to deficiencies in diagnosis, prevention, care, and research [6]. Most TBI cases are often mild in severity, and they are passed off as mere concussions that lead to adverse chronic damage to brain function [2,7].

Direct or indirect mechanical insults to the brain cause TBI—resulting in acute changes such as shearing injuries, contusions, and hematomas [8,9]. In one study, TBI

was categorized based on the physical mechanisms of insults into three categories: (i) closed head, (ii) penetrating, and (iii) explosive blast-induced TBI [10]. These mechanisms usually comprise a rapid coup-counter coup or an acceleration/deceleration injury where the brain undergoes multiple movements in the skull that affect the white matter and damage the blood vessels and axons, leading to diffuse axonal injury [11–13]. The heterogeneity of TBI pathology with diverse manifestations consists of immediate and delayed mechanisms [14]. Most TBI cases involve a prominent physical injury (primary injury) with immediate mechanisms. However, all types of TBI comprise subcellular and biochemical injury (secondary injury) phases with delayed mechanisms that affect the structural and physiological changes to brain function [9,14,15]. Primary injury resulting from impact is considered to be untreatable but preventable, with treatment focused mainly on symptom management. Meanwhile, the secondary phase of the insult allows a time window for intervention. Thus, it has received a lot of attention in a bid to find possible therapeutic targets [14]. This secondary phase of injury may lead to unfavorable consequences such as neuronal necrosis and apoptosis, impaired neurotransmission, damage from reactive species and inflammation, blood-brain barrier impairment, energy deficits, and cognitive dysfunction [16]. Deviation of the central nervous system (CNS) homeostasis is the mainstay after TBI; however, studies have shown that the brain undergoes neurogenesis and plasticity after injury [15]. Many studies argue that neurogenesis after head insult is more likely in pediatric patients than in adults. However, some studies have differing opinions on the effect of age on pediatric response after injury [15]. Alternatively, there is a general agreement that severity and

type of injury play a prominent role in neuroplasticity determination [15] and recovery outcomes.

1.2.1. Challenges and Opportunities in TBI Detection and Treatment. Despite considerable efforts and investments being channeled towards the investigation and treatment of TBI, it remains a challenging process [7,15] due to the complex nature and lack of complete understanding of the pathophysiology of TBI [17]. Candidates for TBI treatment are focused on the known TBI pathology; they are primarily antioxidants, anti-inflammatory, and anti-excitotoxic moieties that can confer neuroprotection after TBI. Additional limitations in finding an effective TBI treatment are the lack of well-designed and controlled clinical investigations, univocal diagnostic criteria, the absence of standardized prognostic biomarkers, assessment methods and guidelines, and safety profiles [18,19]. Also, diagnosis difficulty stems from the variations in the symptoms of the disease presented and can be confounded with comorbidities, age, medical history, substance use and abuse, and concomitant medication [20]. Differences in age-based brain physiology make achieving a uniform diagnosis and treatment nearly impossible. Older patients often have worse outcomes, while pediatric patients have a better chance of recovering to a pre-TBI level of health with time [21]. Blast-related mild TBI (m-TBI) is the most common in military personnel [4,6,22], and existing experimental designs for evaluating this type of injury do not reflect real-life situations. The reported percentage of m-TBI cases may not reflect the actual numbers because of a lack of credible diagnostic and prognostic measures [6]. Prognostic methods for more severe TBI types are more established than m-TBI. Although new prognostic measures are beginning to emerge for m-TBI, validation of this method has not been fully implemented [6].

Combination of neuroimaging techniques like computerized tomography (CT), magnetic resonance imaging (MRI), and positron emission tomography (PET) with Glasgow Coma Scale (GCS), tests for loss of consciousness (LOC), and post-traumatic amnesia (PTA) [4] are routinely used to detect and monitor TBI progression and severity. GCS –a measure of eye-opening (E), verbal response (V), and motor response (M)- of 13 to 15 are classified as mild TBI, nine to 12 as moderate TBI, while a GCS less than eight is classified as severe TBI [4,23]. Although utilization of these techniques has proven handy in evaluating more severe forms of TBI, they are largely insensitive to detecting milder forms of TBI, which happens to be the most prevalent of all TBIs [12]. Most of these techniques, in addition to their lack of sensitivity to m-TBI, are invasive techniques that cause pain and stress to the patient during the diagnostic process. Additionally, some pose radiological exposure risks, prolonged hospital stays, inefficient use of resources, and high costs of operation. Alternative methods for monitoring TBI inception and progression using minimally invasive techniques involving peripheral fluids like urine and blood will improve current practices [15,19]. Additionally, m-TBI cases are prevalent in males, teenagers, and young adults, and most cases do not get treated due to lack of diagnosis [24]. Fluid biomarkers were predicted to emerge as new prognostic indicators for developing more accurate prediction models, risk improvement, clinical decision-making, and pharmacotherapeutic regimens [19]. Noteworthily, people in rural areas and low-income earners may not have access to these expensive and arduous diagnostics techniques, which is why a cheap, easy, and accessible method of diagnosis needs to be developed [21]. Blast-induced TBI is suffered by United States service members in conflict regions, and some successes were recorded in the introduction of military

medical treatments for blast TBI in the war theatre that includes decompressive craniectomy, cerebral angiography, transcranial Doppler, and hypertonic resuscitation fluids, to list a few [25]. Progression in the administration of rehabilitation, stateside neurosurgery, and neurocritical care have also been recorded [25].

The general treatment regimen for acute TBI symptoms includes intracranial pressure minimization and optimization of cerebral perfusion to limit secondary impairment while addressing chronic remedies focused on motor, cognitive, and behavioral outcome improvement. However, newer therapies targeting the prevention of the secondary sequelae for neuroprotection enhancement are necessary due to the repression of existing repair mechanisms and therapies by the severity of the injury, age of the patient, recurring injury, and time-lapse in medical management [15]. Consequently, pharmacotherapeutics such as stem cells, antioxidant therapy, and pharmacological interventions enhance repair and regenerative processes after injury [15]. Most of these available treatments only target a few factors involved with secondary injury, making them less in scope in the overall protection after injury [8]. Expeditious diagnosis and treatment administration are vital in improving patients' treatment outcomes due to the different temporal biochemical changes attached to the pathophysiology of TBI [20]. In summary, treatment timing should be carefully targeted for the best efficacy. The “Prevention is better than cure”’ narrative fits nicely into the treatment of TBI, as it is better for pretreatment with neuroprotective agents that will counteract the secondary sequelae of the disease rather than finding a cure to reverse the effect, which may not be possible as the disease progresses. Hospitals and caregivers often view TBI as a one-time event and, as such, treat it in the same manner rather than as

the continuous event that it is [26]. In the words of Geoffrey Manley, a revered expert in TBI, “Look at the epidemiology of TBI and do the math,” he insists, “The field is underfunded. We should be taking care of this problem with the resources it deserves.” [26]. Another opportunity that could be taken advantage of is the oxidative stress characteristic of the secondary mechanisms that may be improved with antioxidant therapy [18].

Due to the multifactorial involvements in the secondary aspects of injury, finding a target for therapy has proven difficult. However, taking advantage of factors such as BBB permeability increase after injury could improve the bioavailability of specific therapies, thereby improving treatment outcomes. Studies have shown that a combination of pre-and post-exposure administration of treatment is the best course of therapy against TBI [27–29], allowing for possible prevention and repair mechanisms to kick off effectively against TBI.

1.2.2. Mechanical and Biochemical Mechanisms of Traumatic Brain Injury.

The mechanism of mild blast-induced TBI begins with acceleration/deceleration movements of the brain in the skull from blast pressures and overpressure [22]. Participation in activities such as contact sports and military combat or training increases one’s susceptibility to TBI with intricate mechanisms that are yet to be fully understood [22,30]. Physical manifestation is to primary injury, as metabolic changes are to secondary injury. Although different, the mechanisms of both injury phases contribute to the overall consequences of TBI. The severity of injury (mild, moderate, and severe) plays a massive role in the acuteness and physical manifestations of TBI. The more severe type is more acute with observable physical injuries and vice versa. Consequently, physical injury

(acute and repetitive) from contact and blast overpressures initially leads to DAI, which is defined by acceleration/deceleration motion that results in shearing, tearing, or twisting forces to the white matter tracts of the brain. This finally results in dynamic brain parenchyma deformation [31]. Although most DAI affects the white matter, axons at the junction between the white matter and the gray matter experience gross and microscopic damage [23]. The protective covering of the axons (myelin sheath) is adversely affected by these forces, causing integrity changes as the DAI evolves with time. Additionally, progressive demyelination in affected areas and white atrophy can occur up to one-year post-injury [32,33]. Further exacerbation of DAI is fostered by the progression of a molecular and cellular cascade of metabolic changes within the axon after injury-mediated initial stress [31,34]. DAI's clinical presentation in patients correlates with the severity of TBI. With the true incidence of DAI largely unknown, it is estimated that roughly 25% of DAI cases will result in death [23]. Mild TBI patients present with signs and symptoms that reflect concussion, while severe TBI patients may present with loss of consciousness, state of persistent vegetativness, and post-concussive symptoms. Also, the definition of the pathophysiology of m-TBI in terms of anatomical or functional descriptions and mechanism(s) of injury is difficult to ascertain[17,30]. Additionally, only a small fraction of severe TBI patients will regain consciousness in the first-year post injury [23]. Post-mortem pathological examination of brain tissue can yield a definitive DAI diagnosis. However, in clinical settings, DAI diagnosis is done by implementing clinical and radiographic observations which may lack accuracy [23]. Pulmonary and auditory physiological changes resulting from the primary blast are well established, but the effect of the explosion on the CNS is not well known. When military personnel or civilians are

exposed to explosion [25], the energy released outside the body is transformed into bokinetic energy that damages cranial and brain structure due to the overpressure from the blast. Although the damage sustained is mechanistically similar to blunt TBI causes, blast injury contributes an additional level of complexity and uniqueness yet to be fully grasped [30]. Blast-related injury taxonomy is described in Table 1.1.

Table 1.1. Blast-related injury taxonomy of the Department of Defense. As described by Bryden et al., [30].

Blast-related injury taxonomy	
Injury	Properties
Primary	Blast overpressure wave impacting the body—examples: blast lung, tympanic membrane rupture, and non-blunt TBI.
Secondary	Damage from projectiles contacting the body. Examples: penetrating ballistic or blunt injuries.
Tertiary	Physical displacement of the body and striking solid surfaces. Examples: traumatic amputation, closed or open head injury, and crush injuries.
Quaternary	Other “explosive products” effects. Examples: burns and inhaled toxic fire gases.
Quinary	Clinical consequences of post-detonation contaminants. Examples: radiation poisoning and tissues reactions to fuels or metals.

Military-related head trauma can be attributed to three events - ballistic, blunt, and blast overpressures- or a combination of these mechanisms. In ballistic head trauma, projectiles like shrapnels and bullets that can vary in mass, geometry, velocity, and impact regions cause head trauma through lacerations, stretching, and shearing of

adjacent regions from accompanying shockwaves, usually accompanied by hemorrhages. The shockwaves generated cause additional diffuse neural damage, brain tissue herniation, and widespread edema [30,35]. Fortunately, military helmets are designed to withstand blunt impact and foreign body penetration [22,30,35]. In blast wave injury, the injury mechanisms and structural and tissue damage are not immediately apparent [22]. Explosive devices generate combined pressure waves with electromagnetic, acoustic, light, and thermal energies [22,25]. The chemical reaction from the explosion releases an initial positive pressure wave that is subsequently followed by a longer negative pressure wave in a pattern referred to as the the Friedlander curve[22,30,36–38] which varies by distance from the explosive and can be a measure of safe stand-off distance [30,39]. Explosive blast waves can result in reflected pressures that can be two to eight times the incident pressure from reflecting off surrounding objects and edifices[22,30,40]. Although, more often than not, the force from the initial impact is not sufficient to cause skull fractures, but it can lead to diffuse brain insult [31]. Thus, from a single explosion event, an exposed victim can suffer repeated hits from several directions and multiple blast waves [22,30]. Causing head and facial structures to be adversely affected by the blast wave transmission [22,41]. Additional transmission of pressure waves to the brain may also arise from a vascular surge emanating from the thoracic and abdominal cavities[22,42,43]. In summary, blast injuries are due to reflective blast wave forces that impact the body's surface and internal environment and causes unfavorable anatomical and physiological changes [22]. Figure 1.1. pictorially describes blast effects on victims of TBI.

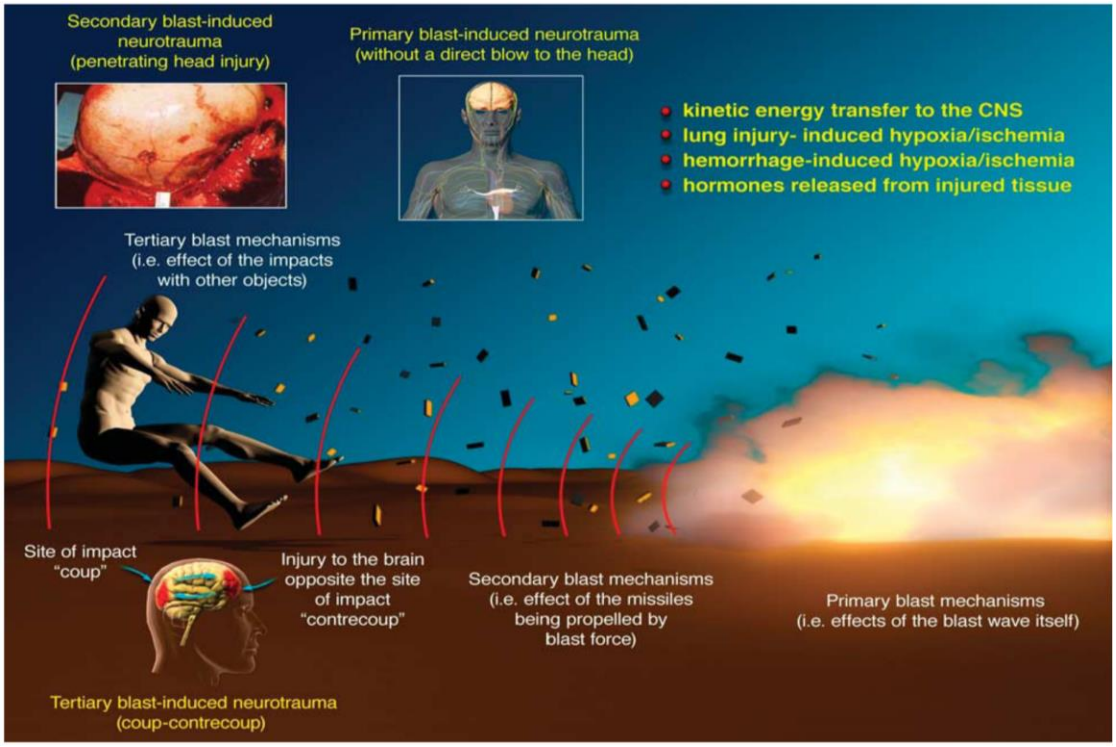

Figure 1.1. Impact and effects of explosion blast on TBI victims [42].

Finally, head trauma from blunt forces common in civilian and military populations alike is sustained from blunt object impact through combat, vehicle crashes, or ballistic generated inward indentation of helmet (backface deformation). This impact results in focal damage to the brain tissue and neurovasculature at the site of impact, causing coup lesions/ contusions and epidural hematomas. This force, if sufficient, can cause linear translation of the brain to contact the skull distal to the impact site, completing the countercoup lesions. Cranial rotation from blunt trauma causes angular rotation that can induce strain and shearing of tissues throughout the brain, causing DAI [30]. Also, blunt trauma may be initiated without external contact with the skull via inertial acceleration from minor vehicular accidents [30]. Overall, regardless of the

difference and how the mechanism of the TBI is initiated, there is an overlap between all the types of mechanisms as they can result in accelerative translational and/or rotational forces that result in focal coup lesions, distal countercoup lesions, and diffuse injury to microstructures in the brain [30] that eventually triggers the eventual biochemical events.

Secondary mechanisms of injury following the DAI from TBI are posited to involve a series of biochemical, cellular, and molecular events that collectively resolve into widespread neurodegeneration [42]. Incidentally, disruption in axonal transport mechanisms results in swelling, secondary axonal degeneration, and Wallerian degeneration [31]. Eventual oxidative stress (Figure 1.2.) arising from an imbalance between reactive species and oxidative stress plays a central role in the genesis of DAI clinical phenotypes linked to the effects of a lot of post-traumatic and cellular changes like the release of proinflammatory cytokines and modifications in calcium metabolism [31]. Ischemia resulting from reduced cerebral blood flow and hematomas caused by damaged CNS vasculature following injury can lead to hypoxia [31,44–47]. With ischemia setting in, the brain, traditionally with a high oxygen demand [48], now has a limited supply, leading to dysfunction of oxygen-dependent cellular processes. Calcium homeostasis dysregulation and glutamate proliferation caused by injury have been strongly correlated with the secondary injury mechanism [31,49]. Both increased calcium ions activate calpains and caspases that play a considerable role in necrosis and apoptosis, and glutamate proliferation results in widespread excitotoxicity [31,50]. Cysteine proteases (calpains and caspases) produce several proteolysis products with potential to be considered as DAI biomarkers [31].

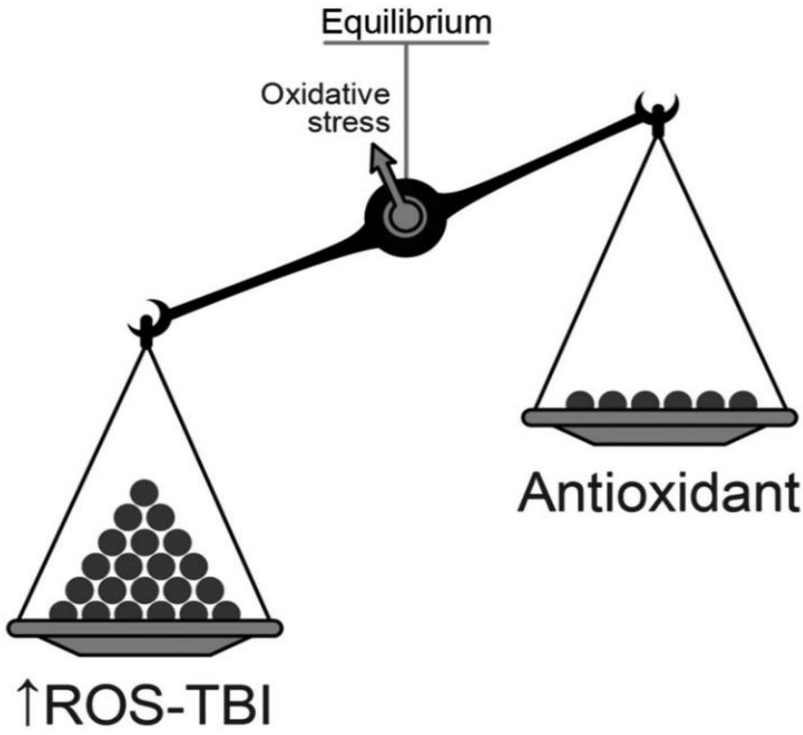

Figure 1.2. Imbalance between reactive oxygen species (ROS) and antioxidants that causes TBI-induced oxidative stress [45].

Neuroinflammatory responses from microglial cells are triggered in the CNS as a reaction to DAI, particularly the accumulation of β-App, phagocytic clean-up, and CNS barrier fortification [31,44]. Cell death from neurodegeneration is regulated by the mitochondria [51] which makes it of utmost importance in TBI pathogenesis [45]. Subsequently, oxidative stress arises from the imbalance between reactive species and antioxidant defenses [45], a consequence of the rampant production of reactive species generated from DAI and mitochondrial dysfunction. Collectively, these brain cellular alterations impair neurologic functions [45]. Differentiating mechanical injury-induced axonal pathology from hypoxia or mass effect due to hematomas or cerebral edema is difficult in severe TBI cases [52], showing how these symptoms and pathologies can

overlap and interact with each other. Figure 1.3. shows the relationship between TBI-induced oxidative damage and neurodegeneration.

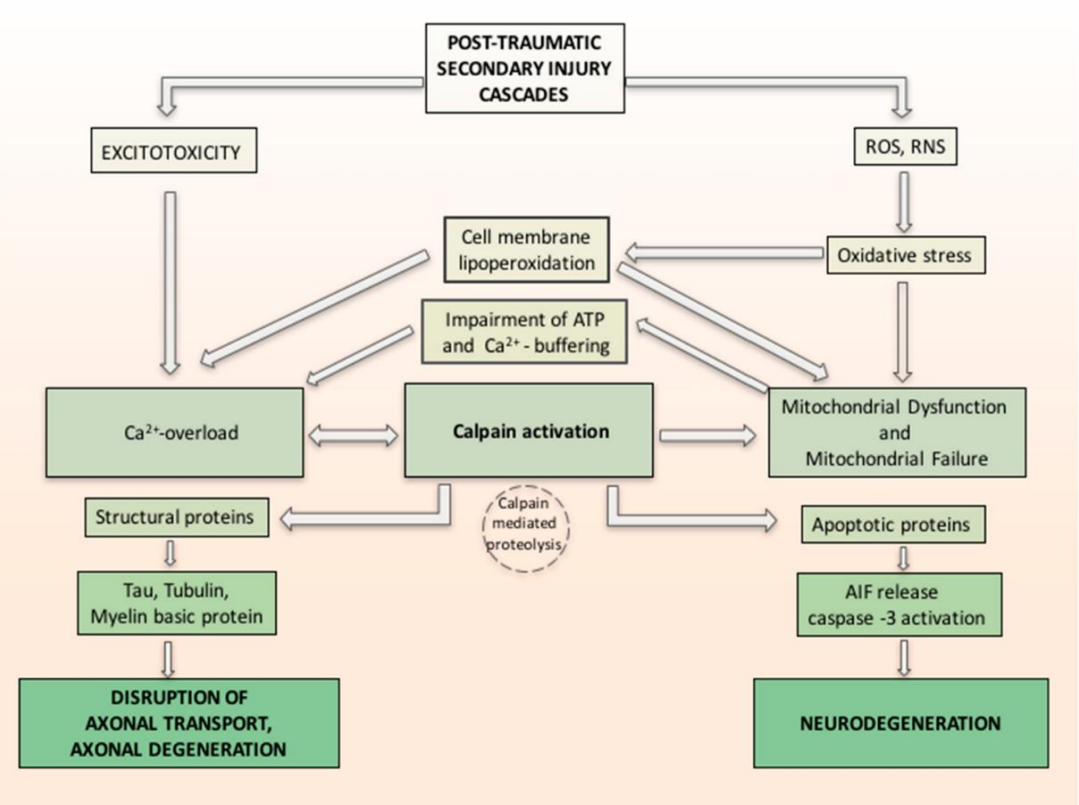

Figure 1.3. Hypothetical inter-relationship between TBI-induced oxidative damage and neurodegeneration. Secondary injury cascade in TBI induces oxidative stress related to increase of free radicals reactive oxygen species/reactive nitrogen species (ROS/RNS) and increase calcium entry both from intracellular stores and injury-induced increases in glutamate (excitotoxicity). Oxidative stress induces cell membrane lipoperoxidation and calcium release, which activates calpain. ROS and RNS induced oxidative damage in neuronal mitochondria and compromise Ca^{2+} homeostasis. Activated calpain mediates further Ca^{2+} entry, forming a positive feedback loop and induces mitochondrial membrane permeability and releases the apoptosis inducing factor (AIF) from mitochondria. Calpain-1 also activates caspase-3. The released AIF and activated caspase-3 together induce neurodegeneration. Activated calpain proteolyzes large groups of cellular proteins varying from structural proteins and soluble proteins (e.g., apoptotic proteins). Changing either or both the structure or activity of the protein substrates can have important effects such as axonal deterioration and neuronal death [31].

1.2.3. Oxidative Stress in Traumatic Brain Injury. Oxygen, comprising approximately 21% of atmospheric oxygen, is critical for the continuous survival of aerobic multicellular organisms [53]. Reactive species such as reactive oxygen species (ROS) and reactive nitrogen species (RNS) are chemically reactive radical and non-radical derivatives of oxygen and nitrogen [53–56]. Their high reactivity is a result of the presence of nonstatic bonds and unpaired valence shell electrons [53]. The unpaired electron in free radicals makes them highly reactive and capable of kicking off chain reactions intracellularly and extracellularly [53]. These reactive species include superoxide, hydrogen peroxide, hypochlorous acid, hydroxyl radical, singlet oxygen, nitric oxide, nitrogen dioxide, and peroxynitrite [53,54]. Figure 1.4. and Figure 1.5. show the reaction mechanism of reactive species and oxidative stress consequences, respectively.

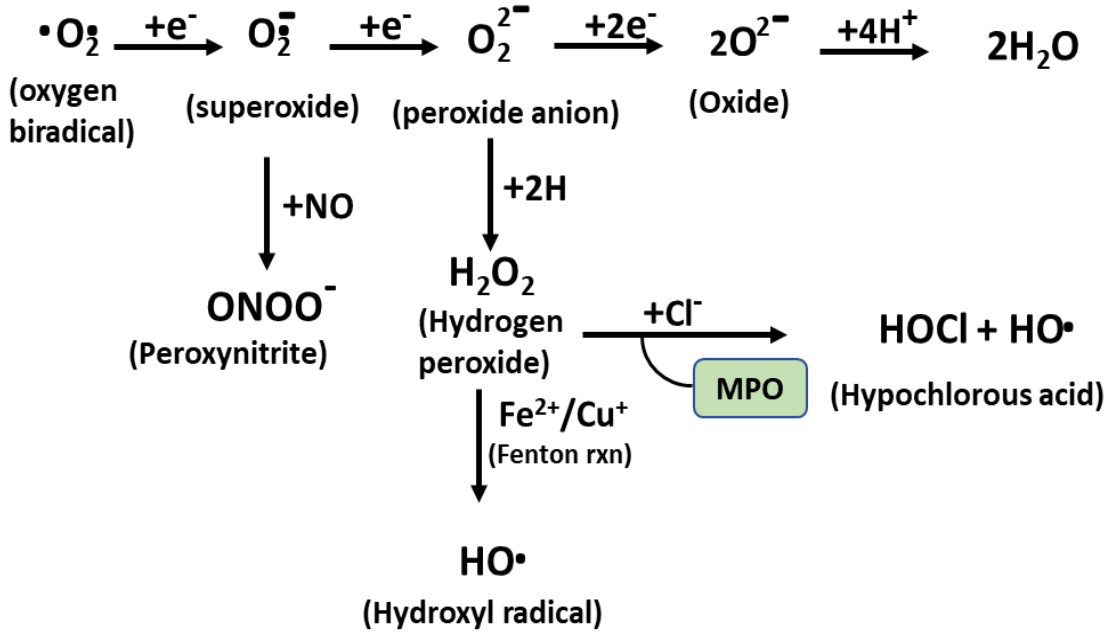

Figure 1.4. Interconversion of some reactive species.

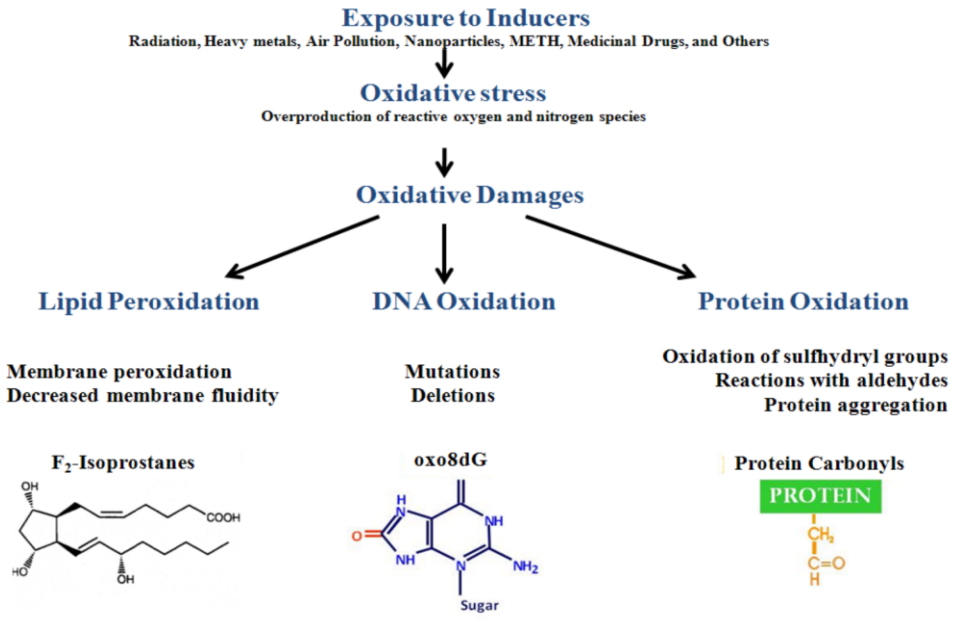

Figure 1.5. Consequences of oxidative stress [57].

These species are essential in cellular metabolism, and they are utilized for signaling cascade, immune response, combating bacterial infections, vasodilation, and overall homeostasis [53,54,58], as well as in redox homeostasis, cardiovascular, and immune system maintenance. However, if their production is not regulated accordingly and/or there are insufficient antioxidant defense actions [54], the results can be devastating for cellular homeostasis, causing oxidative, chlorinative, and nitrosative stress. In contrast, low levels of these reactive species lead to cancer and cardiomyopathy, causing reductive stress [54,59]. The endoplasmic reticulum and mitochondria are two organelles closely linked to these species' production and metabolism [60]. In normal conditions, they are generated by various cellular enzymatic pathways primarily involved in mitochondrial respiration. Other generators of ROS are cytochrome P450, **α**-ketoglutarate dehydrogenase, xanthine oxidoreductase, myeloperoxidase (MPO), and

nicotinamide adenine dinucleotide phosphate oxidase (NADPH oxidase) in the mitochondria [53,54,61–63].

Meanwhile, in disease conditions, their generation may be enhanced by ischemia-reperfusion, hypoxia, hyperoxia, inflammation, enzymes associated with metabolic dysfunction, and mitochondrial dysfunction [54,64–67]. Additionally, environmental factors, xenobiotics, and pathogens may increase the generation of these reactive species [60,68]. Also, this excessive generation of ROS may induce damage to cellular organelles and processes, leading to physiological dysfunction [69]. Hydroxyl radicals, singlet oxygen, and peroxynitrite are the most reactive, making them the most dangerous among known RNSs and ROSs [54]. Their proliferation serves as a marker for disease states as they are heavily involved in diseases such as aging, cancer, atherosclerosis, diabetes mellitus, cardiovascular diseases, neurodegenerative conditions, and TBI [45,54,60,61]. Alternatively, non-enzymatic and enzymatic antioxidant defenses are put up against these reactive species to maintain cellular homeostasis [69,70]. An imbalance in antioxidant and reactive species levels leads to oxidative, nitrosative, and halogenative stress [53,56,64], and these factors have been identified to play critical roles in the pathophysiology and biology of many diseases that are of great concern today [56,64]. Redox health homeostasis in oxidative stress conditions shifts towards the negative, and the high concentrations of reactive species generated readily react with lipids, proteins, nucleic acids, and carbohydrates [53] without much interference from the antioxidant defense system. TBI-induced oxidative stress mechanism is complex [71] compared to many other conditions, and it involves an initial generation of reactive species from hypoxia and ischemia due to the head insult [67] and a subsequent generation of these

reactive species by the TBI-dysfunctionalized mitochondria [71]. Mitochondrial oxidative stress has been implicated in both traumatic and non-traumatic brain injury [48]. Optimal functioning mitochondria and consistent oxygen supply from the blood are necessary to maintain brain homeostasis [48,72], and dysfunctional mitochondria further increase reactive species formation. TBI dysfunctionalizes the mitochondria and shortens the supply of oxygen to CNS cellular functions. As mentioned in the previous section, excessive accumulation of calcium ions in the cytosol activates apoptotic and necrotic proteins, and excessive stimulation of excitatory neurotransmitters both contribute to post-traumatic oxidative stress and excitotoxic cell death [10,72]. Further impairment of the mitochondria from these excesses disrupts the mitochondrial electron transport chain and membrane potential, causing additional proliferation of mitochondria-generated free radicals and cell apoptosis [71,72].

Lipid peroxidation (LPO) occurs when unsaturated fatty acid components of lipids interact with reactive species [73]. Brain and mitochondrial membranes with relatively high lipid content are especially susceptible to LPO [53,74,75] after TBI due to elevated reactive species levels that eventually leads to diruptions in cellular and membrane integrity [76]. This interaction causes the formation of aldehyde-based lipid peroxidation byproducts like malondialdehyde, hexanal, gloxal, acrolein, crotonaldehyde, 2-nonenal, 4-oxo-2-nonenal, and 4-hydroxynonenal (4-HNE) [73]. In TBI, disruption of the membrane phospholipid structure in the brain from oxidative stress leads to lipid peroxidation and generation of cytotoxic lipid peroxidation by-products that bind to cellular proteins and interrupt their normal function [31,50].

1.2.4. Antioxidant Therapy. Due to the complex pathophysiology of TBI, potential therapeutics target different pathophysiologies, including oxidative stress [10]. Enzymatic and non-enzymatic antioxidant defenses are set up in aerobic organisms to counteract the harmful effects of reactive species [70] and maintain cellular homeostasis. Enzymatic antioxidants include all three isoforms of superoxide dismutase (SOD), catalase, glutathione peroxidase (Gpx), glutathione transferase (GST), thioredoxin, and peroxiredoxin [70]. On the other hand, non-enzymatic antioxidants include but are not limited to vitamin C (ascorbic acid), vitamin E (**α**-tocopherol), glutathione, carotenoids (β-carotene), and serotonin [70,77]. Figure 1.6. shows enzymatic scavengers and corresponding catalyzed reactions.

Name of Scavenger	Acronym	Catalyzed Reaction
Superoxide dismutase	SOD	$M^{(n+1)+}\text{-SOD} + O_2^- \rightarrow M^{n+}\text{-SOD} + O_2$ $M^{n+}\text{-SOD} + O_2^- + 2H^+ \rightarrow M^{(n+1)+}\text{-SOD} + H_2O_2$
Catalase	CAT	$2\,H_2O_2 \rightarrow O_2 + 2\,H_2O$ $H_2O_2 + \text{Fe(III)-E} \rightarrow H_2O + O = \text{Fe(IV)-E(.+)}$ $H_2O_2 + O = \text{Fe(IV)-E(.+)} \rightarrow H_2O + \text{Fe(III)-E} + O_2$
Glutathione peroxidase	GTPx	$2GSH + H_2O_2 \rightarrow GSSG + 2H_2O$ $2GSH + ROOH \rightarrow GSSG + ROH + H_2O$
Thioredoxin	TRX	Adenosine monophosphate + sulfite + thioredoxin disulfide = 5'-adenylyl sulfate + thioredoxin Adenosine 3′,5′-bisphosphate + sulfite + thioredoxin disulfide = 3′-phosphoadenylyl sulfate + thioredoxin
Peroxiredoxin	PRX	$2\,R'\text{-SH} + ROOH = R'\text{-S-S-}R' + H_2O + ROH$
Glutathione transferase	GST	RX + GSH = HX + R-S-GSH

Figure 1.6. Enzymatic scavengers of reactive species for antioxidant defense and their catalyzed reactions [70].

Treatment of the acute phase of TBI has seen significant improvements in recent years, and it is mostly focused on symptom management. However, treatment of the chronic phase of TBI from the secondary manifestations is not well established due to a lack of in-depth understanding of the pathophysiology of secondary injury and its progression [14,17]. The substantial role of ROS and oxidative stress in TBI pathophysiology warrants the exploration of antioxidant therapy in combating TBI, especially the milder form that exhibits mostly subcellular and biochemical metabolic changes [44], which may be the key to finding an effective TBI therapy. In pathological conditions where the antioxidant defense systems have been overwhelmed [70], antioxidant therapy can be employed to restore redox homeostasis and improve outcomes. This therapy involves using exogenous substances that may be prodrugs or reactive species scavengers to bolster the already depleting defense system. Mechanism of action of antioxidant therapy can be based on reactive species scavenging, inhibition of reactive species formation, promotion of de novo synthesis of GSH, and lipid peroxidantion initiation and propagation inhibition [76,78]. Trialed and promising antioxidant therapy candidates for TBI include polyethylene glycol-conjugated-SOD (PEG-SOD), tirilazad, U-83836E, melatonin, tempol, curcumin, lipoic acid, OPC-14117, PBN, NXY-059, penicillamine, phenelzine, resveratrol, *N*-acetyl cysteine, *N*-acetylcysteine amide, and small molecule Nrf2/ARE signaling activators [18,28,50,76].

For antioxidant therapy to be effective, it must be neuroprotective. However, one study stated the inexistence of neuroprotective agents that can effectively prevent or reverse the damage from the secondary sequelae of TBI [14]. Other studies have showed that antioxidant therapy with exogenous antioxidants confers neuroprotection that can

prevent and mitigate the damage from the secondary mechanisms, particularly if administered with the neuroprotective time window [28,31]. The neuroprotective time window is defined as the time range between injury and treatment during which the therapy still possesses efficacy [79]. Figure 1.7. shows the proposed role of antioxidant therapy in reducing TBI excitotoxicity.

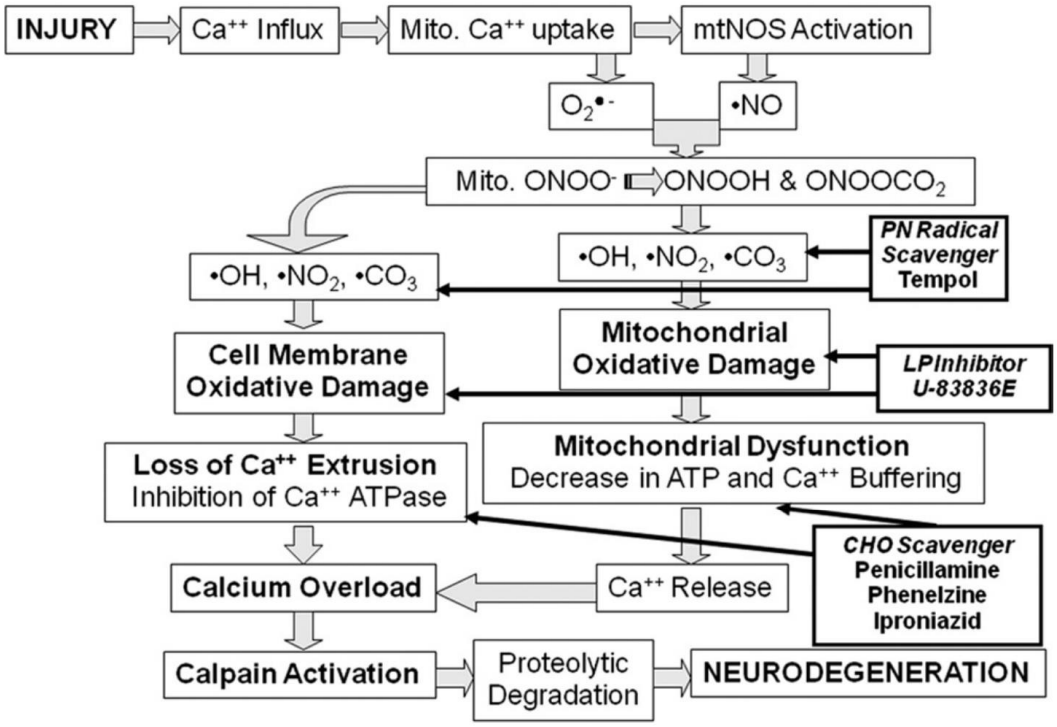

Figure 1.7. Proposed role of antioxidant-based treatment in ameliorating excitotoxicity cascade in TBI [50].

1.2.5. Relationship Between TBI and Other Neurological Disorders. TBI, although classified as a neurological disorder, is a risk factor for the inception, acceleration, and progression of other neurological disorders and diseases in later life [80,81]. Additionally, multiple TBI pathomechanisms, including oxidative stress and

neuroinflammation, have been found to be common between secondary injury TBI and several neurodegenerative conditions [82]. Patients with underlying conditions report worsened symptoms and higher odds of neurological disorders after TBI [83]. As a result, TBI is considered a chronic disease with long-lasting health consequences [84]. Therefore, treatment and management of TBI by health care providers should also be long-term to avoid manifestation of incidences years post-injury [80]. Some of these neurological and non-neurological disorders include psychiatric diseases, seizures, sleep disorders, neuroendocrine diseases, neurodegenerative diseases, sexual dysfunction, systemic metabolic dysregulation, and bladder and bowel incontinence with a chronic nature [80]. Neurodegenerative diseases closely associated with TBI and with overlapping symptoms of TBI include Alzheimer's dementia, depression, bipolar disorder, mild cognitive impairments, neuropsychiatric sequelae, epilepsy, stroke, mixed affective disorders Parkinson's disease, multiple sclerosis, and Lewy body dementia [80,81,83–87]. In some cases, mostly in military personnel, TBI is often misdiagnosed as post-traumatic stress disorder and vice versa due to their similarities. To worsen the situation, both conditions could co-occur as well, causing apparent misdiagnosis or underdiagnosis [25]. Even when the TBI-associated symptoms are addressed, patients who are claimed to have recovered end up with lifelong disability and deterioration that affect the quality of life or even death in some instances [80,84]. Mainly, mild TBI as an evasive form of TBI to diagnose is a silent risk factor and can go unnoticed until it has developed into other neurological diseases; age of victims often increases the risk of succumbing to the chronic effects of TBI [25,84]. Most patients of mild TBI recover and are restored to pre-TBI functional levels. However, a sizeable minority end up with complicated, incomplete, or prolonged

recoveries with unfavorable outcomes worse than what could have been predicted [88]. Post-mortem evaluation of the long-term neuropathology after injury has pinpointed evolving and persisting abnormalities best expressed as polypathology that include chronic traumatic encephalopathy [84]. Both single and repetitive TBI contribute to this late-stage development of neurological consequences, with single TBI having less risk factor than repetitive TBI [84]. Although the clinical correlation of TBI with neurodegeneration has been established, the causative factors connecting these processes have not yet been fully elucidated [82]. Consequently, due to the susceptibility of TBI to devolve into neurodegenerative conditions long term, prophylactic treatments against post-TBI neurodegeneration should be highly encouraged and developed [82]. It is necessary to gain an in-depth understanding of the pathophysiological mechanisms intimately involved in TBI, in particular, oxidative stress that appeared to be crucial in mediating neuroinflammation and excitotoxicity at a molecular level [82]. This would help discover suitable therapeutic targets -particularly targeting reactive species- and reduce post-injury neurodegeneration risks, in turn improving the life quality of victims of TBI, be it civilian or military [82].

1.2.6. Blood-Brain Barrier Pathophysiology after TBI. The blood-brain barrier (BBB), an integral part of the neurovascular unit (NVU), is a restrictive barrier between the CNS and the rest of the body, restricting the free flow of unwanted blood-borne factors [8]. Cerebral homeostasis maintenance by the BBB is performed through molecular reuptake and cerebral blood flow regulation [8]. The NVU is a physiologic entity comprising different interactions between components: endothelial cells, neurons, pericytes, smooth muscles, microglia, astrocytes, and the basement membrane [89,90].

This complex and intimate interaction between the components of the NVU led to their classification as a single functioning unit responsible for developing and upholding a highly selective BBB, cerebral homeostasis, and circulatory function [89]. Controlled movement of biological material through the BBB is facilitated by the inter-endothelial tight and adheren junction protein complexes and by selectively allowing paracellular diffusion [8]. Consequently, the compromisation of BBB integrity after head injury causes these tight junction proteins -claudins and occludins- to weaken and underexpress [8].

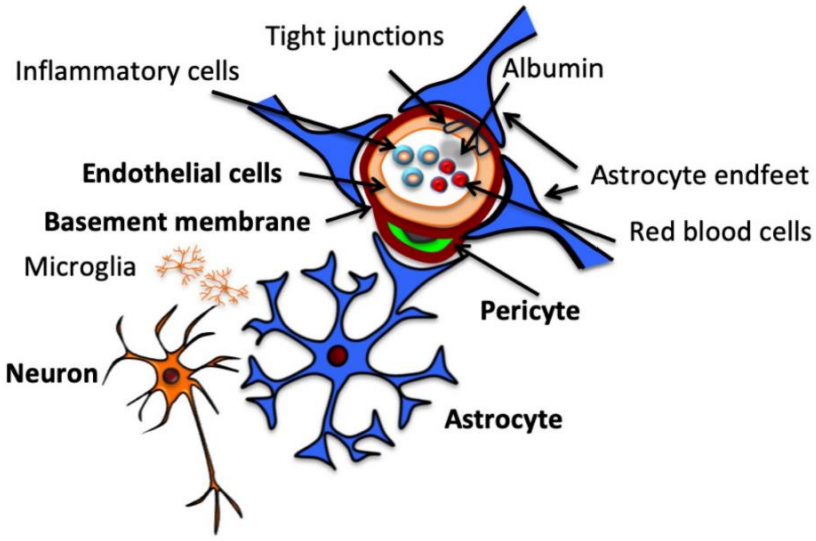

Figure 1.8. Schematic representation of the neurovascular unit (NVU) structure [89].

Pathological insults from TBI impact contributing components to the NVU, especially the BBB. When this disturbance occurs, cerebral homeostasis has a negative shift due to the constituent cells' response to adverse stimuli [89]. Specifically, neurovascular coupling changes may disrupt blood flow and metabolic regulation, and excitotoxicity may be induced by neurotransmitter release-reuptake disruption in neurons

and astrocytes. Gliovascular signaling alterations may underlie BBB disruption and traumatic edema. Finally, a culmination of all these biochemical activities may increase apoptosis and necrosis susceptibility [91]. In summary, these cell-cell interactions play critical roles in CNS disorders [91] and in-depth understanding of these interactions is of utmost importance in designing a treatment regimen. Having established the importance of BBB in the pathophysiology of TBI, it is necessary to elaborate on its specific function, how it is affected by TBI, and how taking advantage of BBB disruption may pave the way to finding effective diagnostics and therapy for TBI [14].

The severity of TBI determines the extent and speed of BBB disruption. Severe forms of TBI show acute BBB changes within minutes of injury, while milder forms show chronic changes to the BBB that can last for days and months [92]. BBB breakdown initiates transcriptional neurovasvular network changes, eventually resulting in delayed neuronal dysfunction and degeneration [14]. Due to the high incidence of BBB breakdown in TBI patients, as confirmed with brain imaging data, the pathology could be utilized as a biomarker clinically and in drug trials [14]. In a normal functioning brain, interaction between the glial cells and endothelial cells in the NVU occurs via paracrine signaling. Following injury, this communication is affected adversely by the glial cells' overproduction and release of signaling and non-signaling molecules [8]. This overproduction and release leads to BBB degradation and eventual weakening of the tight junction proteins [8].

1.2.7. Biomarkers in TBI. Current diagnosis of TBI is heavily focused on surface symptom observations of the mechanical injury of TBI, of which milder TBI forms display neural and structural changes [19]. Neuroimaging techniques can also provide

clinical evidence of TBI, especially those of increased severity [19,93–95]. However, this method cannot easily evaluate secondary biochemical and metabolic changes [12]. For effective evaluation and in-depth understanding of the complex secondary mechanisms of TBI pathophysiology, alteration in biomarkers of the metabolic changes should be easy to measure in accessible fluids and could be carefully evaluated to accurately determine the inception and extent of disease [19,96]. These small molecules represent the complex result of biological processes that occurs in cell, tissue, or organ; thus, they are viewed as attractive candidates for understanding disease phenotypes [97].The diagnostic accuracy of a biomarker or biomarker signature is denoted and quantitatively evaluated by its sensitivity and specificity [98]. Identifying accurate TBI biomarkers may be painstaking because it requires technical expertise and knowledge of the pathomechanisms of TBI and the use of complex instrumentation that may be time-consuming. Certain small molecule and protein biomarkers have been identified to be involved in pathophysiologies of TBI, including oxidative stress, excitotoxicity, mitochondrial dysfunction, neuroinflammation, and lipid peroxidation [93,98]. Additionally, the metabolites constitute a variety of low-molecular-weight structures, including amino acids, lipids, nucleic acids, peptides, and organic acids, which complicates comprehensive analysis using analytical techniques [97]. Biomarkers have been used as objective physiological indicators of the genesis and progression of different disease or injury states [98]. Similarly, TBI biomarkers can give details of pathogenesis, pathoprogression, and in turn, the overall pathophysiology of TBI to provide better insights into understanding this complex process [7,34,99,100]. A combination of advanced neuroimaging techniques with molecular biomarkers could be the key to efficiently diagnosing TBI of even the mildest form, which was found to still

cause disease symptoms in the absence of positive neuroimaging findings [98]. As a standalone, monitoring biomarkers of different pathophysiologies of TBI can be combined to form biomarker signatures for understanding the interactions between these pathophysiologies and how they influence one another. Monitoring TBI biomarkers offers specificity and non-variability in the diagnosis of TBI presentations [101]. After injury, it is widely thought that BBB disruptions result in extravasastion of biomarkers from the site of injury to surrounding circulation [101,102]. This makes investigations of blood, urine, saliva, and cerebrospinal fluid-based biomarkers representative of TBI, especially mild TBI, localized in different brain regions, ideal [7,12,98]. Additionally, detected biomarker level changes would indicate or eliminate the need for brain imaging [98], saving diagnosis time and resources. Also, in rural areas and conflict regions where advanced imaging techniques or diagnostic capabilities may not be available [20,100,103,104], biomarkers could complement or act as a viable replacement for diagnosing TBI. In TBI, the time of diagnosis is very crucial; having biomarkers that could speed up diagnosis time could be the key to positive recovery outcomes [7,105]. Furthermore, the efficacy of experimental treatments could be objectively evaluated by studying biomarker-level changes that represent the TBI-related metabolic changes and treatment involvement [98]. The use of biomarkers for TBI diagnosis can be challenging as there exist a variety of specific and non-specific CNS markers of brain injury [7,98]. Time course changes of biomarkers in response to TBI to study the progression of the disease could indicate different biochemical process involvement in the pathophysiology of the disease[98]. Although a large portion of patients with mild TBI also sustain injuries to other organs. Mild-TBI diagnosis can be challenging if peripheral biomarkers used are not specific to

the brain but also released by the other organs [98]. A good example of such a biomarker is S100B, majority of S100B found in the serum after TBI is sourced from the brain compared to other organs [98,106,107]. Consequently, in diagnosing TBI and TBI with polytrauma comorbidities, the best route of action lies in the combination of specific and non-specific CNS markers, each representing a different time course of the disease [98]. This combinatorial approach is referred to as “biomarker signatures” that are generated to improve overall specificity and accuracy of diagnosis [98]. Applications of potential biomarker signatures may include disease diagnosis, secondary pathology assessment, treatment efficacy assessment, temporal profile of disease states, injury mechanism identification, and determination of disease severity, progression, and recovery outcomes [7,12,98]. As a standalone, presently tested biomarkers are unlikely to have sufficient specificity and sensitivity for TBI diagnosis and outcome predictions. Evidently, the combinatorial approach should be the future of TBI diagnosis [98]. Additionally, serial sampling of biofluids for these biomarkers is a better approach than a single-point sampling because it provides invaluable information on the temporal profile associated with TBI pathophysiological changes [7]. In addition, improvement in identifying numerous blood-based biomarkers that well represent acute and more severe TBI has been recorded. However, mild-TBI blood-based biomarkers still require more evidence to corroborate their utility in TBI diagnosis [7].

Utilization of Protein biomarkers for TBI diagnosis has seen a lot of progress as there are FDA approved biomarkers glial fibrillary acidic protein (GFAP) and ubiquitin C-terminal hydrolase-L1 (UCHL1) and a host of other identified potential biomarkers such as S100 calcium-binding protein B (S100B), neurofilament heavy chain protein

(NF-H), myelin basic protein (MBP), total and phospho Tau, αII-spectrin breakdown products, and neuron specific enolase (NSE) [100](kevin wang, agoston). These protein biomarkers are indicative of TBI pathophysiologies like neuronal cell body injury, neuronal cell death, astroglial injury, axonal injury, white matter injury, post-injury neurodegeneration, and post-injury autoimmune response [7,100]. Figure 1.9. illustrates the connection between protein biomarkers with temporal changes and the pathophysiology of TBI.

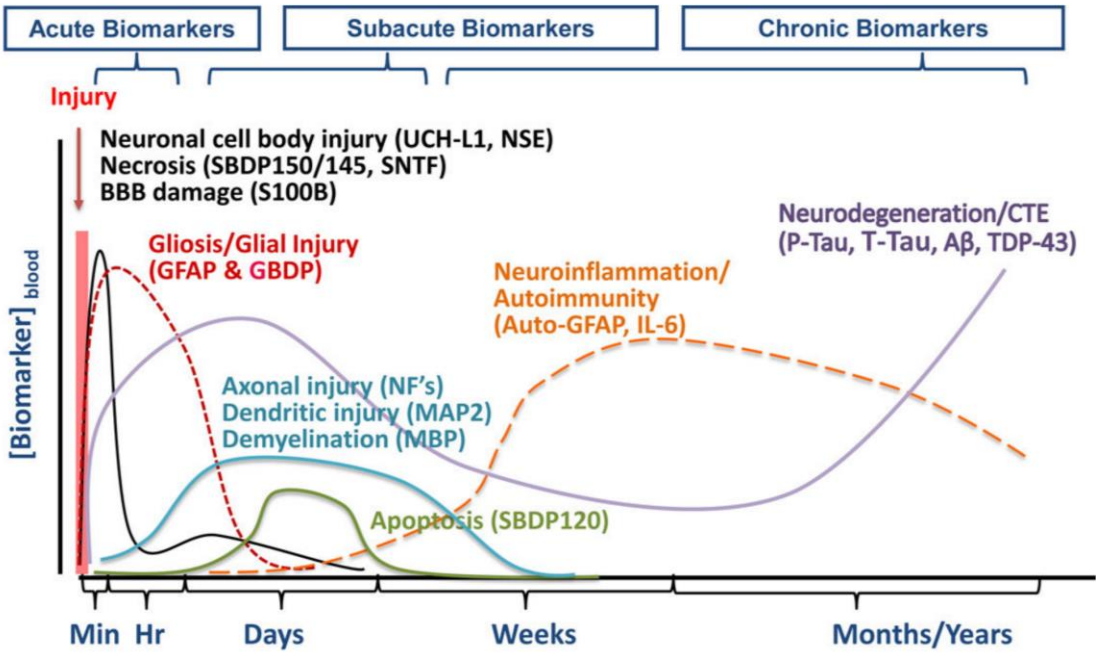

Figure 1.9. Temporal changes of protein biomarkers in different phases and pathophysiology of TBI [100].

Small molecule biomarkers' use in TBI investigation has gained a lot of interest recently due to the identification of the involvement of many small molecules in the biochemical and metabolic changes initiated by TBI [93,98,99]. Such involvements may

include mitochondrial dysfunction, oxidative stress, lipid peroxidation, neuroinflammation, and neurotoxicity [108]. It has been reported that small molecules can move around more freely in and around the injury site after trauma [109], indicating that they possibly end up in peripheral fluids. *N*-acetylaspartic acid (NAA), 5-hydroxyindoleacetic acid (5-HIAA), 4-hydroxynonenal (4-HNE), F2a-isoprostane (F2a), malondialdehyde (MDA), glutathione (GSH), and glutathione disulfide (GSSG) as biomarkers all have indirect and direct relationship with oxidative stress [110–114]. The exact function of NAA, an abundant neuron residing amino acid derivative in the adult brain, is not entirely understood [115,116]. Changes in NAA levels in biofluid and brain, for one, have been implicated in neuronal activity and mitochondrial function deficits in schizophrenic patients and following traumatic brain injury [117,118]. Additionally, these changes may be indicative of intracellular component leakage from neuronal injury or death [115]. Acetyl coenzyme A dependent functions such as energy derivation, lipid synthesis, and protein acetylation reactions in different cell population are distinctively affected by NAA depletion after TBI [116]. The pathway through which NAA is synthesized in the citric acid cycle and used in the brain is depicted in Figure 1.10

5-HIAA is the primary serotonin metabolite that starts as tryptophan within cells. It has been indicted as a marker for neurotoxicity, oxidative stress, neuroinflammation, diseases of malabsorption, and inborn errors of metabolism [114,119,120]. In neurological disorders, 5-HIAA's reduction may be indicative of reduced production or increased reuptake of serotonin from neuronal synapse [121]. Urinary and biofluid 5-HIAA is especially useful in monitoring chronic appendicitis [122], acute kidney injury

[114], and neurological disorders [121]. Figure 1.11. shows 5-HIAA synthesis in the tryptophan metabolic pathway.

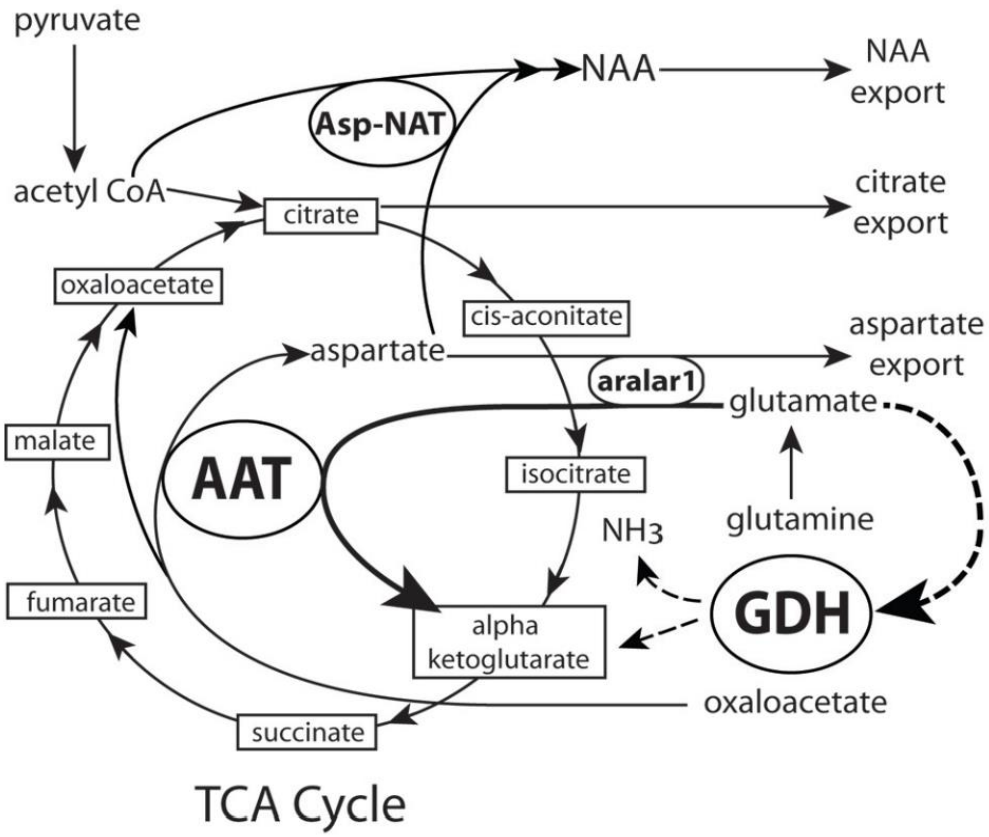

Figure 1.10. Proposed schematic of NAA synthesis in neuronal mitochondria. Dashed lines show α-ketoglutarate pathway through GDH that is bypassed by synthesis through AAT (aspartate amino-transferase). As more pyruvate enters the cycle NAA synthesis is increased, aspartate export from mitochondria is decreased and NAA export is increased [116].

Multiple cellular processes including cell differentiation, proliferation, and apoptosis utilize a tripeptide GSH as essential [124,125]. GSH homeostasis results in redox imbalance that has been implicated in the etiology and/or progression for numerous

diseases [124]. GSH is important in the pathophysiology, combating, and understanding of the complex process of oxidative stress from TBI and other diseases [124,125].

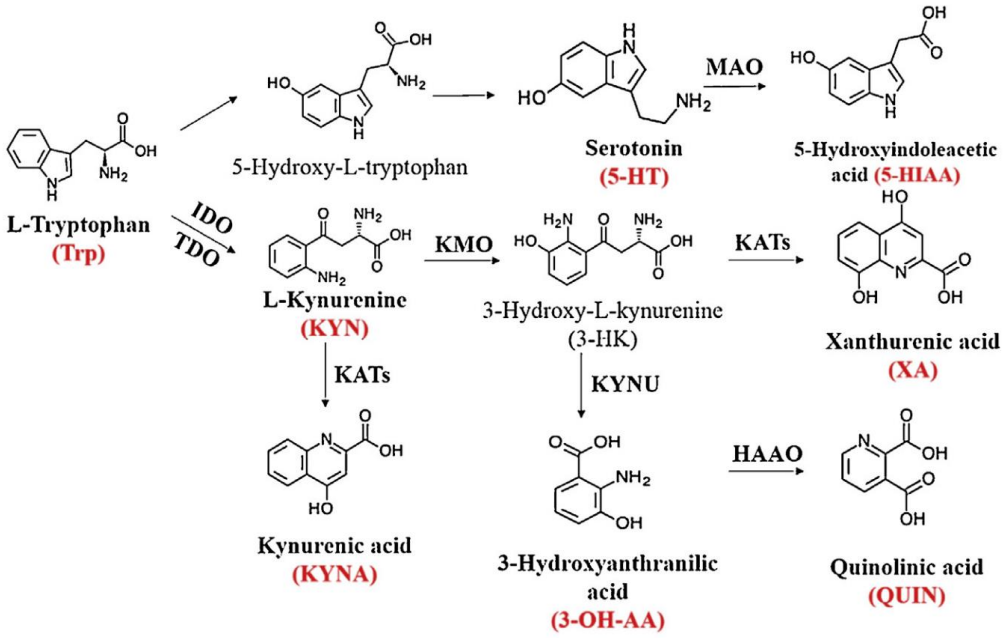

Figure 1.11. The tryptophan metabolic pathway [123].

Additionally, GSH homeostasis is maintained under normal conditions by controlling GSH synthesis rates and exports from the cells [124]. Low intracellular GSH levels indicate reduced antioxidant capacity, while higher GSH levels indicates increased antioxidant capacity against oxidative stress [124]. Biosynthesis of GSH in the cytosol is tightly regulated and controlled by the availability of rate limiting sulfur amino acid precursor (cysteine) and the activity of the rate limiting enzyme, glutamate cysteine ligase (GCL) [125]. Additionally, GSH synthesis can be carried out by the enzyme GSH synthetase [125]. GSH activity works in a redox cycle in which GSH converts into GSSG upon oxidation, largely catalyzed by GSH peroxidase (GPx) enzyme and GSSG produced

can be converted by to GSH using NADPH as substrate by GSH reductase enzyme [56,124,125]. Incidentally, GSH, GSSG, and a ratio of GSH to GSSG can be used as biomarkers to monitor disease states and redox health status of oxidative stress characterized diseases [56]. Some antioxidant therapy strategies aimed at counteracting oxidative stress involves the use of GSH-prodrugs like NAC and γ-glutamylcysteine ethyl ester to confer neuroprotection [126]. Glutathione synthesis and catabolism is described in Figure 1.12.

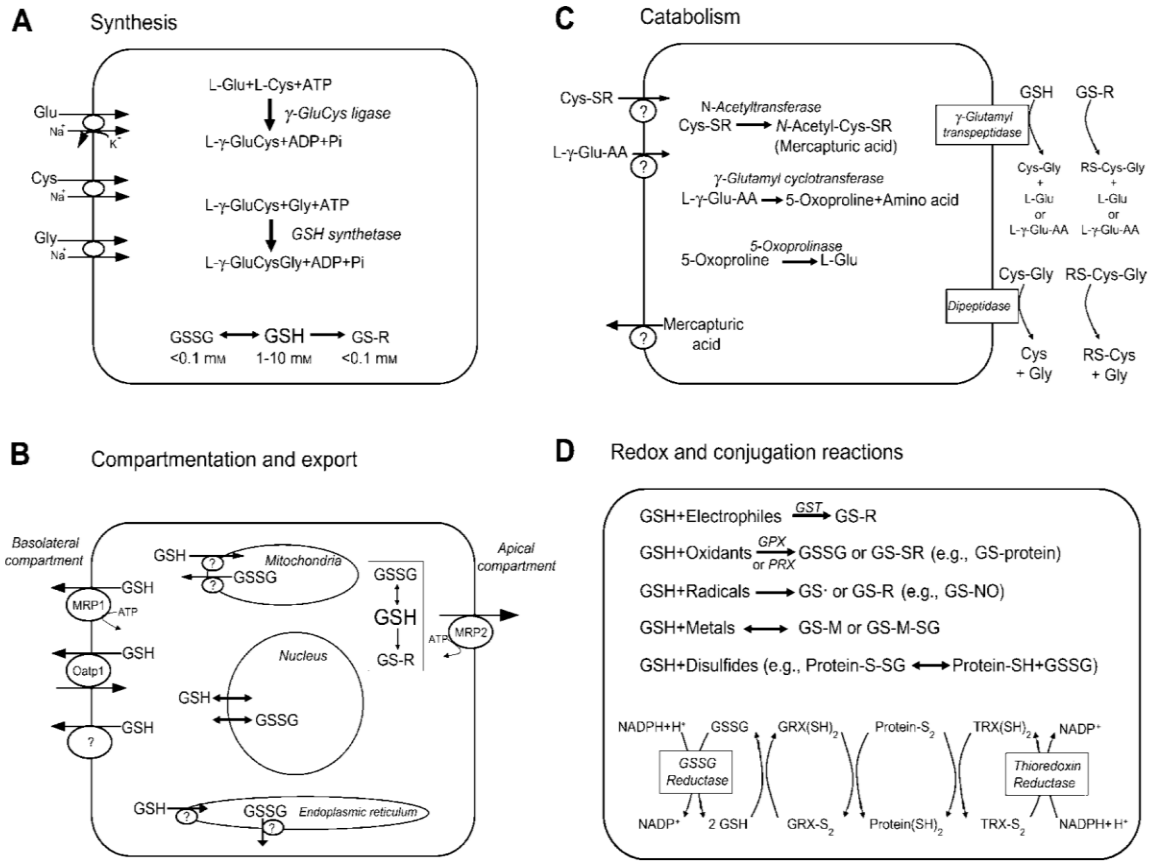

Figure 1.12. Major pathways of glutathione homeostasis in mammalian cells. (A) Synthesis, (B) Catabolism, (C) Compartmentation and export, and (D) Redox and conjugation reactions [124].

1.2.8. Peripheral Fluids and Brain Biomatrices for TBI Investigation.

Peripheral fluids like CSF, blood and urine become connected to brain activities intimately at a biochemical and molecular level in disease conditions [93,127]. In disease conditions, the glymphatic system and BBB breakdown may be responsible for transporting TBI biomarkers into peripheral blood [101,102]. BBB disruption causes extravasation of metabolites and protein into the blood and consequently into urine [7]. This makes the investigation of the brain and peripheral fluids ideal for understanding how the changes occur as a result of injury and hopefully may help in studying treatment efficacy of TBI. Use of peripheral fluid would offer the advantage of using easily collectible minimally invasive fluids for TBI diagnosis [7], thereby relieving stress and pain on victims during biological sample collection and ensuring faster diagnosis time for better recovery outcomes. Use of these fluid-based biomarkers may also be a cheaper option to neuroimaging-based diagnosis. One limitation to the use of peripheral biofluids markers is that the mechanism through which brain interstitial fluid molecules are transferred into peripheral circulation are not well understood and highly complex. Additionally, this transportation across the BBB is largely dependent on solubility, molecular weight, and size of protein or molecule [7].

1.2.9. GSH-Prodrugs NAC and NACA. TBI treatment, which is primarily focused on guidelines and symptom management, may not be well suited for combatting the disease [6,128]. Alternatively, targeting specific mechanisms of injury or a combination can be useful in finding effective therapies against TBI [129]. One particular mechanism of interest is oxidative stress, characterized by redox imbalance. This secondary mechanism of TBI can be counteracted with the use of antioxidants and

medicinal thiols to improve redox homeostasis [18,78,130–132]. Figure 1.15 from Pfaff et al., shows different mechanisms of action of medicinal thiols.

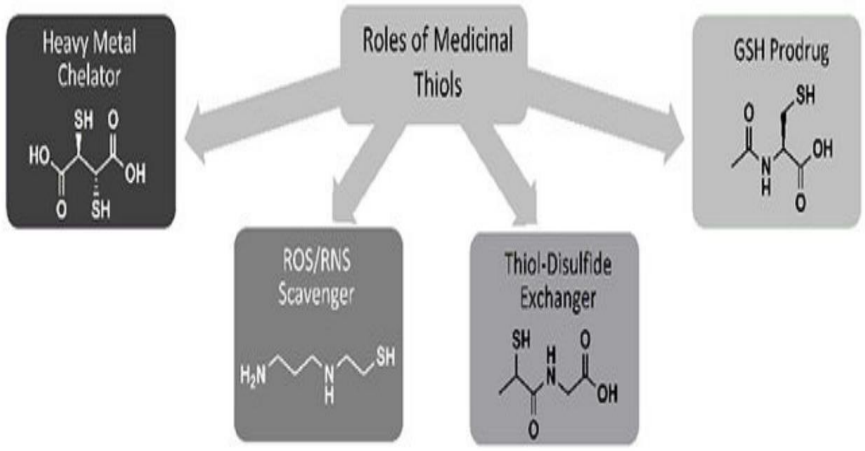

Figure 1.13. Different roles of medicinal thiols [78].

A medicinal thiol drug that fits well into this narrative is *N*-acetylcysteine (NAC-2,3-meso-dimercaptosuccinic acid), which is an FDA-approved GSH prodrug and ROS scavenger used to combat oxidative stress induced by acetaminophen poisoning [78]. However, NAC's action against oxidative stress is limited by its low bioavailability, which leads to higher dosage [78,133]. This limitation was addressed by the synthesis of *N*-acetylcysteine amide (NACA) in 1967 [134], an amide derivative of NAC that has better bioavailability due to its hydrophobic and lipophilic identity that lets it cross the BBB more effectively [135]. The structure of NAC and NACA is shown in Figure 1.16., also, Figure 1.17 shows NACA's mechanism of action.

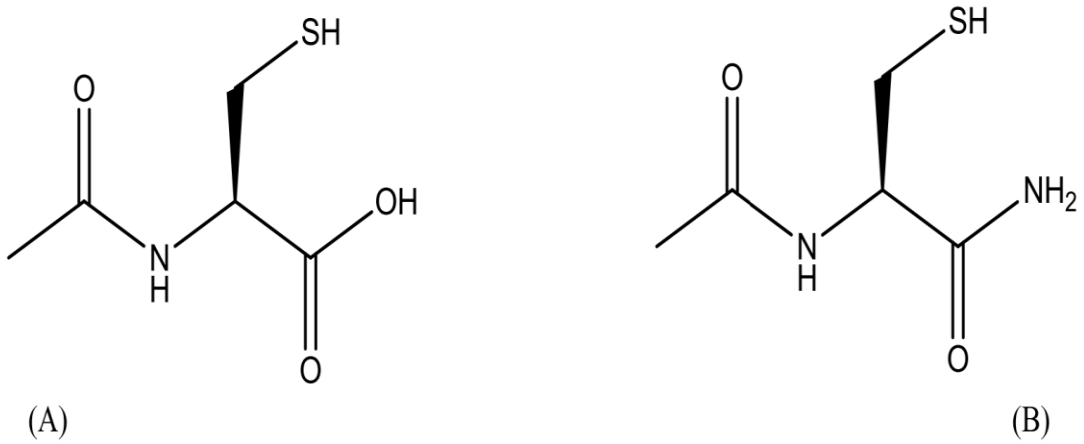

Figure 1.14.The structures of (A) *N*-acetylcysteine and (B) *N*-acetylcysteineamide [57].

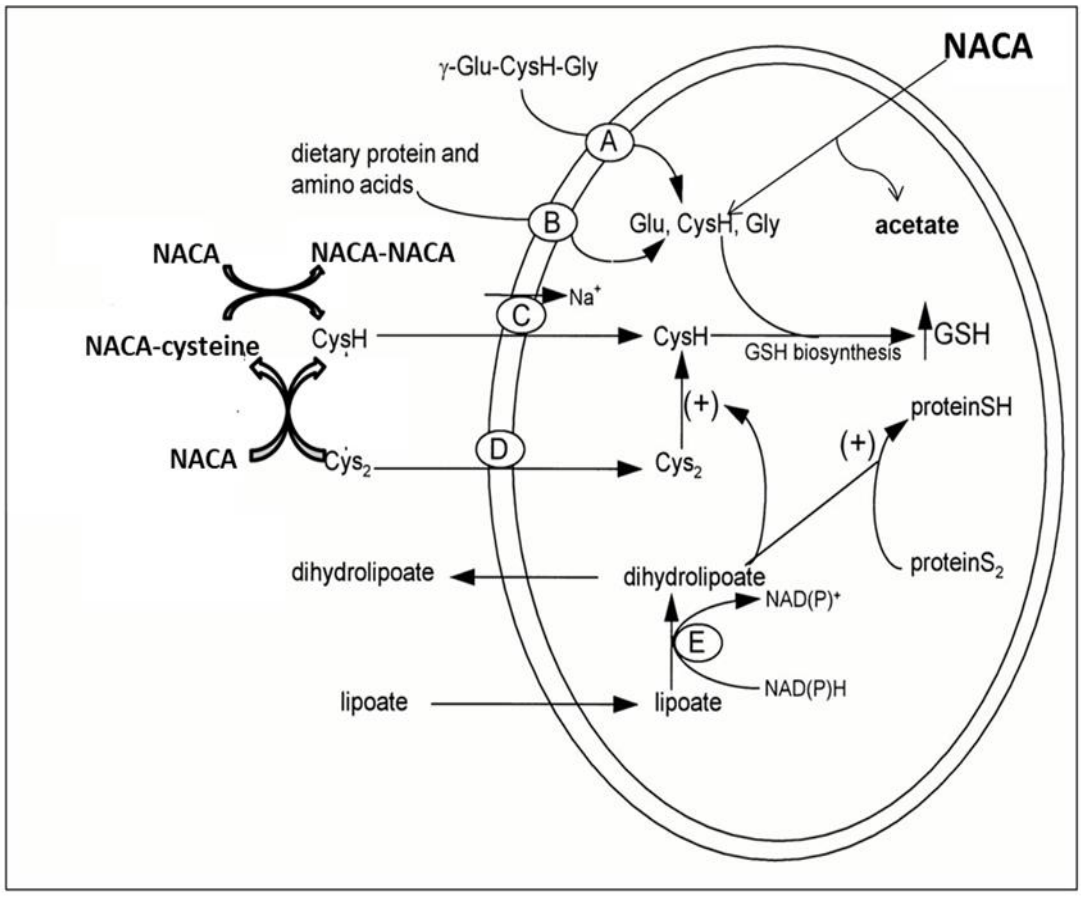

Figure 1.15. Mechansim of action of NACA [136,137].

1.2.10. Animal Models of TBI. Cellular and metabolic deviation from physiological homeostasis that causes physiological components to perform their functions sub-optimally is the cause of disease in humans and animals alike [138]. In research, in-vitro studies, including cell-based assays and tissue culture studies, are used to investigate disease mechanisms, and they provide invaluable pathological information [138]. However, they fail to account for the complex physiological conditions and interactions between different cell types of tissues and organs [138]. On the other hand, animal disease models address these concerns as they are used to unravel different disease mechanisms in physiological and pathological conditions similar to humans [138,139]. Animal models are useful for understanding disease mechanisms and treatment and for prevailing over clinical trial limitations in human subjects [138]. Historically, animal models use dates back to the fourth century B.C. when Williams Harvey used animals in the 1600s to describe the blood circulatory system [138]. Additionally, notable scientists Louis Pasteur (credited as the father of immunology and the pasteurization process [140]) and Emil von Behring (who developed therapies for diphtheria and tetanus [141]) were recorded to have used animal models for experiments and hypotheses proving [138]. Modeling the multitude of dynamic forces of DAI acting on the structurally complex human brain is difficult, and as such, in selecting animal models for TBI, researchers need to consider some important anatomical factors carefully [31,33]. Brain folds and shape in studying TBI are very important considerations to achieving accurate modeling. Animal models are classified as gyrencephalic (non-human primates, porcine, canines, and whales) and lissencephalic models (typically rodents) based on the type of brain-fold they have [33]. The gyrencephalic models most closely represent human brain anatomy and

physiology. However, the categories of animals in this model are not easy to handle during experiments and are economical [33]. Alternatively, the lissencephalic models, which comprise murinae that are small and easy to handle, are most preferred by researchers due to their reproducibility, economy, and capacity for titration of injury magnitude [33,142,143]. In addition, murine share some anatomical, physiological, and genetic similarities to humans, making them ideal for studying the pathophysiology of human-centric diseases [144]. In studying TBI, it is crucial to consider the brain as a semisolid of heterogeneous densities and composition that, when force is applied, is deformed in a manner consistent with its plasticity, elasticity, and viscosity [33,145]. Mechanical injury may be induced by a direct or indirect force that may be focal or diffuse with different severity. Additional variability exists in these two primary modes. For example, direct force may be from a penetrating or blunt force, while indirect force may be from blast overpressures or inertial acceleration/deceleration head trauma movement [33]. In inducing non-blast TBI, controlled cortical impact, impact acceleration, and fluid percussion models are used [33]. However, explosive blast injuries common in the military population require a model that is closely associated with blast neurotrauma. Certain researchers use compressed gas blast-tubes; however, this may not accurately represent heat and toxic organic compounds containing exhaust that are impacted on the subject in real-life scenarios [33]. Open-field blast models have been developed to simulate blast neurotrauma to create blast pressure and overpressures enough to induce mild to severe blast neurotrauma and replicate real-life effects and blast physics in the rodent models [22]. Figure 1.14. shows the different modes of injury animal models are induced with TBI.

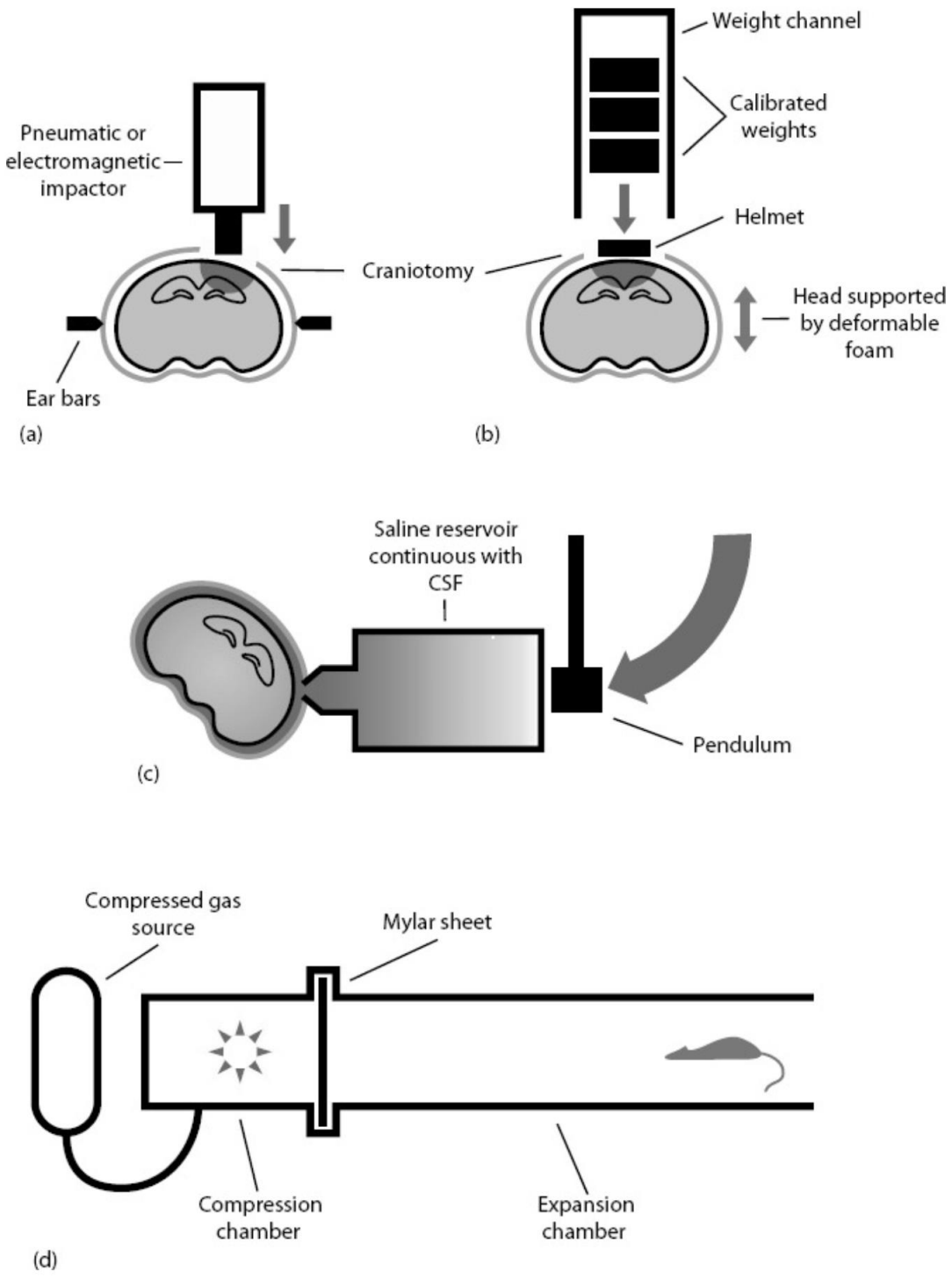

Figure 1.16. Experimental models of traumatic brain injury used in simulating DAI in lissencephalic animals. (a) controlled cortical impact, (b) impact acceleration, (c) fluid percussion, (d) compressed gas blast tube [33].

Finally, fresh approaches to understanding [17] blast overpressure injury mechanisms are critical in establishing in vivo markers of damage unique to blast [30]. Bryden et al. recommended strategic performance of further research in areas of modeling, scaling, and head-only or combined body injury. In this study, we utilized open-field explosive injury in murine models to closely simulate the injury military personnel are exposed to in training and combat.

1.2.11. Analytical Techniques for Small Molecule Metabolites. The importance of small molecule biomarkers in disease diagnosis and treatment design cannot be overstated. These metabolites depict the "composite output" of the cellular machinery that accounts for proteomic, genomic, and transcriptomic variability, and thus, they closely represent the changes to cells, tissue, or organism that are triggered by a disease process [97]. Furthermore, techniques with high specificity and sensitivity are used to analyze these metabolites of interest in a field of studies referred to as metabolomics [97]. Currently, high throughput and highly sensitive analytical tools capable of detection and quantification of low concentrations of metabolites, enable the analyst to follow pathological changes with metabolite alterations and compare them with normal states or different pathological processes [93]. A typical metabolomic experiment operates in four parts: 1.) sample acquisition and preparation, 2) analyte separation and detection, 3) data mining and collection, and 4) data analysis and proofing [97]. The most common platforms with enough sensitivity and specificity used in metabolomics are nuclear magnetic resonance (NMR) and mass spectrometry (MS) [93]. Both techniques are capable of reproducible high-throughput measurement of a large number of metabolites [93]. MS and NMR-based analytical platforms have enabled the separation,

characterization, detection, and quantification of a wide variety of chemical structures [97]. Additionally, integrating bioinformatic techniques with these metabolomics yields a high throughput of analysis of metabolites and data read-out to understand disease process pathology better[97].

NMR spectroscopy operates on the principle of nuclei resonating in a magnetic field at a frequency specific to that nuclei. So, when a compound is placed in a magnetic field, isotopes within the compound (e.g., ^{1}H, ^{13}C, ^{14}N, ^{15}N, ^{17}O) absorb the radiation and resonate at a frequency dependent on its position in the small molecule [97,146]. The resultant data is an NMR spectrum comprising a collection of peaks at different positions (chemical shifts) and intensities, with each compound having its unique pattern [97]. In contrast to MS, NMR is non-discriminating (detecting any compounds with protons, carbon, nitrogen, or oxygen), non-destructive during analysis, and requires minimal or no sample preparation [97]. However, its limitation lies in its low sensitivity, which results in the omission of low abundance metabolites in NMR-based approaches[97,147]. This has led to a preference for MS-based techniques to NMR-based techniques for metabolomic studies [97,148].

MS as a standalone is a powerful technique and can be used to run untargeted and targeted metabolomics. However, for optimal specificity and sensitivity [97,149], MS is routinely coupled with gas chromatography (GC) or liquid chromatography (LC), which helps to separate the analyte of interest from the matrix component and, in turn, improve the analysis. This makes analyzing complex biomatrices like biofluids and tissues easier to analyze. GC is ideal for the separation of volatile compounds such as fatty and organic acids, while LC is ideal for separating non-volatile compounds [97]. The working

principle of MS-based identification of analytes involves sample injection, separation, ionization, mass analysis, data acquisition, data analysis, and metabolite identification [97]. Typical MS workflow is outlined in Figure 1.13.

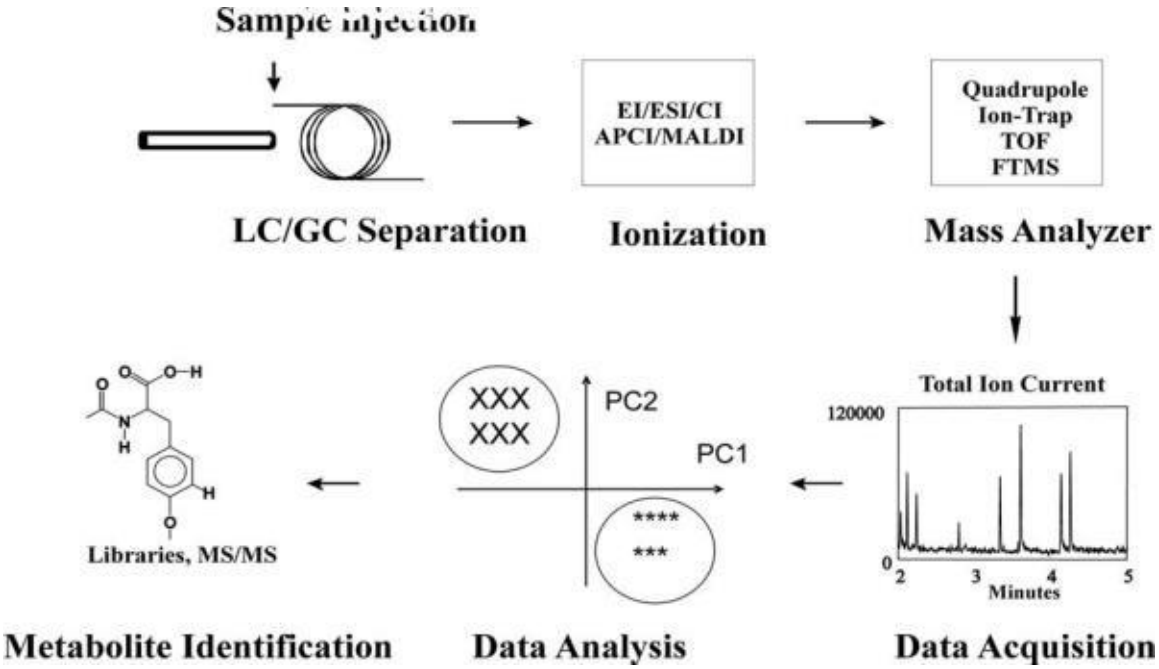

Figure 1.17. Descriptive workflow for mass spectrometry based metabolomic analysis [97].

After separation by LC or GC, the biomolecules are ionized, and the mass-to-charge (m/z) ratio is derived by parent ion fragmentation in the MS. Read-out data is acquired as a full scan mass spectrum of the target analytes [97]. Ionization techniques like chemical ionization (CI) and electron impact ionization (EI) have made it possible to detect and quantify target analytes at sub-femtomole levels [97]. In addition, the development of the soft ionization technique electrospray ionization (ESI) has made LC-MS coupling possible [97,150,151]. The MS mass analyzers could also be oriented in

series to give tandem MS (LC-MS/MS), a combination of different mass analyzers, including triple quadropole, ion-traps, orbitraps, and/or time-of-flight (TOF) [97]. MS limitations lie in the destructive nature of some ionization techniques, discriminative nature (not all samples can be ionized under a specific set of conditions, and ion source polarity may have to be modified), and it requires extensive sample preparation that may result in metabolite loss and cost in time and resources [97].

Untargeted metabolomics is used by researchers to generate hypotheses and discover biomarkers in a way that raises research questions [97]. It is casually referred to as “unbiased or nondirectional metabolomics.” The ultimate goal is possible metabolite detection of an ample amounts in a biomatrix to classify phenotypes based on metabolite patterns or interaction [97]. In contrast, targeted metabolomics are hypothesis-driven to confirm untargeted studies or validate essential biological pathways [97]. This has caused it to be referred to as “biased or directed metabolomics” or “metabolomic profiling.” It involves the predetermination of metabolite sets or classes of specific chemicals of small molecules like lipids and tricarboxylic acid cycle metabolites [97]. Finally, other analytical instrumentation used in metabolomics may include Fourier transform infrared spectroscopy and capillary electrophoresis [152]. Here, we utilized targeted metabolomics to study biomolecules that have been hypothesized to be involved in the pathophysiology of TBI to understand their diagnostic potential and response to antioxidant therapy.

1.3. RESIDUAL SOLVENTS IN PHARMACEUTICAL PRODUCTS

In the drug product manufacturing process, solvents are utilized at major stages of production as synthesis catalyst or vehicles, purification, and formulation of excipients and active pharmaceutical ingredients (APIs) [153,154]. Yield and physicochemical properties of the synthesized API and excipients during the manufacturing process may be enhanced by appropriate selection of solvent [153]. However, after usage some of these solvents offering no therapeutic benefits may be retained in the final drug products and they are hard to get rid of completely [153,154]. Residual solvents (RS) as the retained solvents are called, are present in varying concentrations in these drug products, and they should be removed to a possible extent to meet safety standards [153,154]. The presence of these RS has adverse effects on the quality and durability of the product during packaging, storage, and transportation [155]. More importantly, they may lead to adverse health consequences based on their toxicity, thereby defeating the objective of drugs for addressing disease states [155]. In addition to adverse health consequences posed by these RS, they also contribute to environmental depletion [154]. To control and regulate the amount of residual solvent that is permissible for human use owning to having no or tolerable risks, regulatory bodies ICH (The International Council for Harmonisation of Technical Requirements for Pharmaceuticals for Human Use) and USP (United States Pharmacopeia) have set limits that are generally agreed upon by manufacturing and other regulatory bodies [153–155] alike for how much of these RS can be tolerated based on three classes notably As described in Table 1.2. [153,154]:

Class one- These solvents should be avoided in the production of drug substances, excipients, or drug products unless risk-benefit assessment can be used to justify their

usage. Their lists include known and suspected human carcinogens and environmental hazards.

Class two- These solvents are associated with less severe toxicity and should be limited to protect patients from adverse effect potential. They include solvents suspected of significant but reversible toxicities, non-genotoxic animal carcinogens, causative agents of irreversible neurotoxicity and genotoxicity.

Class three- These solvents should be used only in practical situations. They are known to have low toxic potential to humans, and no health-based exposure is needed for them.

Table 1.2. Classification of residual solvents by ICH [154].

Class 1		Class 2		Class 3	
Solvent	Limit (ppm)	Solvent	Limit (ppm)	Solvent	Limit (w/w%)
Benzene	2	Acetonitrile	410	Acetic acid	0.5
Carbon Tetrachlroide	4	Chlorobenzene	360	Acetone	0.5
1,2-Dichloroethane	5	Chloroform	60	Anisole	0.5
1,1-Dichloroethene	8	Cumene	70	1-Butanol	0.5
1,2-Dichloroethane	1500	Cyclohexane	3880	2-Butanol	0.5
		Cyclopentyl methyl ether	1500	Butyl acetate	0.5
		1,2-Dichloroethene	1870	tert-Butylmethyl ether	0.5

Table 1.2. Classification of residual solvents by ICH [154]. (Cont.)

Class 1		Class 2		Class 3	
Solvent	Limit (ppm)	Solvent	Limit (ppm)	Solvent	Limit (w/w%)
		Dichloromethane	600	Dimethyl sulfoxide	0.5
		1,2-Dimethoxyethane	100	Heptane	0.5
		N,N-Dimethylacetamide	1090	Isobutyl acetate	0.5
		N,N-Dimethylformamide	880	Isopropyl acetate	0.5
		1,4-Dioxane	380	Methyl acetate	0.5
		2-Ethoxyethanol	160	3-Methyl-1-butanol	0.5
		Ethylene glycol	620	Methylethyl ketone	0.5
		Formamide	220	2-Methyl-1-propanol	0.5
		Hexane	290	2-Methyltetrahydrofuran	0.5
		Methanol	3000		
		2-Methoxyethanol	50		

Table 1.2. Classification of residual solvents by ICH [154]. (Cont.)

Class 1		Class 2		Class 3	
Solvent	Limit (ppm)	Solvent	Limit (ppm)	Solvent	Limit (w/w%)
		Methylbutyl ketone	50		
		Methylcyclohexane	1180		
		Methylisobutylketone	4500		
		N-Methylpyrrolidone	530		
		Nitromethane	50		
		Pyridine	200		
		Sulfolane	160		
		Tertiary-butyl alcohol	3500		
		Tetrahydrofuran	720		
		Tetralin	100		
		Toluene	890		
		1,1,2-Trichloroethene	80		
		Xylene	2170		

1.3.1. Residual Solvent Monitoring. The most appropriate and widely used methods for qualitative and quantitative RS determination are static and dynamic

headspace gas chromatography and USP 23 <467> Organic Volatile impurities [155]. Alternatively, sampling using solid phase micro-extraction (SPME) and high-pressure liquid chromatography may be used in place of headspace sampling and gas chromatography. Detectors are imperative in any chromatography technique, and RS analysis may be detected by mass spectrometry (MS), Fourier transform infrared spectroscopy (FTIR), and flame ionization detectors (FID) [156–159]. Incidentally, static headspace gas chromatography coupled with flame ionization detectors (FID) is the most popular and recommended instrumentation used for RS analysis [153,154,160,161]. These techniques, although effective, still lapse in terms of cost, complexity, and size of instrumentation, [161,162] which can be a disadvantage in the fast-paced pharmaceutical drug product manufacturing industry. A solution to these problems will be the availability of cost-effective, selective, sensitive, easy-to-use, and miniaturized instrumentation [163] which fits the description of the Novatest P100 gas chromatography-photoionization detector (GC-PID) with online preconcentration. This instrument is a miniaturized combination of gas chromatography and photoionization detection that can easily satisfy the demand for versatilite, portable, and convenient instrumentation. Additionally, there are GC methods and procedures developed and described by the USP for RS analysis [153].

1.3.2. Miniaturized Instruments. Historically, desire to miniaturize has yielded the development of more powerful devices than was existent initially [164]. For analytical instrumentations, development of “lab-on-a-chip” techniques, micro- and nano- scale chromatography systems, and enhanced professional “point of care” devices were heavily influenced by the desire for smaller and portable instrumentation than what was originally

available [164]. Miniaturized instrumentation has the advantage of ease of movement of equipment to/from the laboratory to be deployed for field testing or in a different area of a manufacturing process that may require analysis of such instruments [164]. This ease of movement reduces the risks of sample manhandling and contamination [164]. Additionally, for chromatographic instrumentation, reduced fluid volume requirement from reduced overall instrumentation size subsequently reduces sample size, analysis time, reagent volume, and operational costs [164]. Also, the miniaturization of photoionization detectors can help develop improved gas analyzers through reduced resource consumption and enhanced sensitivity from the portability [165]. Miniaturized GC-PID has been shown to achieve commendable gas separation and detection reliability for residual solvent mixtures [166]. Also, if there is a desire for lower detection limits, additional preconcentration step can be added to the set-up to preconcentrate the sample before injection into the instrument [166]. Photoionization detectors (PID) can be miniaturized while still retaining comparable sensitivity of RS with bulky PID and other detectors.

1.3.3. Portable GC-PID System. The growing demand for convenience and versatility by academic and private researchers has led to the shrinkage of the GC to be better and improved [163]. Conventional GC is a very powerful and useful analytical technique; however, in the need to deploy it for field analysis, it is impractical due to its size [167]. The onset of micro-electromechanical systems (MEMS) technique development has led to further miniaturization of the portable GC to obtain microsized instruments that are easy to use and suitable for field deployments [168]. GC-PID is commonly used for the detection of volatile organic compounds (VOCs) or RS to prevent

environmental pollution or RS toxicity. Rapid detection of these volatiles is a necessity in a number of lab and on-site settings raising the need for field deployable, high precision, and portable GC-PID system for real time monitoring of volatiles [167]. Miniaturized versions of the GC with micro-GC column and micro pre concentrator coupled with a mini PID will have the advantage of small volume requirements, rapid analysis, low power consumption, and cost compared with conventional GC systems [167]. The miniaturized GC system usually comprises an injection unit, a micro preconcentrator, a micro-GC column, and a mini PID [167], as shown in Figure 1.18.

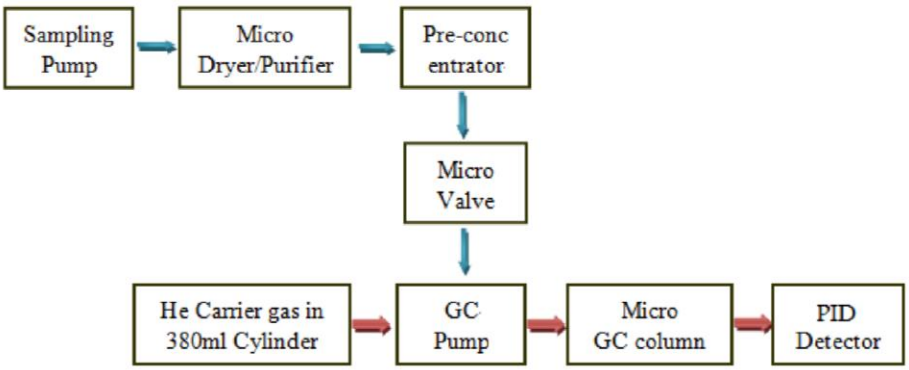

Figure 1.18. A schematic representation of a typical miniaturized GC system architecture [167].

1.3.3.1. Sampling and injection. The successful outcome of a GC analysis is dependent on the sampling technique employed. Monitoring of volatile and semi-volatile compounds is ideal for the GC system [169]. However, the source of these kinds of compounds may be from gaseous, liquid, or solid samples [169]. Samples can be prepared in Tedlar® bags or GC vials for analysis. The liquid injection uses a needle to

introduce volatile and semi-volatile analytes into the GC through an injection port preheated to the initial column temperature [170]. Direct sampling injection is useful for small liquid or solid samples that can fit into a sample cup attached to a heating probe and be directly inserted into the GC-MS ionization chamber, bypassing the GC-column; the heat applied ionizes the sample [170]. In the SPME method, a polymeric stationary phase-coated fiber core needle that can be directly inserted into liquid samples or sample headspace is used for the adsorption of analytes [170]. In direct thermal desorption sampling, solid samples are directly filled into thermal desorption tubes that are heated to release or desorb the volatile analytes via thermal desorption into the GC system [170]. Similarly, in thermal desorption sampling, volatile analytes from thermal desorption tubes filled with large volumes of gas are released into the GC system through heat desorption via an adsorbent trap system [170]. Optionally, the static headspace method for detection of volatile analytes involves preheating liquid samples in an incubating chamber within the autosampler. Pre-heating results in free equilibrium movement of dissolved components between the liquid phase and gas headspace, and the higher incubation chamber temperature causes the more volatile components to converge in the gas phase due to an equilibrium shift [170]. Finally, the dynamic headspace method or purge-and-trap method employed by portable GCPID systems is an advanced form of headspace injection with greater accuracy than the static headspace method. In this method, a purge gas is introduced into a sample, and the volatile target analytes are carried to an adsorbent trap for concentration in the pre concentrator [170]. Heating the trap releases the volatiles into the GC system through a process known as desorption [170]. Supply of the sample to the pre-concentrator or GC column is carried out by the

injection unit [167]. Injection modes usually employed in GC systems may be split injection (sample portioned in a specified ratio), splitless injection (entire sample introduced into the column by carrier gas), on-column injection (sample introduced directly into the column with a thin injection needle), and programmed temperature vaporizer [169,171].

1.3.3.2. Preconcentration. Upon injection, the sample is supplied to the preconcentrator, a sampling and concentrating device that can significantly improve GC system detection limits by 1~3 orders [167]. Existing analyte detection methods do not always satisfy sensitivity needs. However, preconcentrators help increase sensitivity by increasing the concentration of analytes via adsorption/ desorption phenomena in an adsorbent medium [172]. Preconcentrators' sensitivity increase characteristic has granted the ability to miniaturize instruments for portability [172]. The operation principle of prconcentrators occurs in 3 stages [172]:

1. Room-temperature adsorption of gas or vapor molecules.
2. High-temperature desorption of adsorbed molecules and consequent injection into the sample unit connected to a detector.

Room-temperature cooling of the preconcentration in preparation for the subsequent sampling and analysis.

Preconcentrators are usually coupled with GC for analyte separation, and it is popular due to its allowance for miniaturization of the GC [172]. The type of adsorbent used in preconcentrators plays a vital role in its performance[173]. As there is no “one size fits all” for preconcentrator adsorbent material, an ideal adsorbent material must possess strong analyte selectivity, large porosity, and a large adsorption capacity [173].

Carbonaceous materials are the most studied and popular preconcentration materials due to their ease of preparation, low cost, and availability [173]. Other precontration materials used include metal-organic framework, polymers, and silicon-based materials that require more preparation resources, causing them to be less used in experiments than the carbonaceous materials even though they may possess better quality and properties [173]. The preconcentration techniques may also be classified as same-directional and opposite-directional flow during the loading and unloading/desorption of the analyte [173]. Our study used the same direction flow pattern on the preconcentrator. Figure 1.19. shows the working principle of the portable GCPID system employed in this research. In the first stage of analysis, the blue route is open, and the green route is closed, air is pumped into the system as ambient air or from a device connected container by the sampling unit. Volatiles in the sample are trapped by the preconcentrator and the sample excess is vented out of the system. In the second phase of analysis, the green route is open, and the blue route is shut, the preconcentrator heats up instantly to desorb trapped analytes and the carrier gas carries the chemicals from the trapping unit into the GC separation unit and the detection unit [174].

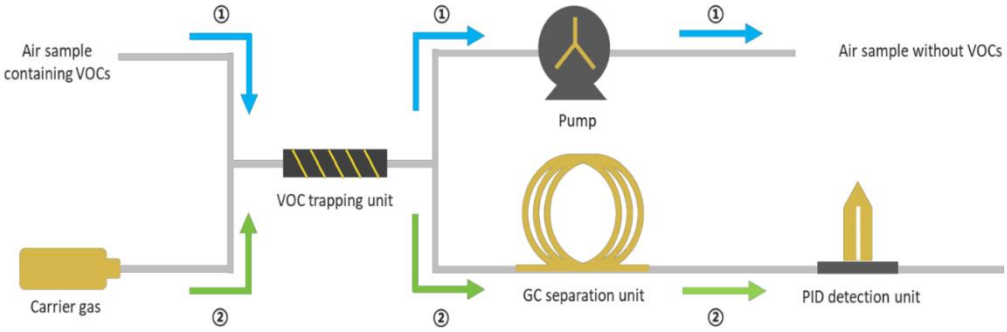

Figure 1.19. Working principle of a Novatest P100 GCPID system [174].

1.3.3.3. Separation. Separation of complex gaseous mixture components of volatile and semi-volatile compounds introduced into the column from the preconcentrator after desorption is carried out by the interaction between the stationary phase and the gaseous component being carried towards the detector by a carrier gas, usually an inert gas, [167]. The types of stationary phases and length of columns used in a GC play a vital role in the overall selectivity of the instrument. GC improves the sensitivity of PID due to the use of small sample sizes required and compound separation efficiency, making it a powerful technique in analytical chemistry [175].

1.3.3.4. Detection. A photoionization detector (PID) quantifies chemicals in gas samples using the ionization of gaseous compounds by light as a working principle [165]. The main components of a PID are the ionization source, electrodes, and ionization chamber [165]. The light is generated by PID lamps used as a light source, and it generates energy in electron volts [165]. When gaseous compounds interact with the lamp, only the compounds with ionization potentials less than the energy generated by the lamp can be photoionized and detected. It is often used to the detect volatile organic compounds and some inorganic substances in ambient air [165]. A disadvantage of PID is its non-specificity, meaning that it will show a response to all analytes with its ionization energy range. This problem is addressed by coupling the PID with a GC that is specific [165]. Alternatively, PID as a standalone can quantify Total Organic Volatile Organic Compounds (TVOC) concentrations in units of isobutylene equivalent [165]. The high-energy light source used to enable photoionization often has wavelengths shorter than 143 nm for chemical species determination [165]. Also, the Classification of the PID is based on the ionization source used. In the first type, the ionization source and ionization

chamber where ionization occurs are integrated. Plasma is generated in a noble gas such as Helium or Argon by a discharge from the ionization source, causing it to be referred to as plasma or discharge photoionization detector (D-PID) [165]. In the second type of PID, the radiation source and ionization chambers are separated into two distinct spaces, causing the ionization chamber to have no fluidic connection to the ionization chamber, and it is known as the lamp photoionization detector (L-PID) [165]. Figure 1.20 a and b show the element and main components of both D-PID and L-PID, respectively.

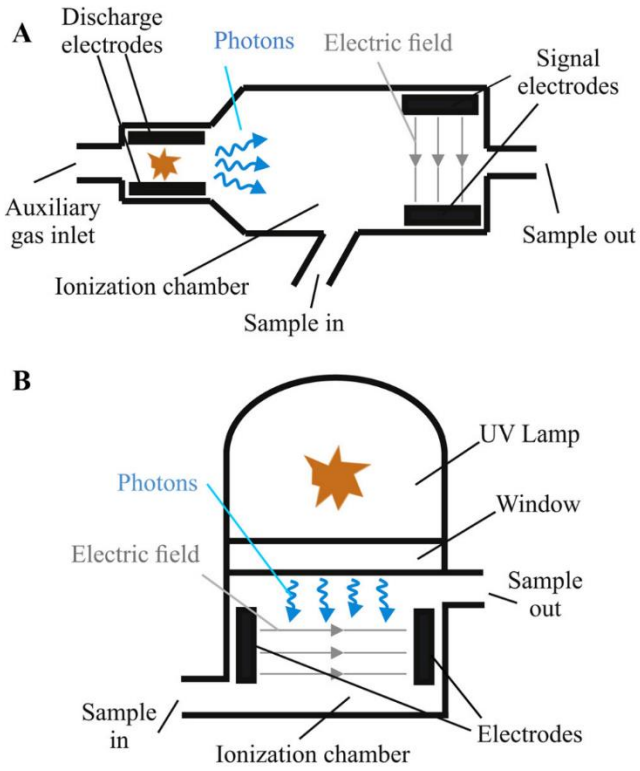

Figure 1.20. Components of photoionization detectors. A) Plasma or Discharge Photoionization Detector (D- PID), where ionization source and ionization chamber are integrated. B) Lamp Photoionization Detector (L-PID), where the ionization source and ionization chamber are physically separated by a window [165].

1.4. OBJECTIVES

The objectives of this research work involve the development of HPLC-MS/MS methods for monitoring potential TBI biomarkers and investigating the therapeutic efficacy of antioxidant therapy using NACA against blast-induced TBI. Secondly, the other objective entails the development of portable GC-PID methods for residual solvent monitoring in pharmaceutical drug products.

PAPER

I. HPLC-MS/MS METHODS FOR ANALYSES OF POTENTIAL TRAUMATIC BRAIN INJURY BIOMARKERS IN URINE, PLASMA AND BRAIN TISSUE OF RAT MODELS

Olajide Adetunji[1#], Jiandong Wu[2#], Annalise Pfaff[1], Austin Sigler[1], Mousumi Bose[1], Catherine Johnson[3], Nuran Ercal[1], Honglan Shi[1], Paul Nam[1, *]

[1]Department of Chemistry, [2]Department of Chemical and Biochemical Engineering, [3]Department of Mining and Explosives Engineering, Missouri University of Science and Technology, Rolla, MO, 65409, USA

#: these authors contributed equally.

ABSTRACT

Traumatic brain injury (TBI) poses an immediate public health concern, as it affects a substantial portion of the population, especially veterans. Milder forms of closed-head TBI can often go undetected with conventional diagnostic methods, increasing the likelihood and severity of long-term effects. TBI initiates a cascade of neurochemical changes; a sensitive small-molecule biomarker panel that monitors such changes would facilitate the investigation of new approaches to diagnosis and treatment. Therefore, two high performance liquid chromatography with tandem mass spectrometry (HPLC-MS/MS) methods were developed and validated to analyze six potential small-molecule TBI biomarkers in rat plasma, urine, and brain tissue at sub-ppb levels. These

levels include glutathione and its oxidized form glutathione disulfide, which reflects tissue redox status altered by the surge of reactive oxygen and nitrogen species after TBI. Other potential biomarkers were investigated, including lipid peroxidation byproducts F2a-isoprostane and 4-hydroxynonenal, along with neurotransmitter metabolites *N*-acetylaspartic acid and 5-hydroxyindoleacetic acid. Analyte stability during storage and handling was drastically improved by incorporating a derivatization step and oxidation inhibitor. The methods developed in both positive and negative ESI modes yielded excellent sensitivity, linearity, accuracy, and reproducibility upon application to urine, plasma, and brain tissue samples obtained from healthy rats. Finally, the method was successfully applied to samples obtained using an open-field blast model of TBI in rodents, and it revealed significant blast-related changes in several of the selected biomarkers.

Key words: Traumatic brain injury, HPLC-MS/MS, biomarkers, urine, plasma, brain.

GRAPHICAL ABSTRACT

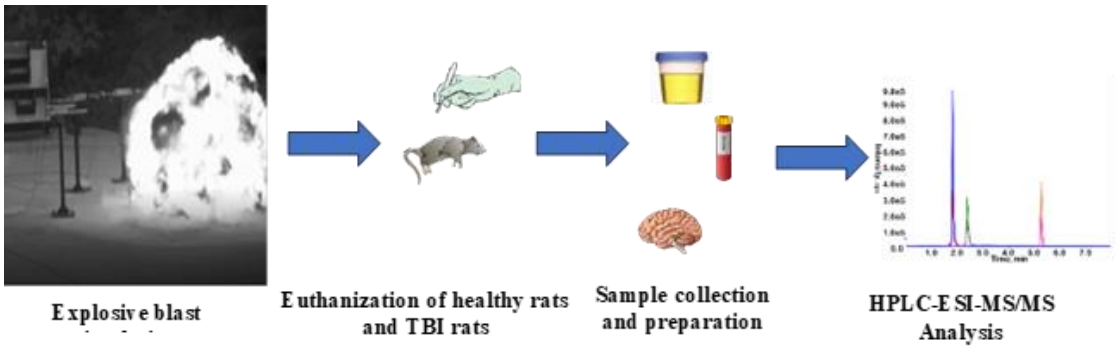

1. INTRODUCTION

TBI affects millions of people each year in the US alone, with 61,000 deaths recorded in 2017 [1, 2]. Closed-head TBI can occur when the brain is subjected to physical insult inside the cranium from a blow, rapid change in momentum (whiplash), or explosive blast. The resulting pressure and shear stress on brain tissue can disrupt blood flow and physically damage neurons and glia, leading to altered brain function. TBI remains a primary cause of death and disability within the military and civilian populations alike [3, 4], with the former mainly being affected by explosive blast overpressures from improvised explosive devices (IEDs) or other explosive apparatus [5] during training or in war-zones [6, 7].

Mild TBI (m-TBI) is the most common form of TBI, but it can be challenging to detect [8, 9]. Traditionally, TBI is diagnosed after a neurological exam coupled with imaging techniques like computerized tomography scans (CT) and magnetic resonance imaging (MRI) [7–9]. However, radiographic techniques may be insensitive to milder forms of TBI [10] due to the lack of macroscopic structural abnormalities [11, 12]. Without adequate symptom management and care, patients with m-TBI are at risk of developing more severe TBI upon subsequent insult to the head [9]. Moreover, even mild-to-moderate TBI can severely disrupt patients' physical, emotional, psychiatric, and cognitive health [4, 9], especially if left untreated. Thus, alternative or additional diagnostic techniques are needed to detect TBI in cases that might otherwise be overlooked [13].

Although TBI primarily affects the central nervous system (CNS), sensitive analytical techniques like GC-MS [14, 15] and LC-MS [14–16] can detect protein

biomarkers of TBI in easily accessible biological fluids [14, 17–19] like urine and plasma [11, 14, 20]. A sensitive test using urinary and plasma biomarkers could augment conventional tests with minimal additional cost or discomfort for the patient [19], this test could also be utilized in animal models of TBI to study the pathophysiologic progression and potential therapeutics of the disease. Additionally, when military personnel or emergency workers are exposed to a blast or concussive force, there is a dire need for a rapid, reliable test for TBI using biological samples that can be collected easily [14, 17, 19, 21] in the field. Individuals who sustain a TBI could be relieved from duty and provided with prompt medical attention, while uninjured individuals could quickly resume their normal duties.

To develop such a test, we selected a panel of small-molecule biomarkers that reflect critical biochemical pathways disrupted by TBI. TBI occurs in two stages, primary and secondary. Primary injury refers to the mechanical damage to the brain occurring immediately upon insult, which is usually irreversible [22, 23]. As the name implies, secondary injury encompasses the downstream effects of the primary injury that operate at a subcellular and biomolecular level, including ischemia, excitotoxicity, oxidative stress, blood-brain barrier disruption, intracranial hypotension, and apoptosis of neurons and glia [3, 4, 8, 24, 25] amongst others [22, 23, 26]. These secondary injury processes can drastically alter concentrations of certain metabolites in the CNS and systemically. Therefore, determination of these compounds in tissue or biological fluids may represent a promising approach for detecting and investigating m-TBI.

Recently, specific small molecules and proteins were identified as possible TBI biomarkers with potential diagnostic utility [10, 27–29]. Selected potential TBI

biomarkers in this study are shown in Table 1. *N*-acetyl aspartate (NAA) is the second most abundant small molecule in the brain after glutamate [30]. Although the mechanism is not fully understood, alterations in brain NAA levels have been linked to mild and moderate TBI [31] and other neurological disorders, like Alzheimer's and Huntington's diseases [10, 30], using analytical techniques like NMR [10, 30] and LC-MS [31]. Levels of the serotonin metabolite 5-hydroxyindoleacetic acid (5-HIAA) are reportedly affected by fluid percussion-induced moderate TBI [32]. In comatose TBI patients, higher than normal CSF concentrations of 5-HIAA may correlate with poorer outcomes [33, 34]. Glutathione (GSH) and its oxidized product, glutathione disulfide (GSSG), represent one of the most critical physiological redox couples. Relatively high levels of GSH compared to GSSG are essential for redox homeostasis in most healthy tissues, with lower GSH/GSSG ratios corresponding to oxidative stress in whole blood [35] and serum [36]. The lipid peroxidation byproducts 4-hydroxynonenal (4-HNE) and F2α-isoprostane (F2a) in urine, CSF, and serum [10, 27, 35] are also elevated following oxidative stress. Due to the high proportion of polyunsaturated fatty acids in the brain, increased levels of these compounds may indicate TBI [27, 35, 36].

Here, we developed two high-throughput, sensitive, selective, and robust LC-MS/MS methods that can detect and quantify the selected potential small-molecule TBI biomarkers in a wide array of biological samples, including urine, plasma, and brain tissue of rats subjected to open-field blast TBI. Monitoring these analytes in urine [28], in addition to plasma and brain, represents a novel approach to investigating TBI. Further, the newly developed methods can simultaneously determine all the analytes mentioned above, which was not possible using previously available methodology. Consequently,

researchers can conveniently monitor thiol redox status, lipid peroxidation byproducts, and neurotransmitter-related analytes at the same time. Thus, these methods will find wide application in animal models of TBI pathology and treatment, and potentially in human studies investigating urine and plasma markers.

Table 1. List of the analytes and the name of pathways of their involvement or significance.

Analyte	Abbreviation	Molecular Structure	Metabolic pathway or significance
N-acetylaspartic acid	NAA	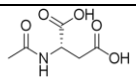	Aspartate
5-hydroxyindoleacetic acid	5-HIAA	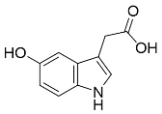	Serotonin Metabolite
8-isoprostanglandin	F2a	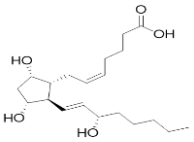	Lipid peroxidation
4-hydroxynonenal	4-HNE	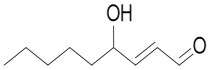	Lipid peroxidation
Glutathione	GSH	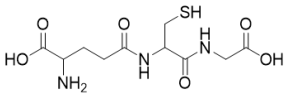	Antioxidant
Glutathione disulfide	GSSG	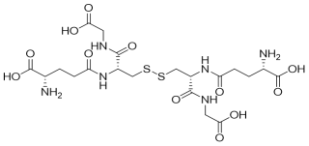	Oxidized GSH
Creatinine	CRT	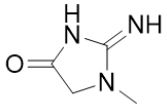	Hydration-dilution Correction

2. MATERIALS AND METHODS

2.1. CHEMICALS AND REAGENTS

Analytical grade standards of butylated hydroxy toluene (BHT), creatinine (CRT), glutathione disulfide (GSSG), glutathione (GSH), and *N*-acetyl aspartic acid (NAA) were

purchased from Sigma-Aldrich (St. Louis, MO, USA). An analytical grade standard of 5-hydroxyindoleacetic acid (5-HIAA) was purchased from Acros Organics (Fair Lawn, NJ, USA). 4-hydroxynonenal (4-HNE) and F2α-isoprostane (F2a) prepared in MeOAc were purchased from Cayman Chemicals, (Ann Arbor, MI, USA). Isotopically labelled compounds were used as internal standards (ISs). Glutathione-(glycine-$^{13}C_2$, ^{15}N) (GSH-IS) was purchased from Sigma-Aldrich (St. Louis, MO, USA), glutathione disulfide-(glycine-$^{13}C_2$, ^{15}N, GSSG-IS) was purchased from Cambridge Isotopes Laboratories (Tewksbury, MA, USA) while *N*-acetyl aspartic acid-D_3 (NAA-IS) was purchased from CDN Isotopes (Pointe-Claire, Quebec, CA). Creatinine-D_3 (CRT-IS) and F2α-isoprostane-D_4 (F2a-IS) prepared in MeOAc were purchased from Cayman Chemicals (Ann Arbor, MI, USA). Analytical grade 5-hydroxyindoleacetic acid-D_5 (5-HIAA-IS) was purchased from Cerilliant (Round Rock, Texas, USA). LC-MS grade methanol (MeOH), acetonitrile (ACN), ethanol (EtOH), and Optima™ LC-MS grade Formic acid (FA) were purchased from Fisher Chemical (Hampton, NH, USA). Centrifugal filters (3k Da molecular weight cut-off) were purchased from VWR North America (Radnor, PA, USA). N-ethylmaleimide (NEM) was purchased from CHEM-IMPEX INT'L INC (Wood Dale, IL, USA). Ultrapure water was produced in-house using a Millipore Elix-3 purification system (Millipore, Billerica, MA, USA). Homogenization was done using a bullet blender tissue homogenizer (Next Advance, Troy, NY, USA).

2.2. STANDARD PREPARATION AND CALIBRATION PROCEDURE

CRT, NAA, NAA-IS, GSSG, GSH stock solutions (1 mg/mL), and CRT-IS, GSH-IS, GSSG-IS stock solution (10 mg/mL) were prepared in 50% (v/v) ACN in water.

5-HIAA (1 mg/mL) and 5-HIAA-IS (0.1 mg/mL) stock solutions were prepared in ACN and MeOH, respectively. Stock solutions of F2a (5 mg/mL), F2a-IS (0.1 mg/mL), and 4-HNE (10 mg/mL) were used to prepare working solutions. Working solutions and calibration standards for GSH, GSSG, CRT, 4-HNE and their corresponding internal standards were prepared in 0.01% FA aqueous solution. ACN 5% (v/v) aqueous solution was used to prepare working solutions for NAA, F2a, 5-HIAA and their corresponding internal standards. BHT stock solution of 10 mg/mL was prepared in pure ethanol, and 100 mM NEM stock solution used for GSH adduct was prepared in ultrapure water.

Calibration standards were prepared at concentrations of 0.5, 1, 2, 5, 10, 20, 50, 100, and 200 ng/mL for all analytes. Additional concentrations of 500, 1000, and 2000 ng/mL were prepared for CRT due to its high concentration in urine samples. Quality control standards were prepared at 5 ng/mL and 20 ng/mL for all analytes except CRT, for which 50 ng/mL and 200 ng/mL standards were prepared.

2.3. SAMPLE COLLECTION AND STORAGE

All animal procedures were approved by the Missouri S&T Animal Care and Use Committee. Fifteen-week-old healthy Fischer CDF male rats (Charles River) were used for all experiments described in this study. Animals were housed in a temperature- and humidity-controlled room with a 12-hr light-dark cycle at the Missouri S&T Animal Research Facility. Animals were allowed food (Purina Lab Diet rat chow) and water (municipal tap) ad libitum. Animals were deeply anesthetized via intraperitoneal injection of ketamine/xylazine. Urine was directly drawn from the bladder with slight pressure. Animals were euthanized by exsanguination via cardiac puncture. Blood was collected in

heparin-coated tubes and centrifuged (3000 g, 10 min; 4 °C) immediately to separate out plasma. Each urine or plasma sample was divided into two aliquots. Upon collection, 10 mg/mL BHT was added to one aliquot of each urine or plasma sample to give a final concentration of 200 µg/mL BHT. To the other aliquot of collected urine or plasma, 100 mM NEM was added (urine or plasma/NEM = 9:1, v/v), and the mixture was vortexed for a few seconds to form the stable GSH-NEM adduct. Whole brains were collected immediately following euthanasia. Stabilized urine, plasma, and brain samples were frozen immediately in liquid nitrogen and stored at -80 °C until analysis.

2.4. RAT MODEL OF OPEN-FIELD BLAST TBI

Twelve animals were divided into two groups: sham (n = 6) and b-TBI (n = 6). All animals were transported to the Experimental Mine facility at Missouri University of Science and Technology. The blast rats (b-TBI) group was subjected to an open-field explosive blast at 2.15 m from a 350 g charge of C4. No explosive was used for the sham group. Animals were anesthetized via ketamine/xylazine (80/12 mg/kg body weight, i.p.) prior to injury. On the 5th day after injury, animals were deeply anesthetized with ketamine/xylazine (i.p.), urine, plasma, and whole brains were collected as described above. The open-field blast model of TBI used here was developed and validated previously in rodents [37, 38].

2.5. SAMPLE PREPARATION FOR HPLC-ESI-MS/MS ANALYSIS

2.5.1. Urine Sample Preparation. Aliquot 1: The BHT-stabilized urine aliquots were used for the analysis of NAA, 5-HIAA, and F2a. After thawing, 10 µL of BHT-

stabilized urine was mixed with 20 µL internal standard mixture (consisting of 1 µg/mL of NAA-IS, 5-HIAA-IS, F2a-IS) and diluted with 970 µL of 5% ACN (v/v) aqueous solution for a 100-fold dilution. Diluted urine was passed through diluent-preconditioned centrifugal filters (13000g, 35 min) and directly used for HPLC-MS/MS analysis.

Aliquot 2: The NEM-derivatized urine aliquots were used for the analyses of GSH, GSSG, and CRT. After thawing, 10 µL of derivatized urine was mixed with 20 µL internal standard mixture (GSH-NEM-IS and GSSG-IS, 1 µg/mL; CRT-IS, 10 µg/mL) and diluted with 970 µL of 0.01% FA for a total 100-fold dilution from the original urine. After the same ultrafiltration procedure as described above, the 100-fold diluted sample was directly used for HPLC-MS/MS analysis of GSH and GSSG. Another 10-fold dilution with 0.01% FA was applied prior to analysis of CRT.

2.5.2. Plasma Sample Preparation. Aliquot 1: The BHT-stabilized plasma aliquots were used for the analysis of NAA, 5-HIAA, and F2a. Thawed BHT-stabilized plasma was diluted 20-fold by mixing 10 µL of sample, 20 µL of internal standard mixture (NAA-IS, 5-HIAA-IS, and F2a-IS, 200 ng/mL) and 170 µL of 5% ACN aqueous solution. Diluted samples were vortex mixed and passed through pre-conditioned centrifugal filters as described above and directly used for HPLC-MS/MS analysis.

Aliquot 2: The NEM-derivatized plasma aliquots were used for the analysis of GSH, GSSG and CRT. Plasma derivatized with NEM was diluted 100-fold and ultrafiltered as described for urine aliquot 2. GSH, GSSG and CRT were analyzed by HPLC-MS/MS without further dilution.

2.5.3. Brain Tissue Sample Preparation. Whole rat brains were gently rinsed with phosphate-buffered saline (pH 7.4) prepared in ultrapure water. Then, each whole

brain was crushed with a mortar and pestle under liquid N2 until a homogenous powder was obtained. Crushed brain tissue was then weighed into ~50 mg aliquots in microcentrifuge tubes. One aliquot was used to determine the dry weight of each brain [39], and the other aliquots were used immediately or stored at –80oC until analysis was conducted. For analysis, the crushed brain tissue was homogenized in BHT solution to extract the analytes into solution for HPLC-MS/MS analysis. About 50 mg of zirconium oxide beads (0.5 mm, Next Advance, Troy, NY) and 200 µL of 200 ug/ mL BHT in MQ: ACN (1:1) were added to the ~50 mg aliquots of crushed brain tissue in microcentrifuge tubes. Homogenization was accomplished using a Bullet Blender Storm (Next Advance) in a –20 ˚C freezer to keep samples cold. Samples were homogenized at speed 8 for two intervals of 3 minutes each. The resulting homogenate was then centrifuged at 10000g for 10 mins at 4 °C. Approximately 150 µL of supernatant was recovered after centrifugation, of which 90 µL was derivatized with 100 mM NEM (supernatant: NEM = 9:1, v/v). The derivatized supernatant was diluted by mixing 10 µL sample, 20 µL of internal standard mixture (GSH-NEM-IS, NAA-IS, and GSSG-IS, 9000 ng/mL; 5-HIAA-IS, F2a-IS, 900 ng/mL) and 870 µL of 5% ACN. Diluted samples were vortexed and passed through pre-conditioned centrifugal filters as described above and directly used for HPLC-MS/MS analysis of 5-HIAA, 4-HNE, and F2a thereafter. Another 10-fold dilution with 0.01% FA was made prior to the analysis of GSH-NEM, GSSG, NAA and CRT. Table S1 describes the dilution factors used for all analytes in different matrices. Figure. 1 describes a workflow from sample collection to HPLC-MS/MS analysis of brain tissue, plasma, and urine.

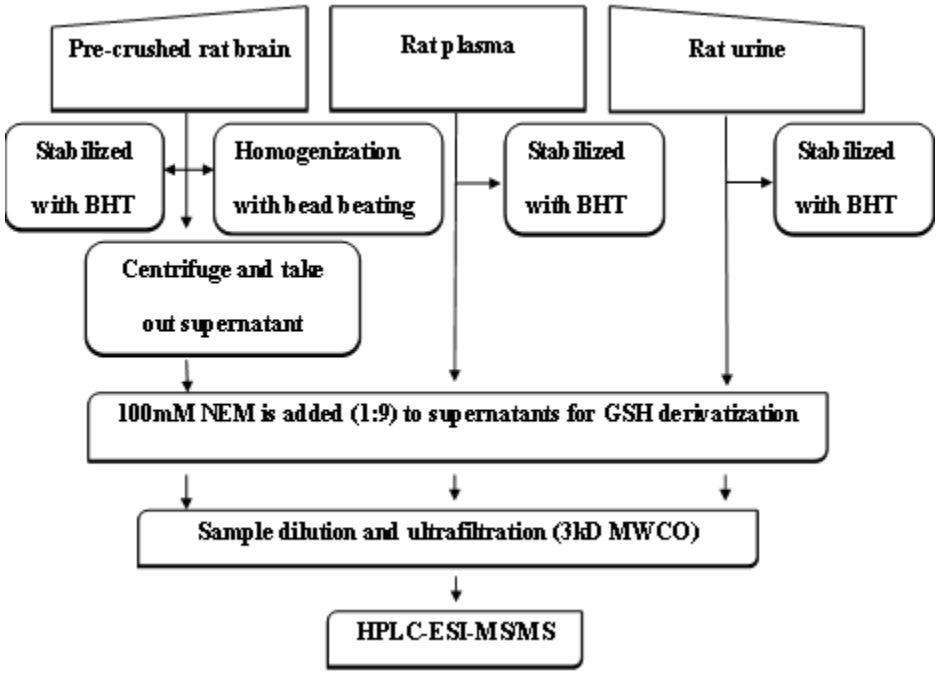

Figure. 1 Analysis procedure flow-chart for rat brain, plasma, and urine

2.6. HPLC-MS/MS METHOD

A Shimadzu (Columbia, MD, USA) Prominence UFLC system comprising an online degasser (DGU-30A3), two pumps (LC-20 AD XR), an autosampler (SIL-20AC XR), and a column oven (CTO-20A), connected to a 4000Q TRAP tandem mass spectrometer system (AB SCIEX, Concord, ON, CA) was used as described previously [28]. Analyst® Software was used for data acquisition and quantitation in this study. All analytes in this study were pre-tested using scan mode in both ionization modes (ESI+ and ESI-). The optimum mode for each analyte was selected based on ionization efficiency. ESI+ was used for GSH-NEM, GSSG, 4-HNE, and CRT while NAA, 5-HIAA and F2a were analyzed using ESI- mode. Ion-source parameters such as the ion source voltage, ion source temperature, curtain gas, and the ion source gas (GS1 and GS2) were determined using flow injection analysis (FIA) and are shown in ESI- (Ion spray voltage,

(-4500); Source Temp., (600 ^{o}C); Curtain gas (psi), (10); GS1 (psi), (30); GS2 (psi), (40)) and ESI+ (Ion spray voltage, (4500); Source Temp., (600 ^{o}C); Curtain gas (psi), (15); GS1 (psi), (40); GS2 (psi), (40).

For HPLC-MS/MS analysis of GSH-NEM, GSSG, 4-HNE, and CRT, chromatographic separation was achieved using a Synergi™ Hydro-RP column (250 × 2 mm, 4 μm, Phenomenex, CA, United States) equipped with a Phenomenex SecurityGaurd guard cartridge, and mobile phase was delivered at a binary flow rate of 0.3 mL/min. Mobile phase A was composed of 0.01 % formic acid in ultrapure water (v/v), and mobile phase B was composed of 0.01 % formic acid in ACN (v/v). The column oven temperature was set at 40 ˚C. Following a 20 μL injection, analytes were separated using the following gradient program: mobile phase composition started at 100% A for 1.0 min, decreased to 20% A from 1.0 to 7.0 min, remained at 20% A from 7.0 min to 9.5 min, and then switched back to 100% A from 9.5 min to 10.5 min. The system was allowed to re-equilibrate for 4.5 min at 100% A before the subsequent injection. For MS/MS detection, scheduled multiple reaction monitoring (SMRM) was used, in which mass transitions were monitored within a 1-min window of the retention time of each analyte. SMRM was used in the ESI+ method specifically to enhance GSSG MS detection sensitivity.

For HPLC-MS/MS analysis of NAA, 5-HIAA and F2a, chromatographic separation was achieved using a Synergi™ Hydro-RP column (150 × 2 mm, 4 μm, Phenomenex, CA, United States) equipped with a Phenomenex SecurityGaurd guard cartridge, and mobile phase was delivered at a binary flow rate of 0.3 mL/min. Mobile phase A was composed of 0.1 % formic acid in ultrapure water (v/v), and mobile phase B

was composed of 0.1% formic acid in ACN (v/v). Binary flow rate, column oven temperature, and injection volume remained the same as described above for the ESI+ method. The method began with a pre-run equilibration of 4 min at 100% A and continued with 100% A after sample injection for first 2 min, followed by a linear gradient increase to 100% B from 2.0 to 8.0 min. After being held at 100% B from 8.0 to 10.0 min, it was finally changed back to 100% A from 10.0 to 10.5 min, followed by re-equilibration at 100% A for 4 min before the next injection. Normal multiple reaction monitoring (MRM) was used for MS/MS detection in ESI- mode.

2.7. DATA ANALYSIS

Data is represented as the mean ± SEM (standard error of the mean) of 4-6 animals. Student's t-tests were used to compare mean biomarker levels between groups (blast vs. sham). Values of $p < 0.05$ were considered statistically significant for analyses discussed here.

3. RESULTS AND DISCUSSION

3.1. OPTIMIZATION OF MASS PARAMETERS AND HPLC MOBILE PHASE

Mass optimization was conducted using direct infusion of analytical standards with a Harvard Apparatus Pump 11 Elite (Holliston, MA, USA) syringe pump operated at 0.6 mL/hr. The upper limits of the precursor ion scans (Q1) for each analyte were set to 150 m/z above the theoretical mass to monitor any formation of possible adduct ions, of which none was found. All analytes formed singly charged ions with the Q1 scans, except for GSSG which formed an extra doubly-charged ion in the ESI+ mode, as previously observed by Wu et al [40]. Product ions and corresponding decluttering potential (DP),

collision energy (CE), collision cell exit potential (CXP) were optimized using "compound optimization" function of Analyst® Software. The optimized MS/MS parameters are shown in Table 2. Additionally, it was also found that the concentration of formic acid influenced signal intensity. For analytes in ESI- mode, optimal sensitivity was achieved with 0.1% formic acid, and for analytes in ESI+ mode, a lower concentration of 0.01% formic acid gave better performance. The optimum concentration of formic acid from direct infusion was further applied in LC mobile phases.

Table 2. MS/MS parameters of standards. DP, declustering potential; CE, collision energy; CXP, collision cell exit potential. (Q), quantitation ion pair; (C), confirmation ion pair.

ESI Mode	Analyte	Ion Pairs (m/z)	(DP, V)	(CE, V)	(CXP, V)
ESI-	NAA	**(Q)** 174.1/88.3	-40	-22	-3
		(C) 174.1/58.3	-40	-30	-7
	5-HIAA	**(Q)** 190.1/146.2	-50	-16	-7
		(C) 190.1/144.3	-50	-28	-7
	F2a	**(Q)** 353.2/193.1	-95	-36	-11
		(C) 353.2/309.2	-95	-28	-7
	NAA-IS	**(Q)** 177.0/91.3	-50	-24	-3
		(C) 177.0/133.3	-50	-18	-7
	5 HIAA-IS	**(Q)** 195.0/151.2	-50	-16	-9
		(C) 195.0/148.3	-50	-30	-7
	F2a-IS	**(Q)** 357.4/197.5	-95	-36	-11
		(C) 357.4/313.6	-95	-28	-7
ESI+	4-HNE	**(Q)** 157.1/138.9	+36	+15	+4
		(C) 157.1/54.9	+36	+31	+4
	GSH-NEM	**(Q)**433.2/304.1	+46	+20	+20
		(C)433.2/201.1	+46	+30	+20
	GSSG	**(Q)**613.2/355.2	+91	+30	+11
		(C)613.2/231.0	+91	+49	+14
	CRT	**(Q)**114.0/43.9	+56	+29	+6
		(C)114.0/85.8	+56	+17	+6
	GSH-NEM-IS	**(Q)** 436.0/307.0	+61	+21	+10
		(C) 436.0/201.0	+61	+31	+12
	GSSG-IS	**(Q)** 619.2/360.9	+20	+30	+11
		(C) 619.2/231.1	+20	+49	+14
	CRT-IS	**(Q)** 117.0/47.0	+26	+27	+14
		(C) 117.0/43.0	+26	+45	+8

3.2. HPLC-MS/MS METHOD VALIDATION

Performance characteristics for the optimized methods are shown in Table 3. Overlaid extracted ion chromatograms from standard mixtures and real samples are shown in Figure 2. The methods exhibited good sensitivity with detection limits (LOD, S/N ≥ 3) of 0.5 ng/mL for most investigated analytes, except 4-HNE and GSSG which were at 5 ng/mL and 1 ng/mL respectively. Limits of quantitation (LOQ, S/N ≥ 10) for these methods were also found to be slightly improved or comparable to extant analytical methods that have been used to investigate these analytes previously [28, 40]. Analyte calibration curves were linear within the concentration range as shown in Table 3 with all R2 values (regression coefficient) greater than 0.99. The linearity was not investigated beyond the range given.

Table 3. HPLC-MS/MS method performance.

Analyte	ESI Mode	RT (min)	LOD (ng/mL)	Linear range (ng/mL)	R^2
NAA	ESI-	1.8	0.5	0.5-500	0.9976
5-HIAA		5.6	0.5	0.5-500	0.9996
F2a		7.1	0.1	0.5-100	0.9946
4-HNE	ESI+	8.7	5.0	5-500	0.9981
GSH-NEM		5.7	0.5	0.5-500	0.9996
GSSG		5.5	1.0	1-500	0.9997
CRT		2.3	0.5	0.5-2000	0.9982

Spike recovery studies were performed at two levels (low and high) for each analyte in each matrix. As show in Table 4, the recovery of all analytes ranged from 86 % to 122% in urine, 75.4% to 113% in plasma, and 78% to 119% in whole brain tissue,

except for one spiked urine sample with 130% recovery for CRT, possibly due to the analyte's high native concentration in urine.

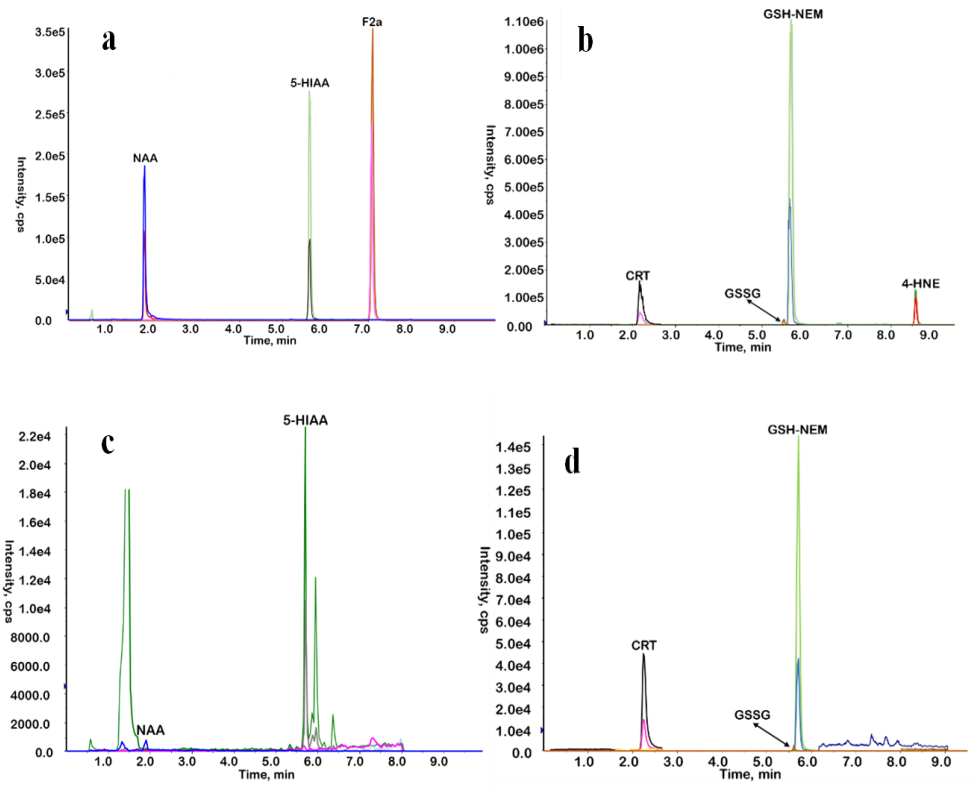

Figure 2. Representative overlaid XIC of a)100 ng/mL standard mixture in the ESI- method, b) 100 ng/mL standard mixture in the ESI+ method, c) urinary analytes in the ESI- method, d) plasma analytes in the ESI+ method.

Percent RSD for spike recovery experiments ranged from 1.4% to 15% in urine, 3.7% to 19% in plasma, and 1.4% to 10% in brain homogenate. This further confirms that both the ESI+ and ESI- methods performed accurately and reproducibly. Concentrations used for spike recovery are depicted in Table S2.

Table 4. Spike recovery and relative standard deviation (recovery% ± RSD%, n =3). Detailed spike levels for different types of samples are shown in Table S2.

Analyte	Spike level	Urine % Recovery ± %RSD (n=3)	Plasma % Recovery ± %RSD (n=3)	Brain %Recovery ± %RSD (n=3)
NAA	Low	106 ± 8.7	75.4 ± 14.9	104.1 ± 6.0
	High	93.2 ± 7.5	83.4 ± 9.6	99.1 ± 4.0
5-HIAA	Low	102.6 ± 15.2	108.1 ± 15.7	97.1 ± 5.7
	High	107.4 ± 6.0	97.7 ± 16.7	87.5 ± 4.9
F2a	Low	83.9 ± 6.1	109.3 ± 6.7	113.4 ± 1.4
	High	82.8 ± 10	100.9 ± 4.3	102.3 ± 3.2
4-HNE	Low	not applied	not applied	78.0 ± 2.4
	High	not applied	not applied	78.0 ± 4.0
GSH-NEM	Low	99.0 ± 4.34	87.0 ± 17.6	90.2 ± 2.9
	High	102.4 ± 2.2	95.0 ± 3.7	118.2 ± 10.7
GSSG	Low	102.8 ± 13.0	113.0 ± 19.2	119.0 ± 3.1
	High	93.6 ± 8.0	112.0 ± 14.0	111.9 ± 2.6
CRT	Low	122.7 ± 8.3	99 ± 13.3	not applied
	High	130.7 ± 1.4	101.0 ± 9.3	not applied

3.3. STABILIZATION WITH ANTIOXIDANT BHT AND DERIVATIZATION OF THIOLS

In the extant literature, antioxidants such as tocopherol, sodium metabisulfite, and BHT were used to stabilize oxidation-prone analytes in biological samples [4, 41]. Oxidative stress plays an important role in the pathogenesis of TBI, and changes in levels of redox-active markers may be key indicators that a TBI has occurred. Following TBI,

increased levels of reactive species deplete endogenous antioxidants such as GSH, leaving polyunsaturated fatty acids and other biomolecules vulnerable to oxidative damage. As a result, byproducts of these reactions, such as GSSG, 4HNE, and F2a, may be elevated in the affected CNS tissues and systemically [22, 42]. Thus, these oxidative stress markers were investigated as potential biomarkers of TBI for this study. However, oxidation can occur in tissue samples under improper storage and processing conditions, resulting in artifactually increased levels of oxidative stress biomarkers. Therefore, steps were taken to prevent oxidation in tissue samples after collection. To determine lipid peroxidation byproducts 4HNE and F2a, BHT was added to prevent further lipid peroxidation between sample collection and analysis. BHT is a lipid-soluble chain-breaking antioxidant that has been employed to prevent lipid peroxidation [43] in numerous biological matrices, including zebrafish tissue [44], plasma [41, 44, 45], urine [41], and canola oil [46].

The ratio of GSH to GSSG is another critical indicator of tissue redox status, with levels of GSH exceeding GSSG levels by a significant factor in most healthy tissues [47]. Thus, oxidation of only a small fraction of free GSH can drastically impact the GSH/GSSG ratio. Therefore, it is critically important to prevent oxidation of GSH during sample manipulation. This can be accomplished by blocking the free thiol group to form a stable derivative suitable for long-term storage, sample preparation, and analysis. In a relatively simple matrix like tear fluid, oxidation of free thiols may be negligible under appropriate conditions [40]. In contrast, free thiols in more complex matrices like urine, plasma, serum, and tissue may undergo significant and rapid oxidation during routine sample preparation and handling. Consequently, the determination of GSH and GSSG in

these matrices may necessitate derivatization of free thiols with agents such as NEM [48–50], 2-vinylpyridine [48, 51], or iodoacetic acid [49, 51] to prevent artifactual oxidation [48]. Out of these, NEM exhibits the fastest reaction time with free thiols, and it does not need to be removed from the sample prior to analysis, hence its widespread use as a derivatization agent in chromatographic and mass spectrometry analysis [48–50] and its incorporation into the method was described here. In preliminary experiments, we did not derivatize urine, plasma, and brain tissue, and we observed a higher GSSG concentration than GSH. Also, GSSG levels increased chronologically as GSH levels decreased, which was an indication that GSH was susceptible to oxidization prior to analysis. Others have noted the artifactual oxidation of GSH [50], which was conveniently remedied by derivatization of the free thiols with a maleimide. Ultimately, stabilization of sample matrix with BHT and derivatization of free thiols substantially improved the accuracy and reproducibility of the method by eliminating the extraneous effects of oxidation on analyte concentrations after sample collection.

3.4. QUANTITATION OF NATIVE CONCENTRATIONS OF POTENTIAL TBI BIOMARKERS IN RAT SAMPLE

Natural concentrations of analytes (Table 5) in rat urine, plasma, and brain tissue were determined using samples collected from healthy rats and subsequently accounting for matrix effects through spike recovery tests on the same samples to ensure accuracy and precision of the detected concentrations. This was necessary to optimize dilutions and sample preparation for each analyte and their collective determination in healthy and diseased samples. However, the concentrations of F2a and 4-HNE were less than the LOD even at dilutions as low as 5-fold. Although matrix effects increased, these less

diluted samples were prepared to detect F2a and 4-HNE for qualitative purposes. Native concentrations of NAA (brain tissue [52, 53] and plasma [52]), 5-HIAA (urine [54, 55], plasma [56], and brain tissue [57–60]), and CRT (urine [61, 62] and plasma [63]) were in agreement with extant literature values. The GSH/GSSG ratio was also within an acceptable range for healthy rat biological samples [64, 65]. To the best of our knowledge, this study was the first to report native NAA concentrations in rat urine.

Optional hydration-dilution correction of analyte concentrations was employed in this study, and it can be done by urine specific gravity (USG) determination or urinary creatinine [66, 67]. However, USG correction requires a sample volume that was impractical for this study. Creatinine correction allows for hydration correction regardless of sample volume because it can be determined alongside the target analytes using HPLC-MS/MS in the same sample. Therefore, creatinine correction was used for hydration dilution correction in urine and plasma samples collected from healthy rats as shown in Table 5. For brain tissues, concentration of analytes was represented as w/w (analyte (ng)/mg of wet tissue).

3.5. ANALYSIS OF BIOLOGICAL MATRICES FROM TBI RAT MODELS

To test the real-world performance of the newly developed HPLC-MS/MS methods, urine, plasma, and brain tissue were obtained from rats subjected to open-field blast injury as described above. Biomarker levels in b-TBI animals were then compared to those from sham-injured animals. Statistical analyses indicated several significant differences between sham and blast-exposed animals, although the concentrations of 4-HNE and F2a were below the LOD in all samples,

Table 5. Native concentrations of analytes in rat urine, plasma, and brain (n =3).

Unnormalized Values			
Analyte	Urine (ng/mL) Mean ± SD	Plasma (ng/mL) Mean ± SD	Brain Tissue (ng/mg of wet tissue) Mean ± SD
NAA	3102 ± 268.6	68 ± 2.9	1062 ± 82.5
5-HIAA	4772 ± 171.3	38 ± 2.1	3.3 ± 0.2
F2a	< 0.5	<0.5	< 0.2
4-HNE	not analyzed	not analyzed	< 2.0
GSH	208 ± 31.7	6608 ± 995.6	300 ± 10.9
GSSG	62 ± 6.0	841 ± 128.6	32.8 ± 3.3
CRT	560,000 ± 109,600	3000 ± 76.3	not analyzed
Creatinine Normalized values			
Analyte	Urine ng/mg CRT Mean ± SD		Plasma ng/mg CRT Mean ± SD
NAA	5.0 ± 0.66		21.9 ± 1.97
5-HIAA	7.2 ± 0.27		12.2 ± 0.77
GSH	0.4 ± 0.09		2164 ± 367.50
GSSG	0.1 ± 0.03		280.2 ± 51.00

In urine, NAA and 5-HIAA were significantly elevated in blast-exposed animals compared to controls ($p < 0.05$). In plasma, the opposite effect was observed for 5-HIAA ($p < 0.01$) which was significantly lower in blast-exposed animals. Plasma NAA was slightly decreased in the b-TBI group, but it was not significantly different from the sham group ($p > 0.05$). No significant differences in NAA or 5-HIAA levels were noted in brain tissue. For GSH-NEM, GSSG, and GSH/GSSG, no significant differences between sham and blast-exposed animals were observed in urine or plasma. However, brain tissue exhibited key changes in the levels of these redox status biomarkers. Most notably, GSH levels were significantly decreased in the blast-exposed group compared to the sham group ($p < 0.05$). Changes in GSH concentration are closely linked to the excitotoxic

processes following initial insult [67]; the ability to monitor these changes is thus highly advantageous for application of this method in TBI models [47, 68, 69]. Neither GSSG nor GSH/GSSG changed appreciably in brain tissue under the blast conditions reported here ($p > 0.05$).

Upon comparison, b-TBI-related changes in biomarker profiles differ substantially between the biomatrix studied. Urine and plasma NAA and 5-HIAA varied significantly between TBI and sham groups, but not in the brain. Only changes of GSH were evident in brain tissue. The apparent discrepancies may be explained in terms of blood-brain barrier (BBB) dysregulation resulting from closed-head blast injury [70]. The permeability of the BBB is tightly controlled by neurovascular endothelial cells connected to each other with tight junction proteins. Even when macroscopic physical damage to the BBB is minimal, ROS generated during secondary injury processes activate matrix metalloproteinases that damage tight junction proteins between the endothelial cells of the BBB [71]. This results in an extended period of increased BBB permeability for efflux of small molecules like NAA and 5-HIAA [14, 70, 72–74] into peripheral fluids. Thus, elevated NAA and 5-HIAA may be present in peripheral fluids after recovery of normal homeostatic control in the brain. It is interesting to note that increased levels of NAA and 5-HIAA were observed in urine but not plasma at 5 days post-blast. However, several studies report that TBI biomarker concentrations tend to peak in urine at later time points than in plasma [12]. Further studies are necessary to elucidate the time course of the selected biomarkers post-injury. In contrast to NAA and 5-HIAA post-injury, passive efflux of GSH through the BBB is negligible in healthy

controls, and therefore elevated brain GSH levels in these individuals may not be reflected in urine or plasma levels.

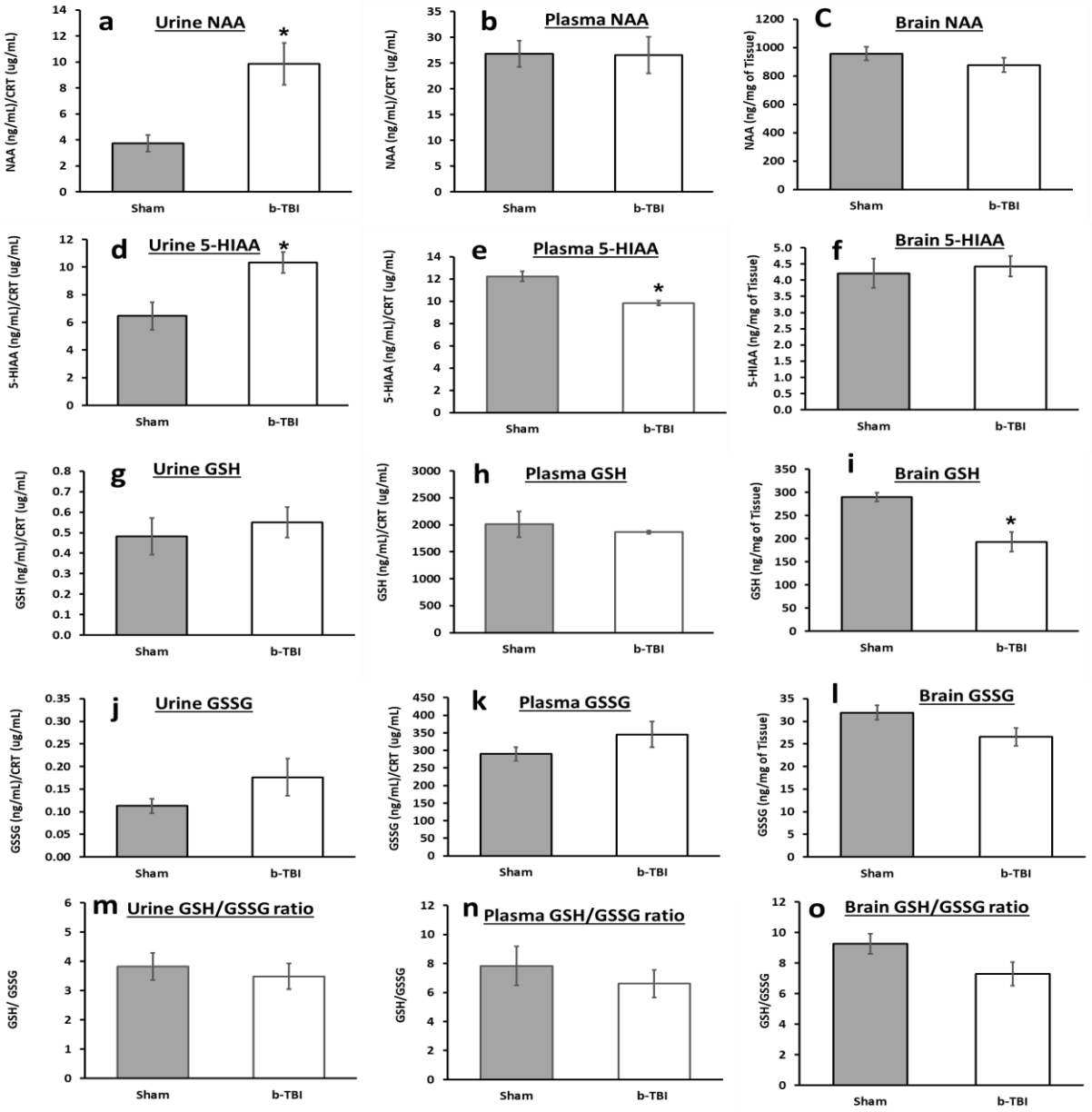

Figure 3. Comparison of normalized analyte concentrations in sham and b-TBI groups. Columns represent the mean ± SEM of 4-6 animals. NAA in (a) urine, (b) plasma, (c) brain; 5-HIAA in (d) urine, (e) plasma, (f) brain; GSH in (g) urine, (h) plasma, (i) brain tissue; GSSG in (j) urine, (k) plasma, (l) brain tissue; GSH/GSSG in (m) urine, (n) plasma, (o) brain tissue. * $p < 0.05$.

Increased GSSG after TBI was observed in other studies but was not detected on this timescale [69]. It is possible that elevated GSSG was present in b-TBI animals at earlier time points in the study and thus not observable in samples taken 5 days after the blast.

Creatinine-normalized plots and data for the test groups are shown in Figure 3 and Table 6, respectively. Analysis of uncorrected urine concentrations indicated significant differences between b-TBI and sham groups for GSH-NEM and 5-HIAA levels, but no significant differences were noted in plasma. Figure S1 and Table S3 report values and column plots.

Table 6. Potential biomarker levels (mean ± SD) in rat urine, plasma, and brain homogenate for sham rats and b-TBI rats.

Biological Matrix	Biomarker	Sham	b-TBI	*P*
Urine	NAA§	3.7 ± 1.6	9.9 ± 3.6	***0.02****
	5-HIAA§	6.5 ± 2.4	10.3 ± 1.7	***0.02****
	GSH§	0.5 ±0.2	0.6 ± 0.2	0.6
	GSSG§	0.1 ± 0.03	0.2 ± 0.09	0.2
	GSH/GSSG	3.8 ± 1.0	3.5 ± 1.3	0.6
Plasma	NAA§	26.8 ± 5.7	26.5 ± 7.1	0.9
	5-HIAA§	12.2 ± 1.0	9.8 ± 0.4	***0.006****
	GSH§	2011.7 ±583.6	1863.8 ± 56.7	0.6
	GSSG§	289.8 ± 43.7	345.4 ± 82.5	0.2
	GSH/GSSG	7.8 ± 2.7	6.6 ± 1.9	0.5
Brain	NAA†	249.3 ± 24.8	235.1 ± 33.5	0.3
	5-HIAA†	1.1 ± 0.3	1.2 ± 0.2	0.6
	GSH†	75.9 ± 7.9	51.77 ± 13.3	***0.01****
	GSSG†	8.3 ± 0.9	7.1 ± 1.19	0.09
	GSH/GSSG	9.3 ± 1.6	7.3 ± 1.7	0.1

§ Normalized with CRT, ng/µg CRT
†ng/mg of wet tissue

4. CONCLUSION

In this study, two HPLC-MS/MS methods were developed and validated for plasma, urine, and brain tissue analyses. Stabilization and derivatization steps were incorporated to facilitate accurate determination of oxidatively labile analytes in complex matrices. Additionally, native concentrations for most of the analytes were successfully measured in these biological samples, including NAA in rat urine that had not yet been reported to the best of our knowledge. Finally, a proof-of-concept study demonstrated that the methods were sufficiently sensitive and reliable for quantitation of analytes in blast-exposed and sham-injured rats. The analytical methods and subsequent statistical treatment revealed significant differences between blast-exposed and sham groups, particularly with respect to NAA and 5-HIAA in urine and plasma as well as GSH levels in the brain. Such changes likely indicate dysregulated neurotransmission and redox status in animals exposed to blast TBI. Based on these results, the HPLC-MS/MS methods developed here may find broad application in investigations of potential therapeutics or diagnostic approaches.

ACKNOWLEDGEMENTS AND FUNDING INFORMATION

This study was supported by the Leonard Wood Institute through a cooperative agreement with the US Army Research Laboratory (W911NF-14-2-0034). The Acute Effects of Neurotrauma Consortium also facilitated this research. The views and conclusions contained in this document are those of the authors and should not be interpreted as representing the official policies, either expressed or implied, of the

CONFLICT OF INTEREST

The authors declare the absence of conflicts of interest financially or in any other capacity.

CREDIT AUTHORSHIP CONTRIBUTION STATEMENT

Olajide Adetunji: Investigation, Methodology, Validation, Writing- original draft preparation.

Jiandong Wu: Investigation, Methodology, Validation, Editing.

Annalise Pfaff: Visualization, Writing – review & editing.

Austin Sigler: Data curation, Methodology.

Mousumi Bose: Formal analysis.

Catherine Johnson: Conceptualization, Supervision, Funding acquisition.

Nuran Ercal: Conceptualization, Supervision, Funding acquisition, Writing – review & editing.

Honglan Shi: Conceptualization, Supervision, Funding acquisition, Writing – review & editing.

Paul Nam: Conceptualization, Supervision, Funding acquisition, Writing – review & editing.

LIST OF ABBREVIATIONS

CNS- Central Nervous System

CSF- Cerebrospinal Fluid

BHT- Butylated Hydroxy Toluene

NEM- N-Ethyl maleimide

GSH- Glutathione-reduced

GSSG- Glutathione-oxidized

F2a- 8-Isoprotanglandin

5 HIAA- 5-Hydroxyindoleacetic acid

4-HNE- 4-Hydroxynonenal

IS- Internal Standard

TBI-Traumatic Brain Injury

NAA- *N*-acetyl aspartic acid

CRT- Creatinine

SUPPLEMENTARY INFORMATION

Table S1. Dilution factor of metabolites in urine, plasma, and brain tissue.

Table S2. Spiked concentrations for spike recovery test.

Figure S.1 Comparison of unnormalized analyte concentrations in sham and b-TBI groups. Columns represent the mean ± SEM of 4-6 animals. NAA in (a) urine, (b) plasma; 5-HIAA in (c) urine, (d) plasma; GSH in (e) urine, (f) plasma; GSSG in (g) urine, (h) plasma; GSH/GSSG in (i) urine, (j) plasma. *Significant at $p < 0.05$

Table S3. Mean ± SD of analytes in rat urine, plasma, and brain homogenate for sham rats and TBI rats.

Table S1. Dilution factor of metabolites in urine, plasma, and brain tissue.

Sample Matrix	NAA	5-HIAA	F2a	GSH-NEM	GSSG	CRT	4-HNE
Urine	100x	100x	100x	100x	100x	1000x	-
Plasma	20x	20x	20x	100x	100x	100x	-
Brain Homogenate	1000x	100x	20x	1000x	1000x	N/A	20x

Table S2. Spiked concentrations for spike recovery test.

Analyte	Spike level	Urine (ng/mL)	Plasma (ng/mL)	Brain (ng/mL)
NAA	Low	20	10	50
	High	50	50	200
5-HIAA	Low	20	5	5
	High	50	20	20
F2a	Low	20	10	5
	High	50	50	20
4-HNE	Low	not applied	not applied	5
	High	not applied	not applied	20

Table S2. Spiked concentrations for spike recovery test. (Cont.)

Analyte	Spike level	Urine (ng/mL)	Plasma (ng/mL)	Brain (ng/mL)
GSH-NEM	Low	5	5	50
	High	20	10	200
GSSG	Low	5	5	5
	High	20	10	20
CRT	Low	200	5	not applied
	High	500	10	not applied

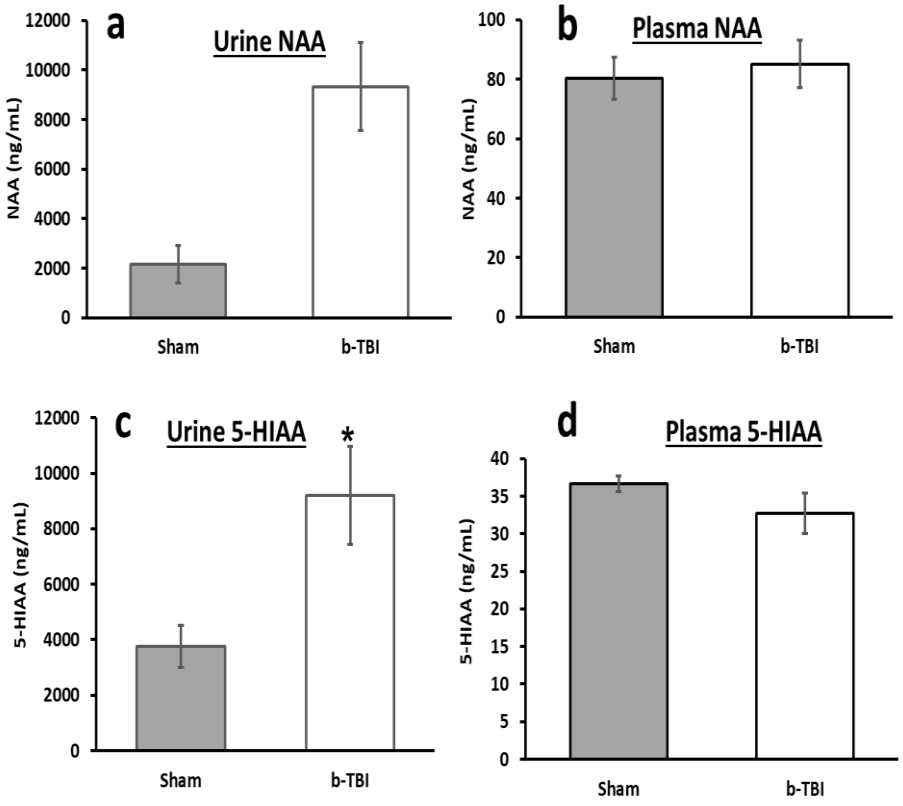

Figure S.1 Comparison of unnormalized analyte concentrations in sham and b-TBI groups. Columns represent the mean ± SEM of 4-6 animals. NAA in (a) urine, (b) plasma; 5-HIAA in (c) urine, (d) plasma; GSH in (e) urine, (f) plasma; GSSG in (g) urine, (h) plasma; GSH/GSSG in (i) urine, (j) plasma. *Significant at $p < 0.05$

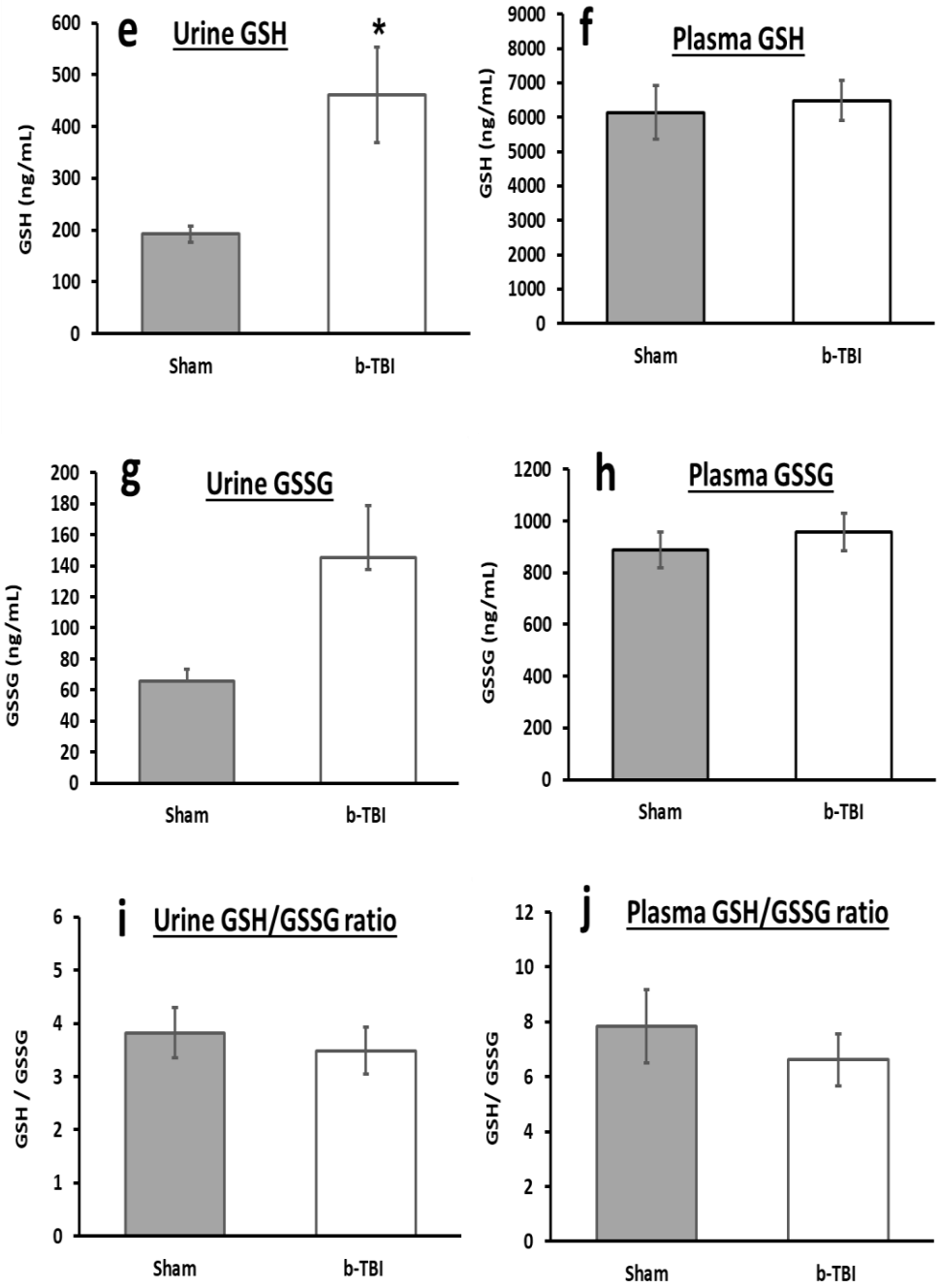

Figure S.1 Comparison of unnormalized analyte concentrations in sham and b-TBI groups. Columns represent the mean ± SEM of 4-6 animals. NAA in (a) urine, (b) plasma; 5-HIAA in (c) urine, (d) plasma; GSH in (e) urine, (f) plasma; GSSG in (g) urine, (h) plasma; GSH/GSSG in (i) urine, (j) plasma. *Significant at $p < 0.05$. (Cont.)

Table S3. Mean ± SD of analytes in rat urine, plasma, and brain homogenate for sham rats and TBI rats.

Biological Matrix	Biomarker	Sham	TBI	*P*
Urine	NAA§	2150.3 ± 1077.8	9322.6 ± 5709.4	0.06
	5-HIAA§	3767.4 ±1860.1	9202.7 ± 3946.8	***0.04****
	GSH-NEM§	192.2 ± 35.6	461.4 ± 205.3	***0.04****
	GSSG§	65.6 ±19.3	145.3 ± 13.0	0.08
	GSH/GSSG	3.8 ± 1.0	3.5 ± 1.3	0.6
Plasma	NAA§	80.26 ± 15.8	85.14 ±15.9	0.7
	5-HIAA§	36.7 ± 2.3	32.8 ± 5.3	0.1
	GSH-NEM§	6136.8 ± 1895.8	6479.6 ±1309.2	0.7
	GSSG§	888.4 ±156.5	956.22 ±144.2	0.5
	GSH/GSSG	7.8 ± 2.7	6.6 ± 1.9	0.5
Brain	NAA†	249.3 ± 24.8	235.1 ± 33.5	0.3
	5-HIAA†	1.1 ± 0.3	1.2 ± 0.2	0.6
	GSH-NEM†	75.9 ± 7.9	51.77 ± 13.3	***0.01****
	GSSG†	8.3 ± 0.9	7.1 ± 1.19	0.09
	GSH/GSSG	9.3 ± 1.6	7.3 ± 1.7	0.1

§ Normalized with CRT, ng/µg CRT
† ng /mg of wet tissue

REFERENCES

1. Coronado VG, McGuire LC, Sarmiento K, Bell J, Lionbarger MR, Jones CD, Geller AI, Khoury N, Xu L (2012) Trends in Traumatic Brain Injury in the U.S. and the public health response: 1995-2009. J Safety Res 43:299–307. https://doi.org/10.1016/j.jsr.2012.08.011

2. Daugherty J, Waltzman D, Sarmiento K, Xu L (2019) Traumatic Brain Injury – Related Deaths by Race / Ethnicity , Sex , Intent , and Mechanism of Injury — United States , 2000 – 2017. 68:1050–1056

3. Ng SY, Lee AYW (2019) Traumatic Brain Injuries: Pathophysiology and Potential Therapeutic Targets. Front Cell Neurosci 13:1–23. https://doi.org/10.3389/fncel.2019.00528

4. Khatri N, Thakur M, Pareek V, Kumar S, Sharma S, Datusalia AK (2018) Oxidative Stress: Major Threat in Traumatic Brain Injury. CNS Neurol Disord - Drug Targets 17:689–695. https://doi.org/10.2174/1871527317666180627120501

5. Hoffer ME, Balaban C, Slade MD, Tsao JW, Hoffer B (2013) Amelioration of Acute Sequelae of Blast Induced Mild Traumatic Brain Injury by N-Acetyl Cysteine: A Double-Blind, Placebo Controlled Study. PLoS One 8:1–10. https://doi.org/10.1371/journal.pone.0054163

6. Champion HR, Holcomb JB, Young LA (2009) Injuries from explosions: Physics, biophysics, pathology, and required research focus. J Trauma - Inj Infect Crit Care 66:1468–1477. https://doi.org/10.1097/TA.0b013e3181a27e7f

7. Su Eric BM Diffuse Axonal Injury. In: Laskowitz D, Grant G, editors. Translational Research in Traumatic Brain Injury. Boca Raton (FL): CRC Press/Taylor and Francis Group; 2016. Chapter 3. Available from: https://www.ncbi.nlm.nih.gov/books/NBK326722/

8. Bramlett HM, Dietrich WD (2015) Long-Term Consequences of Traumatic Brain Injury: Current Status of Potential Mechanisms of Injury and Neurological Outcomes. J Neurotrauma 32:1834–1848. https://doi.org/10.1089/neu.2014.3352

9. Maas AIR, Menon DK, David Adelson PD, Andelic N, Bell MJ, Belli A, Bragge P, *et al.*, (2017) Traumatic brain injury: Integrated approaches to improve prevention, clinical care, and research. Lancet Neurol 16:987–1048. https://doi.org/10.1016/S1474-4422(17)30371-X

10. Sharma R, Laskowitz DT (2012) Biomarkers in traumatic brain injury. Curr Neurol Neurosci Rep 12:560–569. https://doi.org/10.1007/s11910-012-0301-8

11. Kulbe JR, Geddes JW (2016) Current status of fluid biomarkers in mild traumatic brain injury. Exp Neurol 275:334–352. https://doi.org/10.1016/j.expneurol.2015.05.004

12. Adrian H, Mårten K, Salla N, Lasse V (2016) Disorders of the Nervous System Biomarkers of Traumatic Brain Injury: Temporal Changes in Body Fluids. eNeuro 3:1–13

13. Banoei MM, Casault C, Metwaly SM, Winston BW (2018) Metabolomics and Biomarker Discovery in Traumatic Brain Injury. J Neurotrauma 35:1831–1848. https://doi.org/10.1089/neu.2017.5326

14. Ottens AK, Stafflinger JE, Griffin HE, Kunz RD, Cifu DX, Niemeier JP (2014) Post-acute brain injury urinary signature: A new resource for molecular diagnostics. J Neurotrauma 31:782–788. https://doi.org/10.1089/neu.2013.3116

15. Dumas ME, Davidovic L (2015) Metabolic Profiling and Phenotyping of Central Nervous System Diseases: Metabolites Bring Insights into Brain Dysfunctions. J Neuroimmune Pharmacol 10:402–424. https://doi.org/10.1007/s11481-014-9578-5

16. Jeter CB, Hergenroeder GW, Ward NH, Moore AN, Dash PK (2013) Human mild traumatic brain injury decreases circulating branched-chain amino acids and their metabolite levels. J Neurotrauma 30:671–679. https://doi.org/10.1089/neu.2012.2491

17. Walker AL, Imam SZ, Roberts RA (2018) Drug discovery and development: Biomarkers of neurotoxicity and neurodegeneration. Exp Biol Med 243:1037–1045. https://doi.org/10.1177/1535370218801309

18. Sánchez-Illana Á, Piñeiro-Ramos JD, Kuligowski J (2020) Small molecule biomarkers for neonatal hypoxic ischemic encephalopathy. Semin Fetal Neonatal Med 25:101084. https://doi.org/10.1016/j.siny.2020.101084

19. Serpero LD, Bellissima V, Colivicchi M, Sabatini M, Frigiola A, Ricotti A, Ghiglione V, Strozzi MC, Li Volti G, Galvano F, Gazzolo D (2013) Next generation biomarkers for brain injury. J Matern Neonatal Med 26:44–49. https://doi.org/10.3109/14767058.2013.829688

20. Dash PK, Zhao J, Hergenroeder G, Moore AN (2010) Biomarker Prognosis Diagnosis Ttt.Pdf. Neurother J Am Soc Exp Neurother 7:100–114

21. Ramaswamy V, Horton J, Vandermeer B, Buscemi N, Miller S, Yager J (2009) Systematic Review of Biomarkers of Brain Injury in Term Neonatal Encephalopathy. Pediatr Neurol 40:215–226. https://doi.org/10.1016/j.pediatrneurol.2008.09.026

22. Greve, Mark W. BJZ (2009) Pathophysiology of traumatic brain injury. Mt Sinai J Med A J Transl Pers Med A J Transl Pers Med 76,:97-104. https://doi.org/10.1002/MSJ

23. Janich K, Nguyen HS (2016) Management of Adult Traumatic Brain Injury: A Review. J Trauma Treat 5:. https://doi.org/10.4172/2167-1222.1000320

24. Eakin K, Baratz-Goldstein R, Pick CG, Zindel O, Balaban CD, Hoffer ME, Lockwood M, Miller J, Hoffer BJ (2014) Efficacy of N-acetyl cysteine in traumatic brain injury. PLoS One 9:1–7. https://doi.org/10.1371/journal.pone.0090617

25. Corps KN, Roth TL, McGavern DB (2015) Inflammation and neuroprotection in traumatic brain injury. JAMA Neurol 72:355–362. https://doi.org/10.1001/jamaneurol.2014.3558

26. Ding JY, Kreipke CW, Speirs SL, Schafer P, Schafer S, Rafols JA (2009) Hypoxia-inducible factor-1α signaling in aquaporin upregulation after traumatic brain injury. Neurosci Lett 453:68–72. https://doi.org/10.1016/j.neulet.2009.01.077

27. Major BP, McDonald SJ, O'Brien WT, Symons GF, Clough M, Costello D, Sun M, Brady RD, Mccullough J, Aniceto R, Lin IH, Law M, Mychasiuk R, O'Brien TJ, Agoston D V., Shultz SR (2020) Serum Protein Biomarker Findings Reflective of Oxidative Stress and Vascular Abnormalities in Male, but Not Female, Collision Sport Athletes. Front Neurol 11:. https://doi.org/10.3389/fneur.2020.549624

28. Sigler A, He X, Bose M, Cristea A, Liu W, Nam PKS, James D, Burton C, Shi H (2020) Simultaneous Determination of Eight Urinary Metabolites by HPLC-MS/MS for Noninvasive Assessment of Traumatic Brain Injury. J Am Soc Mass Spectrom 31:1910–1917. https://doi.org/10.1021/jasms.0c00181

29. Vorn R, Naunheim R, Lai C, Wagner C, Gill JM, Hubbard WB, Gatto RG (2022) Elevated Axonal Protein Markers Following Repetitive Blast Exposure in Military Personnel. 16:1–6. https://doi.org/10.3389/fnins.2022.853616

30. Tsai G, Coyle JT (1995) N-Acetylaspartate in neuropsychiatric disorders. Prog Neurobiol 46:531–540. https://doi.org/10.1016/0301-0082(95)00014-M

31. Chitturi J, Li Y, Santhakumar V, Kannurpatti SS (2018) Early behavioral and metabolomic change after mild to moderate traumatic brain injury in the developing brain. Elsevier Ltd

32. Busto R, Dietrich WD, Globus MYT, Alonso O, Ginsberg MD (1997) Extracellular release of serotonin following fluid-percussion brain injury in rats. J Neurotrauma 14:35–42. https://doi.org/10.1089/neu.1997.14.35

33. Markianos M, Seretis A, Kotsou S, Baltas I, Sacharogiannis H (1992) CSF neurotransmitter metabolites and short-term outcome of patients in coma after head injury. Acta Neurol Scand 86:190–193. https://doi.org/10.1111/j.1600-0404.1992.tb05064.x

34. Markianos M, Seretis A, Kotsou A, Christopoulos M (1996) CSF neurotransmitter metabolites in comatose head injury patients during changes in their clinical state. Acta Neurochir (Wien) 138:57–59. https://doi.org/10.1007/BF01411725

35. Margonis K, Fatouros IG, Jamurtas AZ, Nikolaidis MG, Douroudos I, Chatzinikolaou A, Mitrakou A, Mastorakos G, Papassotiriou I, Taxildaris K, Kouretas D (2007) Oxidative stress biomarkers responses to physical overtraining: Implications for diagnosis. Free Radic Biol Med 43:901–910. https://doi.org/10.1016/j.freeradbiomed.2007.05.022

36. Blasco H, Garcon G, Patin F, Veyrat-Durebex C, Boyer J, Devos D, Vourc'H P, Andres CR, Corcia P (2017) Panel of Oxidative Stress and Inflammatory Biomarkers in ALS: A Pilot Study. Can J Neurol Sci 44:90–95. https://doi.org/10.1017/cjn.2016.284

37. Song H, Cui J, Simonyi A, Johnson CE, Hubler GK, DePalma RG, Gu Z (2018) Linking blast physics to biological outcomes in mild traumatic brain injury: Narrative review and preliminary report of an open-field blast model. Behav Brain Res 340:147–158. https://doi.org/10.1016/j.bbr.2016.08.037

38. Song H, Konan LM, Cui J, Johnson CE, Langenderfer M, Grant DA, Ndam T, Simonyi A, White T, Demirci U, Mott DR, Schwer D, Hubler GK, Cernak I, DePalma RG, Gu Z (2018) Ultrastructural brain abnormalities and associated behavioral changes in mice after low-intensity blast exposure. Behav Brain Res 347:148–157. https://doi.org/10.1016/j.bbr.2018.03.007

39. LaManna JC, Vendel LM, Farrell RM (1992) Brain adaptation to chronic hypobaric hypoxia in rats. J Appl Physiol 72:2238–2243. https://doi.org/10.1152/jappl.1992.72.6.2238

40. Wu J, Sigler A, Pfaff A, Cen N, Ercal N, Shi H (2021) Development of a HPLC-MS/MS method for assessment of thiol redox status in human tear fluids. Anal Biochem 629:114295. https://doi.org/10.1016/j.ab.2021.114295

41. van de Merbel NC, Bronsema KJ, Gorman SH, Bakhtiar R (2017) Sensitivity improvement of the LC–MS/MS quantification of carbidopa in human plasma and urine by derivatization with 2,4-pentanedione. J Chromatogr B Anal Technol Biomed Life Sci 1064:62–67. https://doi.org/10.1016/j.jchromb.2017.09.010

42. Kempuraj D, Ahmed ME, Selvakumar GP, Thangavel R, Raikwar SP, Zaheer SA, Iyer SS, Govindarajan R, Nattanmai Chandrasekaran P, Burton C, James D, Zaheer A (2021) Acute Traumatic Brain Injury-Induced Neuroinflammatory Response and Neurovascular Disorders in the Brain. Neurotox Res 39:359–368. https://doi.org/10.1007/s12640-020-00288-9

43. Koch E, Mainka M, Dalle C, Ostermann AI, Rund KM, Kutzner L, Froehlich LF, Bertrand-Michel J, Gladine C, Schebb NH (2020) Stability of oxylipins during plasma generation and long-term storage. Talanta 217:121074. https://doi.org/10.1016/j.talanta.2020.121074

44. McDougall M, Choi J, Magnusson K, Truong L, Tanguay R, Traber MG (2017) Chronic vitamin E deficiency impairs cognitive function in adult zebrafish via dysregulation of brain lipids and energy metabolism. Free Radic Biol Med 112:308–317. https://doi.org/10.1016/j.freeradbiomed.2017.08.002

45. Ishikado A, Morino K, Nishio Y, Nakagawa F, Mukose A, Sono Y, Yoshioka N, Kondo K, Sekine O, Yoshizaki T, Ugi S, Uzu T, Kawai H, Makino T, Okamura T, Yamamoto M, Kashiwagi A, Maegawa H (2013) 4-Hydroxy Hexenal Derived from Docosahexaenoic Acid Protects Endothelial Cells via Nrf2 Activation. PLoS One 8:. https://doi.org/10.1371/journal.pone.0069415

46. Gómez B, Strozzi I, Barba FJ, Vargas FC, Saraiva JA, Marszałek K, Sobral PJ do A, Lorenzo JM (2018) Evaluation of the Antioxidant Capacity of a Guarana Seed Extract on Canola Oil Lipid Stability Using Accelerated Storage. Eur J Lipid Sci Technol 120:1–29. https://doi.org/10.1002/ejlt.201800293

47. Halliwell B, Gutteridge JMC (2015) Free Radicals in Biology and Medicine. Oxford University Press

48. Sun X, Berger RS, Heinrich P, Marchiq I, Pouyssegur J, Renner K, Oefner PJ, Dettmer K (2020) Optimized protocol for the in situ derivatization of glutathione with n-ethylmaleimide in cultured cells and the simultaneous determination of glutathione/glutathione disulfide ratio by hplc-uv-qtof-ms. Metabolites 10:1–15. https://doi.org/10.3390/metabo10070292

49. Sutton TR, Minnion M, Barbarino F, Koster G, Fernandez BO, Cumpstey AF, Wischmann P, Madhani M, Frenneaux MP, Postle AD, Cortese-Krott MM, Feelisch M (2018) A robust and versatile mass spectrometry platform for comprehensive assessment of the thiol redox metabolome. Redox Biol 16:359–380. https://doi.org/10.1016/j.redox.2018.02.012

50. Giustarini D, Dalle-Donne I, Milzani A, Fanti P, Rossi R (2013) Analysis of GSH and GSSG after derivatization with N-ethylmaleimide. Nat Protoc 8:1660–1669. https://doi.org/10.1038/nprot.2013.095

51. Forman HJ, Zhang H, Rinna A (2009) Glutathione: Overview of its protective roles, measurement, and biosynthesis. Mol Aspects Med 30:1–12. https://doi.org/10.1016/j.mam.2008.08.006

52. Sangaraju D, Shahidi-Latham SK, Burgess BL, Dean B, Ding X (2017) A multi-matrix HILIC-MS/MS method for the quantitation of endogenous small molecule neurological biomarker N-acetyl aspartic acid (NAA). J Pharm Biomed Anal 140:11–19. https://doi.org/10.1016/j.jpba.2017.03.020

53. Al-Samsam RH, Alessandri B, Bullock R (2000) Extracellular N-acetyl-aspartate as a biochemical marker of the severity of neuronal damage following experimental acute traumatic brain injury. J Neurotrauma 17:31–39. https://doi.org/10.1089/neu.2000.17.31

54. Xu T, Lu C, Feng L, Fan LX, Sun J, Fan B, Wang Q, Wang Y, Liu XM, Wang FZ (2019) Liquid chromatography–mass spectrometry-based urinary metabolomics study on a rat model of simulated microgravity-induced depression. J Pharm Biomed Anal 165:31–40. https://doi.org/10.1016/j.jpba.2018.11.058

55. Zhai XJ, Chen F, Zhu CR, Lu YN (2015) A simple LC-MS/MS method for quantitative analysis of underivatized neurotransmitters in rats urine: Assay development, validation and application in the CUMS rat model. Biomed Chromatogr 29:1737–1743. https://doi.org/10.1002/bmc.3487

56. Han XM, Qin YJ, Zhu Y, Zhang XL, Wang NX, Rang Y, Zhai XJ, Lu YN (2019) Development of an underivatized LC-MS/MS method for quantitation of 14 neurotransmitters in rat hippocampus, plasma and urine: Application to CUMS induced depression rats. J Pharm Biomed Anal 174:683–695. https://doi.org/10.1016/j.jpba.2019.06.043

57. Tareke E, Bowyer JF, Doerge DR (2007) Quantification of rat brain neurotransmitters and metabolites using liquid chromatography/electrospray tandem mass spectrometry and comparison with liquid chromatography/electrochemical detection. Rapid Commun Mass Spectrom 21:3898–3904. https://doi.org/10.1002/rcm.3295

58. He B, Bi K, Jia Y, Wang J, Lv C, Liu R, Zhao L, Xu H, Chen X, Li Q (2013) Rapid analysis of neurotransmitters in rat brain using ultra-fast liquid chromatography and tandem mass spectrometry: Application to a comparative study in normal and insomnic rats. J Mass Spectrom 48:969–978. https://doi.org/10.1002/jms.3243

59. Su F, Wang F, Zhu R, Li H (2009) Determination of 5-Hydroxytryptamine, norepinephrine, dopamine and their metabolites in rat brain tissue by LC-ESI-MS-MS. Chromatographia 69:207–213. https://doi.org/10.1365/s10337-008-0879-9

60. Liu H, Liu N, Teng W, Chen J (2018) Study on a dSPE-LC-MS/MS method for lysophosphatidylcholines and underivatized neurotransmitters in rat brain tissues. J Chromatogr B Anal Technol Biomed Life Sci 1096:11–19. https://doi.org/10.1016/j.jchromb.2018.07.040

61. Andreoli R, Manini P, Corradi M, Mutti A, Niessen WMA (2003) Determination of patterns of biologically relevant aldehydes in exhaled breath condensate of healthy subjects by liquid chromatography/atmospheric chemical ionization tandem mass spectrometry. Rapid Commun Mass Spectrom 17:637–645. https://doi.org/10.1002/rcm.960

62. Hušková R, Chrastina P, Adam T, Schneiderka P (2004) Determination of creatinine in urine by tandem mass spectrometry. Clin Chim Acta 350:99–106. https://doi.org/10.1016/j.cccn.2004.07.007

63. Palm M, Lundblad A (2005) Creatinine concentration in plasma from dog, rat, and mouse: A comparison of 3 different methods. Vet Clin Pathol 34:232–236. https://doi.org/10.1111/j.1939-165X.2005.tb00046.x

64. Giustarini D, Dalle-Donne I, Milzani A, Rossi R (2011) Low molecular mass thiols, disulfides and protein mixed disulfides in rat tissues: Influence of sample manipulation, oxidative stress and ageing. Mech Ageing Dev 132:141–148. https://doi.org/10.1016/j.mad.2011.02.001

65. Olmos Moya PM, Martínez Alfaro M, Kazemi R, Alpuche-Avilés MA, Griveau S, Bedioui F, Gutiérrez Granados S (2017) Simultaneous Electrochemical Speciation of Oxidized and Reduced Glutathione. Redox Profiling of Oxidative Stress in Biological Fluids with a Modified Carbon Electrode. Anal Chem 89:10726–10733. https://doi.org/10.1021/acs.analchem.7b01690

66. Miller RC, Brindle E, Holman DJ, Shofer J, Klein NA, Soules MR, O'Connor KA (2004) Comparison of specific gravity and creatinine for normalizing urinary reproductive hormone concentrations. Clin Chem 50:924–932. https://doi.org/10.1373/clinchem.2004.032292

67. Burton C, Shi H, Ma Y (2014) Normalization of urinary pteridines by urine specific gravity for early cancer detection. Clin Chim Acta 435:42–47. https://doi.org/10.1016/j.cca.2014.04.022

68. Rodriguez-Rodriguez A, Egea-Guerrero J, Murillo-Cabezas F, Carrillo-Vico A (2014) Oxidative Stress in Traumatic Brain Injury. Curr Med Chem 21:1201–1211. https://doi.org/10.2174/09298673216661312171533 10

69. Ansari MA, Roberts KN, Scheff SW (2008) Oxidative stress and modification of synaptic proteins in hippocampus after traumatic brain injury. Free Radic Biol Med 45:443–452. https://doi.org/10.1016/j.freeradbiomed.2008.04.038

70. Prakash R, Carmichael ST (2015) Blood−brain barrier breakdown and neovascularization processes after stroke and traumatic brain injury. Curr Opin Neurol 28:556–564. https://doi.org/10.1097/WCO.0000000000000248

71. Kuriakose M, Younger D, Ravula AR, Alay E, Rama Rao K V., Chandra N (2019) Synergistic Role of Oxidative Stress and Blood-Brain Barrier Permeability as Injury Mechanisms in the Acute Pathophysiology of Blast-induced Neurotrauma. Sci Rep 9:1–12. https://doi.org/10.1038/s41598-019-44147-w

72. Gabathuler R (2010) Approaches to transport therapeutic drugs across the blood-brain barrier to treat brain diseases. Neurobiol Dis 37:48–57. https://doi.org/10.1016/j.nbd.2009.07.028

73. Sorby-Adams AJ, Marcoionni AM, Dempsey ER, Woenig JA, Turner RJ (2017) The role of neurogenic inflammation in blood-brain barrier disruption and development of cerebral oedema following acute central nervous system (CNS) injury. Int J Mol Sci 18:1–24. https://doi.org/10.3390/ijms18081788

74. Nitta T, Hata M, Gotoh S, Seo Y, Sasaki H, Hashimoto N, Furuse M, Tsukita S (2003) Size-selective loosening of the blood-brain barrier in claudin-5-deficient mice. J Cell Biol 161:653–660. https://doi.org/10.1083/jcb.200302070

II. EVALUATION OF ANTIOXIDANT THERAPY ON TRAUMATIC BRAIN INJURY IN RAT MODELS USING HPLC-MS/MS

Olajide Adetunji[1#], Jiandong Wu[2#], Annalise Pfaff[1], Austin Sigler[1], Mousumi Bose[1], Catherine Johnson[3], Nuran Ercal[1], Honglan Shi[1], Paul Nam[1, *]

[1]Department of Chemistry, [2]Department of Chemical and Biochemical Engineering, [3]Department of Mining and Explosives Engineering, Missouri University of Science and Technology, Rolla, MO, 65409, USA

#: these authors contributed equally.

ABSTRACT

Oxidative stress (OS) stemming from traumatic brain injury (TBI) is a preceding factor that leads to a cascade of excitotoxic events, including blood-brain barrier (BBB) disruption, and it remains an essential factor in understanding the pathophysiology of TBI. Private and government institutions invest considerable finances in finding effective therapies against TBI, yet there is no well-established treatment regimen. Rather, therapies are focused on the management of TBI-associated symptoms. Targeting OS characteristics of TBI can make the much-needed difference in finding effective pharmacotherapy against TBI. Antioxidant therapy using glutathione (GSH) prodrug, *N*-acetylcysteine amide (NACA), can improve symptoms, maintain brain homeostasis, and reestablish BBB integrity that was disturbed by the secondary sequelae of head insult. Therefore, in our study, we evaluated the neuroprotective effects of pre-and post-exposure use of NACA (500 mg/Kg) in rat models that were exposed to blast-induced TBI (b-TBI) using an open-field blast model that was simulated to represent what military personnel are regularly exposed to in combat. Selected potential small-molecule

TBI biomarkers were used to measure the TBI-induced and therapeutic efficacy of NACA in urine, plasma, and whole brain tissue of the rat models using HPLC-MS/MS. Significant level changes and trends in OS and neurotoxicity markers were observed as a response to both the b-TBI and the NACA treatment administered. From our findings, NACA may be an effective therapeutic approach for abrogating or reversing some of the OS and neuroinflammatory effects of b-TBI; thereby, NACA may find utility in the treatment and management of the disease. Therefore, future works on evaluating NACA as a therapeutic for TBI should be encouraged.

Keywords: Traumatic brain injury, HPLC-MS/MS, biomarkers, *N*-acetylcysteine amide, urine, plasma, whole-brain.

1. INTRODUCTION

Despite sizeable investments from private and government entities, there are no well-established absolute pharmacotherapeutic protection or clinical outcome improvements for TBI [1–3]. The establishment of a known and widely accepted therapeutic regimen for traumatic brain injury (TBI) has been hampered by the absence of well-designed-controlled clinical investigations, therapeutic evaluation outcomes, well-defined interpretation of safety profiles and limits, and, most importantly, predictive biomarkers of TBI [2,4,5]. In the USA alone, TBI accounts for more than 230,000 hospitalizations, and therapy is largely focused on symptom management because of a lack of a definitive treatment regimen [2,6–9]. This resulted in financial implications of up to $US400 billion globally, owning to hospital visits and TBI-induced disabilities like mental-health aberrations, and severe motor and cognitive impairment [4,6].

Blast-induced traumatic brain injury (b-TBI) incurred during training and on the battlefield is the most common type of TBI in military personnel [1,10,11]. Additional causes are the blunt or piercing forces [3,10], and they all alter the morphological structure of the brain and brain-dependent organs [9]; this initial phase is referred to as the primary injury [12,13]. Notably, most sufferers of TBI are affected by the least severe form of TBI, mild TBI (m-TBI), which is the hardest to identify and can have chronic and long-lasting effects due to systemic manifestations [1,9,14–16]. Due to the diffuse nature of b-TBI, the injury is usually widespread in the brain, causing it to be otherwise known as diffuse axonal injury (DAI) [14,17]. Consequently, a follow-up injury phase (secondary injury) occurring after the primary injury [10] involves numerous neurochemical and subcellular events, reduced cerebral blood flow, and hypoxia [3,9,18]. Additionally, widespread excitotoxicity with secondary disease mechanisms like increased intracranial pressure, loss of consciousness, cerebral edema, lipid peroxidation, blood-brain barrier BBB permeability increase, and oxidative stress (OS) are all critical contributors to the exacerbation of secondary injury [1,12,13]. All these mechanisms play a part in the chronic nature of the disease that translates to other neurodegenerative diseases like ischemic stroke, Parkinson's disease, multiple sclerosis, Alzheimer's disease, and dementia in later life [19–21]. Also, violation of the BBB integrity from systemic inflammation activation and other secondary mechanisms [1] perturbs cerebral homeostasis, which leads to unwanted passage of biological materials in and out of the endothelial cell lining of the BBB into surrounding peripheral fluids [19,22,23]. Therefore, this disruption can be associated with disease states [24].

Early detection and treatment administration could be vital in restoring cerebral homeostasis after the onslaught of this disease [1,25]. TBI diagnosis, although not well established [26], utilizes some protein biomarkers [23,27], the Glasgow Coma Scale (GCS) [28], and symptom observation to monitor disease inception and progression. However, having clear and effective diagnostics sensitive to m-TBI [16,26,28], like that of small molecule biomarkers, will considerably improve early disease detection and treatment outcomes. Additionally, treatment primarily focuses on guidelines and symptom management, which is not the most effective therapeutic approach [4,28]. b-TBI-induced OS from impairment of antioxidant defenses (including enzymes) by reactive species plays a vital role in the secondary events leading to neuronal apoptosis [12,17,18,29]. This phenomenon of redox imbalance [20,21], characterized by the proliferation of reactive oxygen species (ROS), reactive nitrogen species (RNS), free radicals, and a reduction in antioxidant defense setup, can be counteracted by antioxidant therapy [21,30]. Antioxidant therapy in b-TBI, like any other OS-related disease using exogenous and endogenous molecules, is designed to act on any form of OS by neutralizing reactive species, moderating adverse metabolic changes, interrupting and modulating neuronal protein for cellular homeostasis restoration [20,21,31]. Hence, the utilization of neurotransmitters and other markers of neurotoxicity would go a long way in monitoring disease states and drug efficacy in b-TBI [22,25].

Glutathione (GSH), a thiol-based low-molecular weight endogenous antioxidant, is critical in ROS scavenging, and TBI depletes both cellular and mitochondrial levels of GSH [8,32]. *N*-acetylcysteine (NAC) is an endogenous amino acid L-cysteine derivative, a rate-limiting precursor to GSH [29]. Hence, it is referred to as a GSH prodrug [33].

NAC has received FDA approval [3] and is used to combat OS related to acetaminophen poisoning and is employed as a supplement [29,34]. However, a downside of this drug is low BBB permeability, which leads to low bioavailability and high drug dosage [29,34]. In 1967, *N*-acetylcysteine amide (NACA) was synthesized [35], described as an amide derivative of NAC with similar structural properties as NAC but with better bioavailability due to its lipophilic and hydrophobic nature [36]. Due to these minor modifications in its chemical structure, the physicochemical and pharmacological properties of NACA enhance penetration of cell membranes, mitochondria, and the central nervous system, providing NACA an efficacy advantage over NAC [1,36]. However, NACA has not received the same level of acceptance as it does not have FDA approval at the time of this study.

Secondary actions of TBI leading to BBB breakdown result in an unconfined biomarker distribution in the central nervous system (CNS) and peripheral fluids like urine and blood. Understanding the complex kinetic behaviors of biomarkers will help researchers define the pathophysiology of TBI [23]. Furthermore, evolution of the secondary injury mechanisms activated after head insult spans from minutes to days and even months [5,37] due to delayed metabolic, neurochemical, and subcellular changes [1]. Taking advantage of the delayed activation of detrimental processes to administer pre- and post-exposure prophylactic therapeutics could mitigate the effect of TBI or even reverse some of the unfavorable events. NACA's CNS bioavailability, antioxidant and GSH-prodrug nature, anti-inflammatory properties, and minimal side effects indicate its therapeutic candidacy against oxidative damage from b-TBI. In this study, we carried out blast simulation mimicking combat b-TBI on animal models and administered NACA

treatment to the studied animals. We evaluated the impact of TBI and NACA treatment on potential small-molecule biomarkers -*N*-acetyl aspartic acid (NAA), 5-hydroxyindoleacetic acid (5-HIAA), GSH, glutathione disulfide (GSSG), GSH/GSSG ratio, 4-hydroxynonenal (4-HNE), and F2α-isoprostane (F2a)- to understand TBI pathophysiology and therapy. Collectively, these were markers that represented redox status [38], neurotoxicity [39,40], inflammation [41], and lipid peroxidation [42].

2. MATERIALS AND METHODS

2.1. CHEMICALS AND REAGENTS

An analytical grade standard of 5-HIAA was purchased from Acros Organics (Fair Lawn, NJ, USA). Ketamine, butylated hydroxytoluene (BHT), creatinine (CRT), GSSG, GSH, and NAA analytical grade standards were purchased from Sigma-Aldrich (St. Louis, MO, USA). 4-HNE and F2a prepared in MeOAc were purchased from Cayman Chemicals (Ann Arbor, MI, USA). Isotopically labeled compounds were used as internal standards (ISs). Glutathione-(glycine-$^{13}C_2$, ^{15}N) (GSH-IS) was purchased from Sigma-Aldrich (St. Louis, MO, USA), glutathione disulfide-(glycine-$^{13}C_2$, ^{15}N, GSSG-IS) was purchased from Cambridge Isotopes Laboratories (Tewksbury, MA, USA) while *N*-acetyl aspartic acid-D_3 (NAA-IS) was purchased from CDN Isotopes (Pointe-Claire, Quebec, CA). Creatinine-D_3 (CRT-IS) and F2α-isoprostane-D_4 (F2a-IS) prepared in MeOAc were purchased from Cayman Chemicals (Ann Arbor, MI, USA). Analytical grade 5-hydroxyindoleacetic acid-D_5 (5-HIAA-IS) was purchased from Cerilliant (Round Rock, Texas, USA). LC-MS grade methanol (MeOH), acetonitrile (ACN), ethanol (EtOH), and Optima™ LC-MS grade Formic acid (FA) were purchased from Fisher

Chemical (Hampton, NH, USA). Centrifugal filters (3 kDa molecular weight cut-off) were purchased from VWR North America (Radnor, PA, USA). *N*-ethylmaleimide (NEM) was purchased from CHEM-IMPEX INT'L INC (Wood Dale, IL, USA). *N*-acetylcysteine amide was purchased from Alfa Chemistry (Holbrook, NY, USA). Ultrapure water was generated in-house using a Millipore Elix-3 purification system (Millipore, Billerica, MA, USA).

2.2. ANIMALS AND HOUSING CONDITIONS

All animal procedures were reviewed and approved by the Missouri S&T Animal Care and Use Committee in compliance with Federal regulations regarding the protection of animals used in research. Fifteen-week-old Fischer CDF male rats (weight = 250-270 g; Charles River, MA, USA) were used for the experiments described in this study, and they were housed in a temperature and humidity-controlled animal facility. The animals were provided precisely one week of acclimatization before studies were conducted. Access to food (Purina Lab Diet rat chow) and water (municipal tap) were allowed for the animals *ad libitum*, and a 12-hour light-dark cycle was provided for the animals at the Missouri S&T Animal Research Facility.

2.3. EXPLOSIVE BLAST MODEL

Twenty-three animals were divided into four groups: Sham (n = 6), NACA (n=5), b-TBI & NACA (n=6), and b-TBI (n = 6). All animals were transported to the Missouri University of Science and Technology experimental mine facility. Animals were anesthetized via ketamine/xylazine (80/12 mg/kg body weight, i.p.) prior to injury. No

explosive device was detonated for control groups: 1. Sham, and 2. NACA, however, the animals were kept in the same conditions as the blast rats during the blast exercise for equilibration. The experimental (blast-induced) rat groups: 3. b-TBI & NACA and 4. b-TBI were suspended at a height of 60 cm in modified cages and subjected to an open-field explosive blast at 2.15 m from a 350 g charge of C4. The open-field blast model of TBI used here was developed and validated previously in rodents [43–45]. Table 1 shows a description of the groups. The severity of the TBI from the blast-induced was considered mild.

2.4. ANTIOXIDANT THERAPY

On the day of the scheduled blast, animals were treated with s.c. injection of either PBS (1. Sham, and 4. b-TBI) or 500 mg/kg NACA (2. NACA, and 3. b-TBI & NACA) 1 h prior to injury. Animals were transported to the Experimental Mine facility at Missouri University of Science and Technology and were subjected to open blast injury as described in Section 2.3. All animals were treated with s.c injection of 500 mg/kg NACA or PBS for four more days after the blast exposure. Animals were fasted overnight on the 5th day, and they were anesthetized with ketamine/xylazine injection (i.p.) for collection of urine, blood, and whole brain. Table 1 shows a description of the treatment details of the groups.

Table 1. Blast simulation and NACA treatment description.

Group	Blast Conducted	Injection	Injury	Number
1. Sham	No Blast	PBS	Sham	6

Table 1. Blast simulation and NACA treatment description. (Cont.)

Group	Blast Conducted	Injection	Injury	Number
2. NACA	No Blast	NACA	Sham	5
3. b-TBI & NACA	Blast at 2.15m	NACA	Blast	6
4. b-TBI	Blast at 2.15m	PBS	Blast	6

2.5. SURGICAL PROCEDURE AND SAMPLE COLLECTION

Euthanasia, harvesting of tissues, and collections of biological fluids were conducted in the animal surgery theatre at the Missouri S&T Animal Research Facility on the 5^{th} day after the blast. Animals were deeply anesthetized via i.p injection of ketamine/xylazine. Animals were euthanized by exsanguination via cardiac puncture. Blood was collected into heparin-coated tubes and centrifuged (3000 g, 10 min; 4 °C) immediately to separate plasma. Urine was drawn directly from the bladder. Each urine or plasma sample was divided into two aliquots. Upon collection, 10 mg/mL BHT was added to one aliquot of each urine or plasma sample to give a final 200 µg/mL BHT concentration. To the other aliquot of collected urine or plasma, 100 mM NEM was added (urine or plasma/NEM = 9:1, v/v), and the mixture was vortexed for a few seconds to form the stable GSH-NEM adduct. Whole brains were collected immediately following euthanasia. Stabilized urine, plasma, and brain samples were frozen immediately in liquid N_2 and stored at -80 °C until analysis.

2.6. SAMPLE PREPARATION

Biological fluids (urine and plasma) were diluted as needed and ultrafiltered in 3 KDa molecular weight cut-off filters. Whole brain tissues were homogenized using a bullet blender tissue homogenizer (Next Advance, Troy, NY, USA)., followed by dilution and ultrafiltration in a 3 KDa molecular weight cut-off filters. Further details on sample preparation are in a method to be published elsewhere.

2.7. HPLC-MS/ MS METHOD

Two high-performance-tandem mass spectrometry (HPLC-MS/MS) methods in positive and negative electrospray ionization mode (ESI) were used for the analysis of the metabolites on a Shimadzu (Columbia, MD, USA) Prominence UFLC system connected to a 4000Q TRAP tandem mass spectrometer system (AB SCIEX, Concord, ON, CA). Chromatographic separation of NAA, 5-HIAA, and F2a in the negative ESI mode was done with a Hydro-RP column (150 × 2 mm, 4 μm, Phenomenex, CA, United States), 0.1% formic acid in ultrapure water (v/v) as mobile phase A, and 0.1% formic acid in ACN (v/v) as mobile phase B at 0.3 mL/min with a gradient that runs at 100% A after sample injection for the first 2 min, followed by a linear gradient increase to 100% B from 2.0 to 8.0 min. The gradient is held at 100% B from 8.0 to 10.0 min before changing back to 100% A from 10.0 to 10.5 min.

Chromatographic separation of GSH-NEM, GSSG, 4-HNE, and CRT in the positive ESI mode was done with a Hydro-RP column (250 × 2 mm, 4 μm, Phenomenex, CA, United States), 0.01% formic acid in ultrapure water (v/v) as mobile phase A, and 0.01% formic acid in ACN (v/v) as mobile phase B at 0.3 mL/min with a gradient that

runs at 100% A after sample injection for first 1 min, followed by a linear gradient increase to 80% B from 1.0 to 7.0 min. The gradient is held at 80% B from 7.0 to 9.5 min before changing back to 100% A from 9.5 to 10.5 min. Full details of the HPLC-MS/MS method used are described in a yet-to-be-published work (O.A. et al)

2.8. QUALITY CONTROL AND ASSURANCE

Analytical methods were validated in healthy rat samples prior to analysis. Analytical replicates, matrix spikes, and quality control samples were added during analysis to ensure consistency with sample preparation and instrumentation between each batch run.

2.9. DATA PROCESSING AND STATISTICAL ANALYSIS

Hydration in urine and plasma was corrected with the creatinine level detected [46]. The limit of detection (LOD) was defined as the signal-to-noise ratio (S/N) = 3, while the limit of quantitation was defined as S/N = 10. Data is represented as the mean ± SEM (standard error of the mean) of 4-6 animals. GraphPad Prism 6 (San Diego, California) was used to conduct One-way ANOVA to compare mean biomarker levels between all groups. Fisher LSD pair-wise test was used to compare two individual groups in the study. Values of $p \leq 0.05$ were considered statistically significant, and $p \leq 0.1$ were defined to approach statistical significance for analyses discussed here.

3. RESULTS

3.1. EFFECTS OF NACA ON WHOLE BRAIN TISSUE METABOLITES

The exposure to blast overpressure (BOP) caused observable changes to the investigated metabolites in brain tissue. Brain tissue metabolites levels were recorded as ng(analyte)/mg(wet weight) of the tissue and the one-way ANOVA results are as follows: NAA; ($F = 4.68$, $p = 0.0130$), 5-HIAA; ($F = 3.26$, $p = 0.0442$), GSH; ($F = 17.01$, $p \leq 0.0001$), GSSG; ($F = 5.86$, $p = 0.0052$), GSH/GSSG ratio; ($F = 1.48$, $p = 0.252$). Further statistical post-hoc probing using Fisher LSD pair-wise comparison showed a $p < 0.05$ and a 16% reduction in NAA levels between the b-TBI and b-TBI & NACA groups, indicating NACA's ability to reduce NAA levels after b-TBI. NACA also showed a significant difference ($p \leq 0.01$) and a 23% reduction between the sham vs b-TBI & NACA groups. This was an indicator that both NACA and TBI influence NAA levels. This phenomenon was further bolstered by the 13 % reduction in NAA levels between the sham vs NACA groups, which was marginally significant ($p = 0.0511$). The activity of 5-HIAA in the brain as a response to b-TBI and NACA treatment was unclear from our data. We observed that GSH levels in the brain were highest in the sham and NACA rats and lowest in the b-TBI rats. However, a 34% decrease ($p < 0.0001$) observed between the sham and b-TBI rats showed GSH's utility as a TBI biomarker. NACA group rats showed a ($p = 0.0017$) significant 26% GSH reduction difference to the b-TBI group. The use of NACA in non-blast animals can maintain GSH levels in the brain, and b-TBI depletes that level even with NACA treatment administration ($p =0.0004$, NACA vs. b-TBI & NACA). Also, a significantly different $p \leq 0.0001$ was observed between the sham vs. b-TBI & NACA rats, and the similarity between the GSH levels of the sham vs.

NACA rats showed that the b-TBI was the major contributor to the GSH decrease observed in the b-TBI & NACA group. We did not observe NACA's GSH replenishing properties in the b-TBI & NACA group. However, GSSG levels in the b-TBI & NACA group were the lowest of all the groups indicating that NACA was acting more as a ROS scavenger and not a GSH-prodrug in the b-TBI animals treated with NACA. The GSSG levels observed followed a similar trend as the GSH in brain tissue; to better understand the redox status, it is necessary to evaluate the GSH/GSSG ratio [47]. Although not statistically significant, the observed GSH/GSSG ratio was highest in the sham and NACA rats, with the b-TBI & NACA coming next; however, the lowest GSH/GSSG ratio was observed in the b-TBI rats. This was an indication that the b-TBI rats were mainly affected by the redox imbalance from BOP, and NACA treatment was able to improve redox status by 24% in the b-TBI & NACA rats by acting as a ROS scavenger. F2a and 4-HNE levels in brain tissue were less than the LOD. Results are represented in the boxplot in Figure 1, and the p-values of the one-way ANOVA and the Fisher LSD multiple pair-wise comparison are shown in Tables 2 and 3, respectively.

Table 2. One-way ANOVA *p*-values of different metabolites in the whole brain, urine, and plasma.

Analyte	**Biological matrix**		
	Brain	**Plasma**	**Urine**
NAA	**0.0130**	0.3310	**0.0004**
5-HIAA	**0.0442**	**<0.0001**	**0.0269**
GSH	**<0.0001**	0.2576	0.2465
sGSSG	**0.0052**	0.1700	0.2451
GSH/GSSG	0.2521	0.3637	0.4929

Table 3. Fisher LSD pairwise comparison of whole brain tissue metabolites between different groups in the study. Significant *p*-values and approaching statistical significance *p*-values are in bold font.

	Brain				
Comparison	**NAA**	**5-HIAA**	**GSH**	**GSSG**	**GSH/GSSG**
Sham vs. NACA	**0.0511**	0.2517	**0.0908**	**0.0719**	0.7914
Sham vs. b-TBI & NACA	**0.0016**	**0.0708**	**< 0.0001**	**0.0005**	0.837
Sham vs. b-TBI	0.2219	0.727	**< 0.0001**	**0.0491**	0.1067
NACA vs. b-TBI &NACA	0.1277	**0.0059**	**0.0004**	**0.0347**	0.6389
NACA vs. b-TBI	0.4792	0.1549	**0.0017**	0.7785	**0.0662**
b-TBI &NACA vs. b-TBI	**0.0372**	0.1577	0.651	**0.075**	0.1514

3.2. EFFECTS OF NACA ON PLASMA METABOLITES

Plasma metabolites levels were recorded as (Analyte)(ng/mL)/(CRT) (ug/mL) and the one-way ANOVA results are as follows: NAA; ($F = 1.25$, $p = 0.3310$), 5-HIAA; ($F = 18.85$, $p < 0.0001$), GSH; ($F = 1.94$, $p = 0.1700$), GSSG; ($F = 1.49$, $p = 0.2576$, GSH/GSSG ratio; ($F = 1.19$, $p = 0.3637$). From the ANOVA data, only 5-HIAA showed a $p < 0.05$; upon further post-hoc test using Fisher LSD, it was observed that one of the significant differences was between the sham vs. b-TBI groups ($p < 0.05$), and a 20% decrease in biomarker level was noticed between these two groups. The sham group had considerably statistically significant ($p < 0.05$) higher levels than all the other groups. Between the b-TBI vs. b-TBI & NACA groups, a $p < 0.1$ approaching statistical significance with a 16% decrease, indicating the possibility of NACA affecting plasma 5-HIAA levels.

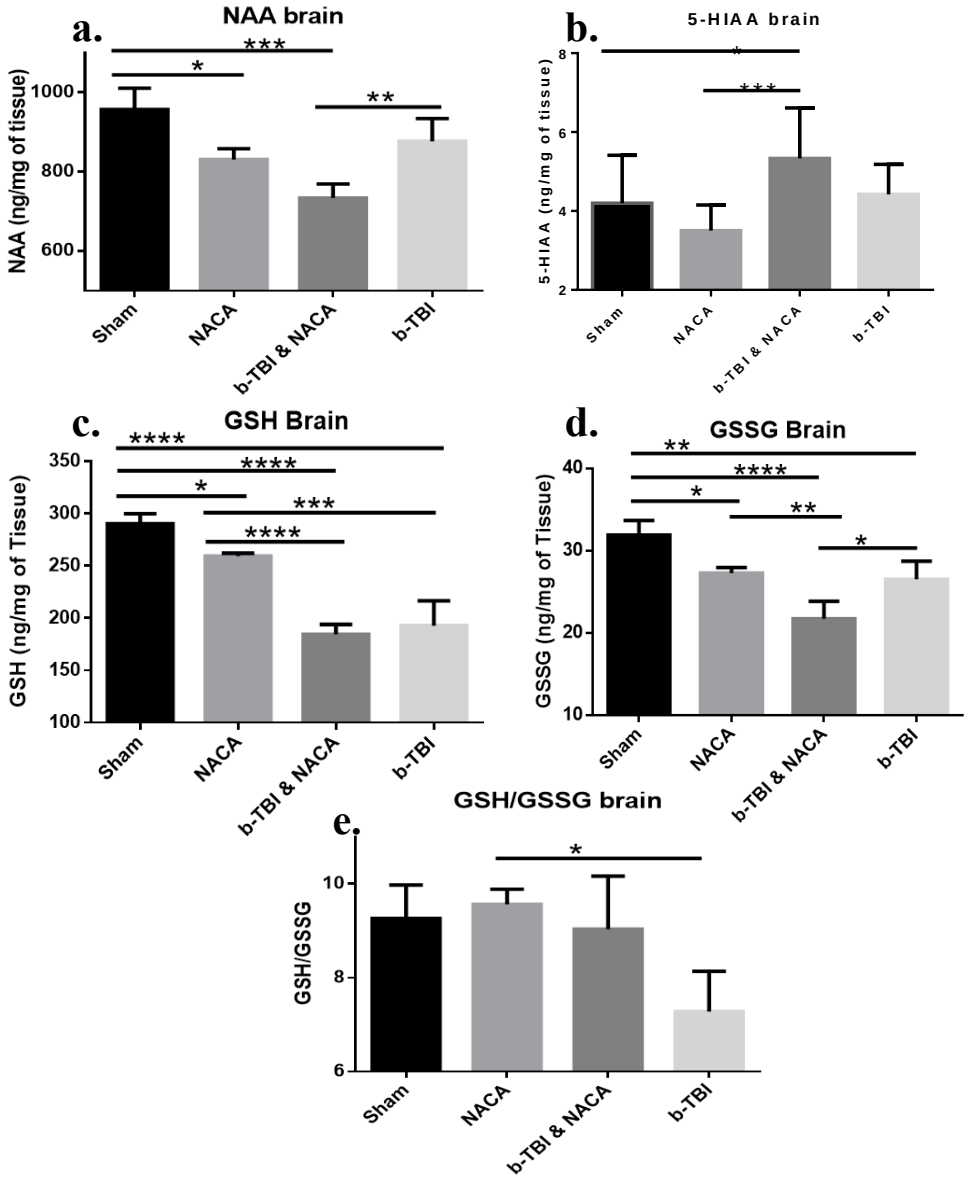

Figure 1. Whole brain tissue metabolite levels in Sham; NACA; b-TBI & NACA; and b-TBI groups for a) NAA, b) 5-HIAA, c) GSH, d) GSSG, e) GSH/GSSG ratio. Values represent mean ± SEM (n = 4-6). $p \leq 0.1$ (*), $p \leq 0.05$ (**), $p \leq 0.01$ (***), $p \leq 0.001$ (****). [Sham = no blast + no treatment, NACA = no blast + NACA treatment, b-TBI & NACA = blast + NACA treatment, b-TBI = blast + no treatment]

This was further corroborated by comparing the sham vs. NACA groups, which showed a statistically significant $p < 0.001$ and a 53% decrease in 5-HIAA level between

the groups. NACA's ability to lower 5-HIAA levels in plasma regardless of TBI was also observed with the 30% level difference between the NACA vs. b-TBI & NACA groups with a $p < 0.05$. No notable differences were observed between the groups for NAA, GSH, GSSG, and GSH/GSSG ratio in plasma. F2a and 4-HNE levels in plasma were less than the LOD. Results are represented in the boxplot in Figure 2, and the *p*-values of the one-way ANOVA and the Fisher LSD multiple pair-wise comparison are shown in Tables 2 and 4, respectively.

Table 4. Fisher LSD pairwise comparison of plasma metabolites between different groups in the study. Significant *p*-values and approaching statistical significance *p*-values are in bold font.

	Plasma				
Comparison	**NAA**	**5-HIAA**	**GSH**	**GSSG**	**GSH/GSSG**
Sham vs. NACA	0.1166	**< 0.0001**	**0.0643**	0.8179	**0.0986**
Sham vs. b-TBI &NACA	0.9384	**0.0003**	**0.0776**	**0.069**	0.256
Sham vs. b-TBI	0.9607	**0.018**	0.5358	0.2795	0.4111
NACA vs. b-TBI &NACA	0.1323	**0.0141**	0.7201	0.1718	0.5771
NACA vs. b-TBI	0.1461	**0.0007**	0.207	0.4722	0.3287
b-TBI & NACA vs. b-TBI	0.9812	**0.0941**	0.2864	0.4438	0.69

3.3. EFFECTS OF NACA ON URINARY METABOLITES

Urinary metabolites levels were recorded as (Analyte)(ng/mL)/(CRT) (ug/mL) and the one-way ANOVA results are as follows: NAA; ($F = 11.33$, $p = 0.0004$), 5-HIAA; ($F = 4.06$, $p = 0.0269$), GSH; ($F = 1.53$, $p = 0.2465$), GSSG; ($F = 1.55$, $p = 0.2451$), and

GSH/GSSG ratio; ($F = 0.84$, $p = 0.4929$). Post-hoc test using Fisher LSD for NAA showed that there were significant differences between the b-TBI group and all the other groups (sham, NACA, and b-TBI & NACA) with $p \leq 0.001$ for all. This indicated that NAA in urine could serve as a TBI biomarker, and NACA treatment had a significant effect in lowering NAA levels by 75% in the b-TBI & NACA rats as compared with the b-TBI rats. The NACA treatment regimen used in this study was able to keep NAA levels in b-TBI & NACA group like levels found in the sham and NACA groups. This proves that NACA might have therapeutic effects against b-TBI. Urinary 5-HIAA levels Fisher LSD tests showed significant differences ($p \leq 0.01$) of 37% decrease between the sham vs. b-TBI rats, indicating 5-HIAA's potential as a urinary TBI biomarker. Approaching statistical significance, sham and NACA rats had similar levels and were approximately 27% lesser than b-TBI & NACA 5-HIAA levels. Although no statistically significant difference was observed between the b-TBI vs. b-TBI & NACA groups, a 15 % decrease in 5-HIAA levels was seen in the groups. OS-related biomarkers, GSH, GSSG, and GSH/GSSG ratio showed no significant differences or trends amongst groups. Urinary F2a and 4-HNE levels were less than the LOD. Results are represented in the boxplot in Figure 3, and the *p*-values of the one-way ANOVA and the Fisher LSD multiple pair-wise comparison are shown in Tables 2 and 5, respectively.

4. DISCUSSION

Although with the least common usage in studies, b-TBI in rat models most accurately represents the diffusivity associated with most TBI [2]. Additionally, it is closest to the kind of TBI military personnel are exposed to in the line of duty.

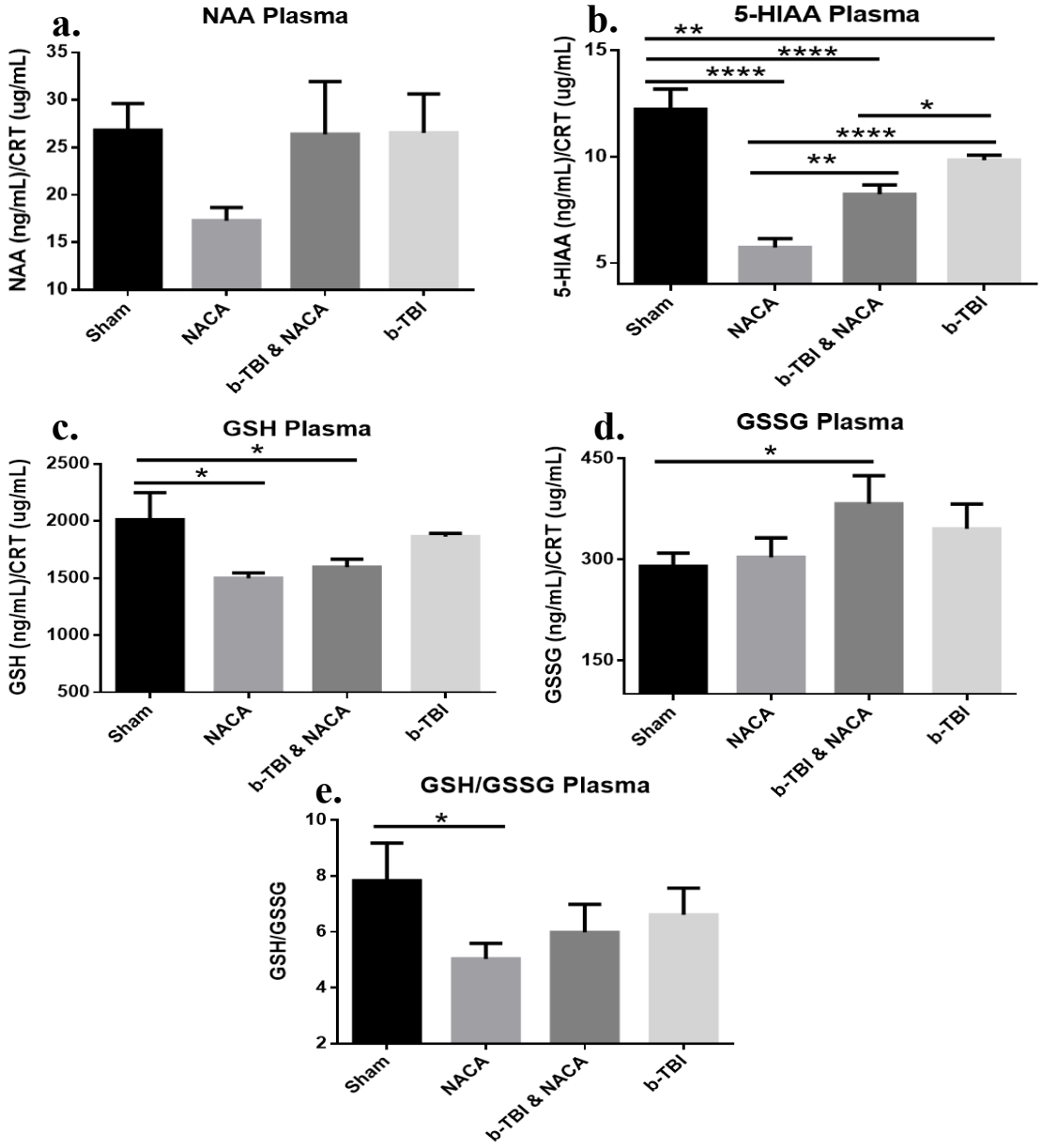

Figure 2. Plasma metabolite levels in Sham; NACA; b-TBI & NACA; and b-TBI groups for a) NAA, b) 5-HIAA, c) GSH, d) GSSG, e) GSH/GSSG ratio. Values represent mean ± SEM (n = 4-6). $p \leq 0.1$ (*), $p \leq 0.05$ (**), $p \leq 0.01$ (***), $p \leq 0.001$ (****). [Sham = no blast + no treatment, NACA = no blast + NACA treatment, b-TBI & NACA = blast + NACA treatment, b-TBI = blast + no treatment].

Table 5. Fisher LSD pairwise comparison of urinary metabolites between different groups in the study. Significant *p*-values and approaching statistical significance *p*-values are in bold font.

	Urine				
Comparison	**NAA**	**5-HIAA**	**GSH**	**GSSG**	**GSH/GSSG**
Sham vs. NACA	0.2229	0.8772	0.1396	0.6183	0.932
Sham vs. b-TBI &NACA	0.4354	**0.0941**	0.5877	0.3113	0.1891
Sham vs. b-TBI	**0.0007**	**0.0071**	0.5435	0.1674	0.6175
NACA vs. b-TBI &NACA	0.674	0.1574	0.373	0.161	0.1856
NACA vs. b-TBI	**0.0001**	**0.0177**	**0.0569**	**0.0807**	0.5787
b-TBI & NACA vs. b-TBI	**0.0003**	0.2913	0.2911	0.7519	0.3838

Other injury models used to evaluate TBI include but are not limited to controlled cortical impact (CCI), fluid percussion injury, impact acceleration, and compressed gas tube injury [48]. The diffuse and heterogenous character of b-TBI in the white matter causes physical damage to the axons and triggers a cascade of secondary mechanisms, of which OS is one [48]. Given the reasons above, in this study, we induced m-TBI with explosive devices as adapted from previous research [43,44]. Furthermore, Insufficient attention is paid to m-TBI as the most common form of TBI, and treatment remains hindered due to a lack of definitive symptoms and biomarkers for prognosis [16,49,50]. As we did in this study, associating small molecule biomarkers with other pathophysiological implications related to TBI provided sufficient evidence of m-TBI's accurate identification and sensitivity to antioxidant therapy. TBI can adversely affect multiple organ systems [9] and cause changes to different peripheral fluids [51]. Control of efflux of compounds by the BBB protects the CNS and regulates brain homeostasis [52].

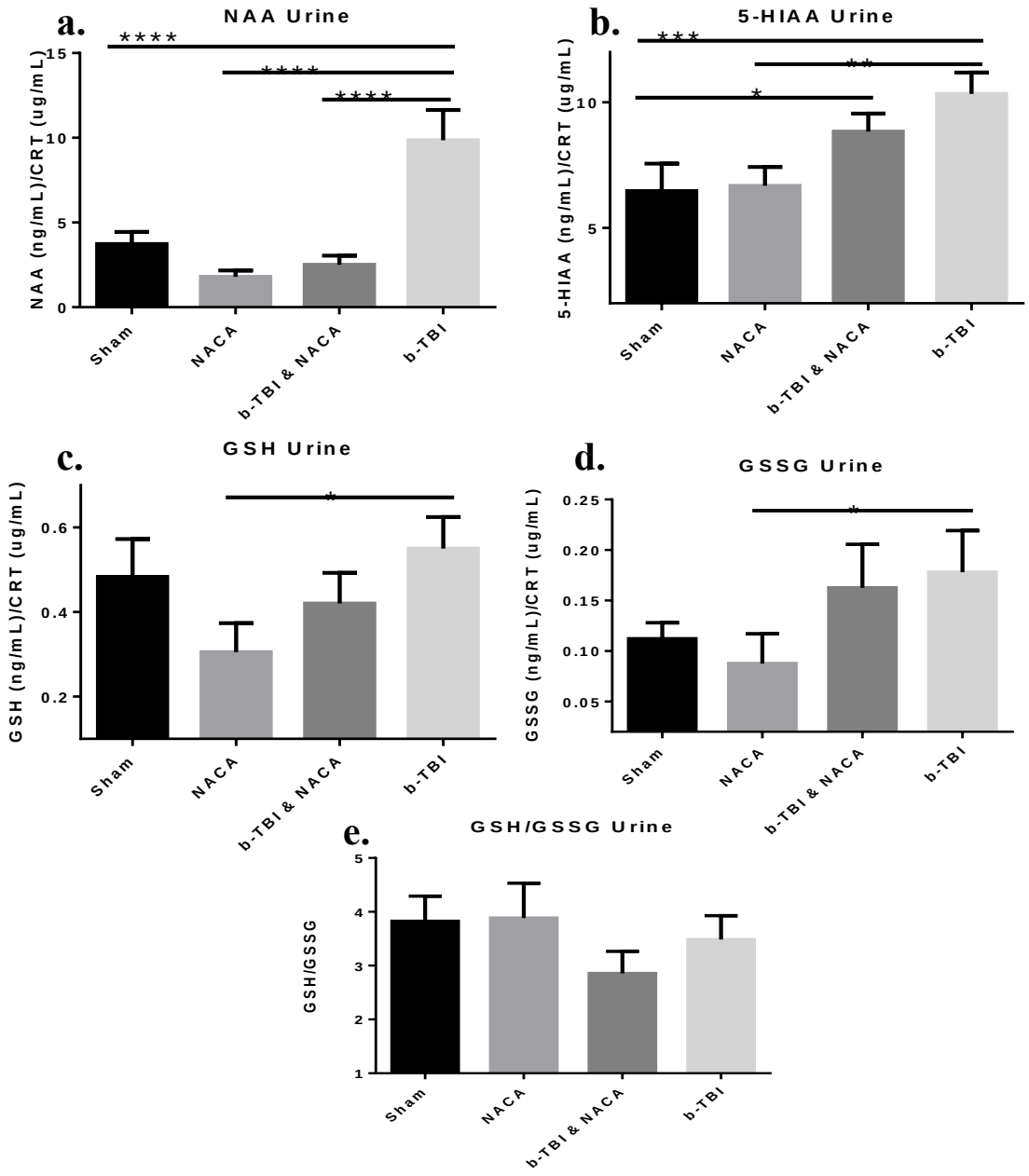

Figure 3. Urinary metabolite levels in Sham; NACA; b-TBI & NACA; and b-TBI groups for a) NAA, b) 5-HIAA, c) GSH, d) GSSG, e) GSH/GSSG ratio. Values represent mean ± SEM (n = 4-6). $p \leq 0.1$ (*), $p \leq 0.05$ (**), $p \leq 0.01$ (***), $p \leq 0.001$ (****). [Sham = no blast + no treatment, NACA = no blast + NACA treatment, b-TBI & NACA = blast + NACA treatment, b-TBI = blast + no treatment]

Consequently, changes can be observed by monitoring specific small molecule biomarkers related to TBI [23,53,54]. Molecular efflux into a peripheral fluid is enhanced for smaller, ionic molecules representing ongoing neurobiological processes in disease and non-disease states [52,55–57]. Additionally, BBB disruption increases this molecular efflux [19]. Our results showed that urinary NAA and 5-HIAA (Figure 3a, b.) increased significantly as a response to b-TBI, and plasma 5-HIAA (Figure 2b) also reduced considerably as a response to b-TBI. Incidentally, increased excitatory amino acids (aspartates) extracellularly and in peripheral fluids were observed as a pathogenesis of TBI [22,58,59]. Additionally, serotonin metabolizes into 5-HIAA and is released into the blood and other peripheral fluids upon inflammation [60].

NAC and NACA both have similar pharmacological activity but different effectiveness [61]. NACA, as an antioxidant therapeutic modality, was also used as an anti-inflammatory and anti-apoptotic agent [61–63]; additionally, NAC was reported to act as a precursor to the most abundant neurotransmitter (glutamate) in the brain that is also a marker of neurotoxicity [61]. In a study that evaluated the reducing power of four antioxidants, NACA>NAC>BHT>**α**-tocopherol was shown in this order [64]; this was ample evidence for the stellar antioxidant capacity of NACA. Indeed, the neuroprotective efficacy of antioxidant therapy is confounded largely on BBB permeability efficiency [55]; conditionally addressing the TBI-induced BBB breakdown with NACA's BBB permeability was shown to improve TBI symptoms [1]. The dysfunction of the BBB also contributes to improving the drug's permeability. NACA's enhanced bioavailability over other antioxidant drugs allows for its usage at lower dosages, thereby reducing the risk of side effects from high dosages.

The full extent of NACA's pharmacokinetic properties is yet to be fully understood [34]. However, studies have shown NACA's neuroprotective mechanism as a GSH prodrug, ROS/RNS scavenger, heavy metal chelator, anti-inflammatory, and disulfide exchanger [3,29]. Additionally, one study proposed NACA to be a NAC prodrug [36]. In summary, these properties make NACA to be a good prooxidant antagonist. The extent and progression of TBI-induced OS can be measured by observing GSH deficiency and GSH/GSSG ratio [51]. The use of NAC and NACA in animal studies for neurological disorders takes different approaches regarding loading mechanisms and dosage, treatment intervals, durations, and routes of administration. Consequently, standardization of antioxidant therapy administration regimens, like dosage and route of administration, will hasten the search for a TBI-effective therapy and solidify NACA's efficacy for the reduction of TBI-related OS [2]. The CNS can recover and adapt to the secondary mechanisms of TBI in a process termed as neuroplasticity, where positive adaptive alterations at the molecular, synaptic, and cellular levels conform structure and function to improve overall cerebral homeostasis [65]. NACA usage can complement neuroplasticity to better improve recovery of cerebral homeostasis. To achieve the full benefit of NACA's efficacy, early administration, dosage, and follow-up treatment of NAC and NACA must be carefully selected and designed to alleviate GSH reduction effectively [1,66]. Incidentally, NACA does not always return GSH to normal levels; instead seeks to minimize the effect of GSH reduction and alleviate some of the symptoms. Additionally, the efficiency of antioxidant therapy is increased when used as both a pre-and post-exposure prophylaxis drug, along with a follow-up treatment after an insult to the head [1,67]. This treatment regimen provides enough antioxidant defenses to

counter initial reactive species, and the follow-up treatment is to bolster the initial treatment and improve treatment outcomes [1]. In this study, NACA's reactive species scavenging property could be observed by the GSH/GSSG ratio being lowest in the b-TBI rats even though GSH levels in the brain tissue were not replenished by NACA treatment (Figure 1c, d, e.). NACA's effectiveness and ability to protect, maintain and restore BBB integrity from methamphetamine-induced OS and neurotoxicity caused one study to propose its application to other neurodegenerative disease like TBI with OS characteristics [68]. The metabolism of excitatory amino acids like NAA in the brain is a factory for ROS generation [21]. Antioxidant therapy with NACA might have an effect of cutting this metabolism short, as we saw in our results, where NACA treatment reduced NAA levels in both healthy and diseased rats. Additionally, depleting NAA concentrations can signal mitochondrial dysfunction [69] from TBI. From our results, we observed that NAA concentrations were depleted in the TBI rats that did not undergo NACA treatment. In summary, both TBI and NACA treatment had effects on NAA levels, as seen in Figure 3a. In peripheral fluids, NACA's downregulatory impact on inflammatory markers [2] (NAA and 5-HIAA) was observed, as shown in Figures 2b and 3a, b.

We observed here that TBI may disturb BBB homeostasis and lead to an unbridled movement of specific small molecules from the brain into the peripheral fluids, suggesting that peripheral fluids may reflect TBI pathogenesis and progression along with therapeutic intervention efficacy [53]. Additionally, NACA treatment was observed to significantly affect some markers of neurotoxicity, inflammation, and oxidation in the brain, plasma, and urine after TBI. This effect may result from the drug's antioxidant

character, bioavailability, and TBI-induced BBB permeability. Interestingly, we observed NACA's action on markers of neurotoxicity and inflammation (NAA and 5-HIAA) in the brain and peripheral fluids even though they are not the main target of the antioxidant therapy, which signifies that NACA may help improve neuroinflammatory and OS-induced metabolic changes. The possibility of NACA to maintain and protect BBB integrity after OS [68] was also noted in this study as the b-TBI rats without NACA treatment tended to have more biomarker levels in urine and plasma than the non-TBI rats and NACA-treated rats, which possibly a result of the efflux and extravasation of small molecules in the brain into the peripheral fluids like urine and blood. Finally, peripheral fluid metabolites' sensitivity to TBI and NACA treatment could mean early detection for patients, which may be able to improve disease monitoring and treatment outcomes.

5. CONCLUSION

In this study, small molecule metabolites of neurotoxicity, inflammation, and oxidation were evaluated in different biomatrices following mild b-TBI and NACA treatment was carried out. The efficacy of antioxidant therapy with NACA on b-TBI was assessed using these biomarkers. Specific markers were found to be sensitive to the mild b-TBI and/or NACA treatment through statistically significant changes in our results. In particular, brain tissue GSH, GSH/GSSG ratio, and NAA, plasma 5-HIAA, and urinary NAA and 5-HIAA were significantly altered following blast and/or treatment. Therefore, NACA may be able to improve inflammation and OS-induced metabolic changes arising from b-TBI. These results showed the interconnection between TBI localized in the brain

and responses observed in peripheral fluids like urine and plasma, showing evidence of possible BBB breach following TBI. Additionally, this study suggests that NACA treatment can be evaluated by taking advantage of this interconnectedness. Finally, we observed that the severity of the TBI correlates directly with OS and neuroinflammatory biomarkers observed. Further efforts to understand the relationship between the neuropathological mechanisms of TBI and NACA should be carried out to establish NACA's utility as a TBI therapeutic fully.

ACKNOWLEDGEMENTS AND FUNDING INFORMATION

The Leonard Wood Institute supported this study through a cooperative agreement with the US Army Research Laboratory (W911NF-14-2-0034). The Acute Effects of Neurotrauma Consortium also facilitated this research. The views and conclusions contained in this document are those of the authors. They should not be interpreted as representing the official policies, either expressed or implied, of the Leonard Wood Institute, the Army Research Laboratory, or the U.S. Government. The U.S. Government is authorized to reproduce and distribute reprints for government purposes, notwithstanding any copyright notation herein.

CONFLICT OF INTEREST

The authors declare the absence of conflicts of interest financially or in any other capacity.

CREDIT AUTHORSHIP CONTRIBUTION STATEMENT

Olajide Adetunji: Investigation, Methodology, Validation, Writing- original draft preparation.

Jiandong Wu: Investigation, Methodology, Validation, Editing.

Annalise Pfaff: Visualization, Writing – review & editing.

Austin Sigler: Methodology.

Mousumi Bose: Formal analysis.

Catherine Johnson: Conceptualization, Supervision, Funding acquisition.

Nuran Ercal: Conceptualization, Supervision, Funding acquisition, Writing – review & editing.

Honglan Shi: Conceptualization, Supervision, Funding acquisition, Writing – review & editing.

Paul Nam: Conceptualization, Supervision, Funding acquisition, Writing – review & editing.

LIST OF ABBREVIATIONS

TBI- Traumatic Brain Injury

BBB- Blood-Brain Barrier

GSH- Glutathione

NACA- *N*-Acetylcysteine Amide

b-TBI- Blast Induced TBI

m-TBI- Mild-TBI

DAI- Diffuse Axonal Injury

ROS- Reactive Oxygen Species

RNS- Reactive Nitrogen Species

NAC- *N*-Acetylcysteine

CNS- Central Nervous System

BHT- Butylated Hydroxytoluene

NAA- *N*-Acetyl Aspartic Acid

5-HIAA- 5-Hydroxyindoleacetic Acid

GSSG- Glutathione Disulfide

4-HNE- 4-Hydroxynonenal

F2a- F2α-Isoprostane

IS- Internal Standards

NEM- *N*-Ethylmaleimide

LOD- Limit of detection

HPLC-MS/MS- High Performance-Tandem Mass Spectrometry

BOP- Blast Overpressure

REFERENCES

[1] U. Kawoos, R.M. McCarron, M. Chavko, Protective effect of N-acetylcysteine amide on blast-induced increase in intracranial pressure in rats, Front Neurol 8 (2017) 1–8. https://doi.org/10.3389/fneur.2017.00219.

[2] J. Bhatti, B. Nascimento, U. Akhtar, S.G. Rhind, H. Tien, A. Nathens, L.T. da Luz, Systematic review of human and animal studies examining the efficacy and safety of N-acetylcysteine (NAC) and N-Acetylcysteine Amide (NACA) in traumatic brain injury: Impact on neurofunctional outcome and biomarkers of oxidative stress and inflammation, Front Neurol 8 (2018). https://doi.org/10.3389/fneur.2017.00744.

[3] K. Eakin, R. Baratz-Goldstein, C.G. Pick, O. Zindel, C.D. Balaban, M.E. Hoffer, M. Lockwood, J. Miller, B.J. Hoffer, Efficacy of N-acetyl cysteine in traumatic brain injury, PLoS One 9 (2014) 1–7. https://doi.org/10.1371/journal.pone.0090617.

[4] A.I.R. Maas, D.K. Menon, P.D. David Adelson et al., Traumatic brain injury: Integrated approaches to improve prevention, clinical care, and research, Lancet Neurol 16 (2017) 987–1048. https://doi.org/10.1016/S1474-4422(17)30371-X.

[5] H.M. Bramlett, W.D. Dietrich, Long-Term Consequences of Traumatic Brain Injury: Current Status of Potential Mechanisms of Injury and Neurological Outcomes, J Neurotrauma 32 (2015) 1834–1848. https://doi.org/10.1089/neu.2014.3352.

[6] D. Thurman et al., Traumatic Brain Injury in the United States: A Report to Congress, Centers for Disease Control, (1999). http://www.cdc.gov/traumaticbraininjury/pdf/tbi_in_ the_us.pdf.

[7] D.J. Thurman, C. Alverson, K.A. Dunn, J. Guerrero, J.E. Sniezek, Traumatic brain injury in the United States: A public health perspective, Journal of Head Trauma Rehabilitation 14 (1999) 602–615. https://doi.org/10.1097/00001199-199912000-00009.

[8] J.D. Pandya, R.D. Readnower, S.P. Patel, H.M. Yonutas, J.R. Pauly, G.A. Goldstein, A.G. Rabchevsky, P.G. Sullivan, N-acetylcysteine amide confers neuroprotection, improves bioenergetics and behavioral outcome following TBI, Exp Neurol 257 (2014) 106–113. https://doi.org/10.1016/j.expneurol.2014.04.020.

[9] S.S.K. Gaddam, T. Buell, C.S. Robertson, Systemic manifestations of traumatic brain injury, 1st ed., Elsevier B.V., 2015. https://doi.org/10.1016/B978-0-444-52892-6.00014-3.

[10] A.C. McKee, M.E. Robinson, A. Dement Author manuscript, Military-related traumatic brain injury and neurodegeneration NIH Public Access Author Manuscript, Alzheimers Dement 10 (2014) 242–253. https://doi.org/10.1016/j.jalz.2014.04.003.Military-related.

[11] R.S. Bell, A.H. Vo, C.J. Neal, J. Tigno, R. Roberts, C. Mossop, J.R. Dunne, R.A. Armonda, Military Traumatic Brain and Spinal Column Injury: A 5-Year Study of the Impact Blast and Other Military Grade Weaponry on the Central Nervous System, Journal of Trauma: Injury, Infection & Critical Care 66 (2009) S104–S111. https://doi.org/10.1097/TA.0b013e31819d88c8.

[12] N. Khatri, M. Thakur, V. Pareek, S. Kumar, S. Sharma, A.K. Datusalia, Oxidative Stress: Major Threat in Traumatic Brain Injury, CNS Neurol Disord Drug Targets 17 (2018) 689–695. https://doi.org/10.2174/1871527317666180627120501.

[13] B.J.Zink. Greve, Mark W., Pathophysiology of traumatic brain injury., Mount Sinai Journal of Medicine: A Journal of Translational and Personalized Medicine: A Journal of Translational and Personalized Medicine 76, (2009) 97-104. https://doi.org/10.1002/MSJ.

[14] D.H. Smith, D.F. Meaney, W.H. Shull, Diffuse axonal injury in head trauma, Journal of Head Trauma Rehabilitation 18 (2003) 307–316. https://doi.org/10.1097/00001199-200307000-00003.

[15] S.Y. Ng, A.Y.W. Lee, Traumatic Brain Injuries: Pathophysiology and Potential Therapeutic Targets, Front Cell Neurosci 13 (2019) 1–23. https://doi.org/10.3389/fncel.2019.00528.

[16] P. Leo, M. McCrea, Epidemiology. In: Laskowitz D, Grant G, editors. Translational Research in Traumatic Brain Injury. Boca Raton (FL): CRC Press/Taylor and Francis Group; 2016. Chapter 1. Available from: https://www.ncbi.nlm.nih.gov/books/NBK326722/, (n.d.).

[17] A. Frati, D. Cerretani, A.I. Fiaschi, P. Frati, V. Gatto, R. La Russa, A. Pesce, E. Pinchi, A. Santurro, F. Fraschetti, V. Fineschi, Diffuse axonal injury and oxidative stress: A comprehensive review, Int J Mol Sci 18 (2017) 1–20. https://doi.org/10.3390/ijms18122600.

[18] H.M. Yonutas, H.J. Vekaria, P.G. Sullivan, Mitochondrial specific therapeutic targets following brain injury, Elsevier, 2016. https://doi.org/10.1016/j.brainres.2016.02.007.

[19] K. Song, Y. Li, H. Zhang, N. An, Y. Wei, L. Wang, C. Tian, M. Yuan, Y. Sun, Y. Xing, Y. Gao, J.F. Santibañez, Oxidative Stress-Mediated Blood-Brain Barrier (BBB) Disruption in Neurological Diseases, Oxid Med Cell Longev 2020 (2020). https://doi.org/10.1155/2020/4356386.

[20] I. Liguori, G. Russo, F. Curcio, G. Bulli, L. Aran, D. Della-Morte, G. Gargiulo, G. Testa, F. Cacciatore, D. Bonaduce, P. Abete, Oxidative stress, aging, and diseases, Clin Interv Aging 13 (2018) 757–772. https://doi.org/10.2147/CIA.S158513.

[21] B. Uttara, A. V Singh, P. Zamboni, R.T. Mahajan, Oxidative Stress and Neurodegenerative Diseases : A Review of Upstream and Downstream Antioxidant Therapeutic Options, (2009) 65–74.

[22] S.K. Ray, C.E. Dixon, N.L. Banik, Molecular mechanisms in the pathogenesis of traumatic brain injury, Histol Histopathol 17 (2002) 1137–1152.

[23] A. Dadas, J. Washington, R. Diaz-Arrastia, D. Janigro, Biomarkers in traumatic brain injury (TBI): a review, Neuropsychiatr Dis Treat Volume 14 (2018) 2989–3000. https://doi.org/10.2147/NDT.S125620.

[24] V. Ebrahimi, Z. Gholinejad, N-Acetylcysteine amide and central nervous system: human studies and animal models, 4 (2023) 39–45. https://doi.org/10.30495/jbcvm.2023.1978678.1036.

[25] A.L. Walker, S.Z. Imam, R.A. Roberts, Drug discovery and development: Biomarkers of neurotoxicity and neurodegeneration, Exp Biol Med 243 (2018) 1037–1045. https://doi.org/10.1177/1535370218801309.

[26] R. Sharma, D.T. Laskowitz, Biomarkers in traumatic brain injury, Curr Neurol Neurosci Rep 12 (2012) 560–569. https://doi.org/10.1007/s11910-012-0301-8.

[27] J.R. Kulbe, J.W. Geddes, Current status of fluid biomarkers in mild traumatic brain injury, Exp Neurol 275 (2016) 334–352. https://doi.org/10.1016/j.expneurol.2015.05.004.

[28] F.K. Pearl Chung, Traumatic Brain Injury (TBI): Overview of Diagnosis and Treatment, J Neurol Neurophysiol 05 (2013) 1–10. https://doi.org/10.4172/2155-9562.1000182.

[29] A.R. Pfaff, J. Beltz, E. King, N. Ercal, Medicinal Thiols: Current Status and New Perspectives, Mini-Reviews in Medicinal Chemistry 20 (2019) 513–529. https://doi.org/10.2174/1389557519666191119144100.

[30] M. Zafarullah, W.Q. Li, J. Sylvester, M. Ahmad, Molecular mechanisms of N-acetylcysteine actions, Cellular and Molecular Life Sciences 60 (2003) 6–20. https://doi.org/10.1007/s000180300001.

[31] H.J. Forman, H. Zhang, Targeting oxidative stress in disease: promise and limitations of antioxidant therapy, Nat Rev Drug Discov 20 (2021) 689–709. https://doi.org/10.1038/s41573-021-00233-1.

[32] H.J. Forman, H. Zhang, A. Rinna, Glutathione: Overview of its protective roles, measurement, and biosynthesis, Mol Aspects Med 30 (2009) 1–12. https://doi.org/10.1016/j.mam.2008.08.006.

[33] S. Tobwala, N. Ercal, N-acetylcysteine amide (NACA), a novel GSH prodrug: Its metabolism and implications in health, 2013.

[34] S. Tobwala, A. Khayyat, W. Fan, N. Ercal, Comparative evaluation of N-acetylcysteine and N-acetylcysteineamide in acetaminophen-induced hepatotoxicity in human hepatoma HepaRG cells, Exp Biol Med 240 (2015) 261–272. https://doi.org/10.1177/1535370214549520.

[35] J.R. Martin, T.A., Causey, D.H., Sheffner, A.L., Wheeler, A.G., Corrigan, Amides of N-Acylcysteines as mucolytic agents., J. Med. Chem. 10, 1172–1176 (1967) 89. http://www.nber.org/papers/w16019.

[36] R. He, W. Zheng, T. Ginman, H. Ottosson, S. Norgren, Y. Zhao, M. Hassan, Pharmacokinetic profile of N-acetylcysteine amide and its main metabolite in mice using new analytical method, European Journal of Pharmaceutical Sciences 143 (2020) 105158. https://doi.org/10.1016/j.ejps.2019.105158.

[37] K.K.W. Wang, A. Moghieb, Z. Yang, Z. Zhang, Systems biomarkers as acute diagnostics and chronic monitoring tools for traumatic brain injury, Sensing Technologies for Global Health, Military Medicine, and Environmental Monitoring III 8723 (2013) 87230O. https://doi.org/10.1117/12.2020030.

[38] S.G. Lee, J. Yim, Y. Lim, J.H. Kim, Validation of a liquid chromatography tandem mass spectrometry method to measure oxidized and reduced forms of glutathione in whole blood and verification in a mouse model as an indicator of oxidative stress, J Chromatogr B Analyt Technol Biomed Life Sci 1019 (2016) 45–50. https://doi.org/10.1016/j.jchromb.2015.10.041.

[39] E. Liemburg, A. Sibeijn-Kuiper, L. Bais, G. Pijnenborg, H. Knegtering, J. Van Der Velde, E. Opmeer, A. De Vos, J. Dlabac-De Lange, L. Wunderink, A. Aleman, Prefrontal NAA and Glx Levels in Different Stages of Psychotic Disorders: A 3T 1 H-MRS Study, Sci Rep 6 (2016) 1–8. https://doi.org/10.1038/srep21873.

[40] G. Tsai, J.T. Coyle, N-Acetylaspartate in neuropsychiatric disorders, Prog Neurobiol 46 (1995) 531–540. https://doi.org/10.1016/0301-0082(95)00014-M.

[41] H.S. Lee, S.M. Kim, J.H. Jang, H.D. Park, S.Y. Lee, Serum 5-hydroxyindoleacetic acid and ratio of 5-hydroxyindoleacetic acid to serotonin as metabolomics indicators for acute oxidative stress and inflammation in vancomycin-associated acute kidney injury, Antioxidants 10 (2021). https://doi.org/10.3390/antiox10060895.

[42] D. Tsikas, Assessment of lipid peroxidation by measuring malondialdehyde (MDA) and relatives in biological samples: Analytical and biological challenges, Anal Biochem 524 (2017) 13–30. https://doi.org/10.1016/j.ab.2016.10.021.

[43] H. Song, J. Cui, A. Simonyi, C.E. Johnson, G.K. Hubler, R.G. DePalma, Z. Gu, Linking blast physics to biological outcomes in mild traumatic brain injury: Narrative review and preliminary report of an open-field blast model, Behavioural Brain Research 340 (2018) 147–158. https://doi.org/10.1016/j.bbr.2016.08.037.

[44] H. Song, L.M. Konan, J. Cui, C.E. Johnson, M. Langenderfer, D.A. Grant, T. Ndam, A. Simonyi, T. White, U. Demirci, D.R. Mott, D. Schwer, G.K. Hubler, I. Cernak, R.G. DePalma, Z. Gu, Ultrastructural brain abnormalities and associated behavioral changes in mice after low-intensity blast exposure, Behavioural Brain Research 347 (2018) 148–157. https://doi.org/10.1016/j.bbr.2018.03.007.

[45] C. Johnson, K. Graham, I. Cernak, A. Zuckerman, G. Ralph, C. Johnson, Open-field blast (OFB) model in mice Jiankun, (2023) 1–6.

[46] D.R.S. Middleton, M.J. Watts, D.A. Polya, A comparative assessment of dilution correction methods for spot urinary analyte concentrations in a UK population exposed to arsenic in drinking water, Environ Int 130 (2019) 104721. https://doi.org/10.1016/j.envint.2019.03.069.

[47] L. Cao, D. Waldon, Y. Teffera, J. Roberts, M. Wells, M. Langley, Z. Zhao, Ratios of biliary glutathione disulfide (GSSG) to glutathione (GSH): A potential index to screen drug-induced hepatic oxidative stress in rats and mice, Anal Bioanal Chem (2013).

[48] B.Michael. Su Eric, Diffuse Axonal Injury. In: Laskowitz D, Grant G, editors. Translational Research in Traumatic Brain Injury. Boca Raton (FL): CRC Press/Taylor and Francis Group; 2016. Chapter 3. Available from: https://www.ncbi.nlm.nih.gov/books/NBK326722/, (n.d.).

[49] J.D. Cassidy, L.J. Carroll, P.M. Peloso, J. Borg, H. von Holst, L. Holm, J. Kraus, V.G. Coronado, Incidence, risk factors and prevention of mild traumatic brain injury: Results of the WHO Collaborating Centre Task Force on Mild Traumatic Brain Injury, J Rehabil Med Suppl (2004) 28–60. https://doi.org/10.1080/16501960410023732.

[50] L.J. Carroll, J.D. Cassidy, P.M. Peloso, J. Borg, H. von Holst, L. Holm, C. Paniak, M. Pépin, Prognosis for mild traumatic brain injury: Results of the WHO Collaborating Centre Task Force on Mild Traumatic Brain Injury, J Rehabil Med Suppl (2004) 84–105. https://doi.org/10.1080/16501960410023859.

[51] N. Ballatori, S.M. Krance, S. Notenboom, S. Shi, K. Tieu, C.L. Hammond, Glutathione dysregulation and the etiology and progression of human diseases, Biol Chem 390 (2009) 191–214. https://doi.org/10.1515/BC.2009.033.

[52] R. Gabathuler, Approaches to transport therapeutic drugs across the blood-brain barrier to treat brain diseases, Neurobiol Dis 37 (2010) 48–57. https://doi.org/10.1016/j.nbd.2009.07.028.

[53] V. Ramaswamy, J. Horton, B. Vandermeer, N. Buscemi, S. Miller, J. Yager, Systematic Review of Biomarkers of Brain Injury in Term Neonatal Encephalopathy, Pediatr Neurol 40 (2009) 215–226. https://doi.org/10.1016/j.pediatrneurol.2008.09.026.

[54] A. Sigler, J. Wu, A. Pfaff, O. Adetunji, P. Nam, D. James, C. Burton, H. Shi, Repeated Low-Level Blast Exposure Alters Urinary and Serum Metabolites, Metabolites 13 (2023). https://doi.org/10.3390/metabo13050638.

[55] A.K. Ottens, J.E. Stafflinger, H.E. Griffin, R.D. Kunz, D.X. Cifu, J.P. Niemeier, Post-acute brain injury urinary signature: A new resource for molecular diagnostics, J Neurotrauma 31 (2014) 782–788. https://doi.org/10.1089/neu.2013.3116.

[56] H. Kusuhara, Y. Sugiyama, Active efflux across the blood-brain barrier: Role of the solute carrier family, NeuroRx 2 (2005) 73–85. https://doi.org/10.1602/neurorx.2.1.73.

[57] K.A. Witt, T.J. Gillespie, J.D. Huber, R.D. Egleton, T.P. Davis, Peptide drug modifications to enhance bioavailability and blood-brain barrier permeability., Peptides (N.Y.) 22 (2001) 2329–2343. https://doi.org/10.1016/S0196-9781(01)00537-X.

[58] A.I. Faden, P. Demediuk, S.S. Panter, R. Vink, The role of excitatory amino acids and NMDA receptors in traumatic brain injury, Science (1979) 244 (1989) 798–800. https://doi.org/10.1126/science.2567056.

[59] A.M. Palmer, D.W. Marion, M.L. Botscheller, P.E. Swedlow, S.D. Styren, S.T. DeKosky, Traumatic Brain Injury-Induced Excitotoxicity Assessed in a Controlled Cortical Impact Model, J Neurochem 61 (1993) 2015–2024. https://doi.org/10.1111/j.1471-4159.1993.tb07437.x.

[60] S. Bolandparvaz, M. Vasei, A.A. Owji, N. Ata-Ee, A. Amin, Y. Daneshbod, S.V. Hosseini, Urinary 5-hydroxy indole acetic acid as a test for early diagnosis of acute appendicitis, Clin Biochem 37 (2004) 985–989. https://doi.org/10.1016/j.clinbiochem.2004.07.003.

[61] K. Sunitha, M. Hemshekhar, R.M. Thushara, M.S. Santhosh, M. Yariswamy, K. Kemparaju, K.S. Girish, N-Acetylcysteine amide: A derivative to fulfill the promises of N-Acetylcysteine, Free Radic Res 47 (2013) 357–367. https://doi.org/10.3109/10715762.2013.781595.

[62] A. Banerjee, M.B. Trueblood, X. Zhang, K.R. Manda, P. Lobo, P.D. Whitefield, D.E. Hagen, N. Ercal, N-acetylcysteineamide (NACA) prevents inflammation and oxidative stress in animals exposed to diesel engine exhaust, Toxicol Lett 187 (2009) 187–193. https://doi.org/10.1016/j.toxlet.2009.02.022.

[63] T. Benterud, M.B. Ystgaard, S. Manueldas, L. Pankratov, C. Alfaro-Cervello, G. Florholmen, M.S. Ahmed, L. Sandvik, S. Norgren, M. Bjørås, L.O. Baumbusch, R. Solberg, O.Di. Saugstad, N-Acetylcysteine Amide Exerts Possible Neuroprotective Effects in Newborn Pigs after Perinatal Asphyxia, Neonatology 111 (2016) 12–21. https://doi.org/10.1159/000447255.

[64] B. Ates, L. Abraham, N. Ercal, Antioxidant and free radical scavenging properties of N-acetylcysteine amide (NACA) and comparison with N-acetylcysteine (NAC), 42 (2008) 372–377. https://doi.org/10.1080/10715760801998638.

[65] Y. Sophie Su, A. Veeravagu, G. Grant, Neuroplasticity after Traumatic Brain Injury. In: Laskowitz D, Grant G, editors. Translational Research in Traumatic Brain Injury. Boca Raton (FL): CRC Press/Taylor and Francis Group; 2016. Chapter 8. Available from: https://www.ncbi.nlm.nih.gov/books/NBK, (n.d.).

[66] Y. Xiong, P.L. Peterson, C.P. Lee, Effect of N-acetylcysteine on mitochondrial function following traumatic brain injury in rats, J Neurotrauma 16 (1999) 1067–1082. https://doi.org/10.1089/neu.1999.16.1067.

[67] M.E. Hoffer, C. Balaban, M.D. Slade, J.W. Tsao, B. Hoffer, Amelioration of Acute Sequelae of Blast Induced Mild Traumatic Brain Injury by N-Acetyl Cysteine: A Double-Blind, Placebo Controlled Study, PLoS One 8 (2013) 1–10. https://doi.org/10.1371/journal.pone.0054163.

[68] X. Zhang, A. Banerjee, W.A. Banks, N. Ercal, N-Acetylcysteine amide protects against methamphetamine-induced oxidative stress and neurotoxicity in immortalized human brain endothelial cells, Brain Res 1275 (2009) 87–95. https://doi.org/10.1016/j.brainres.2009.04.008.

[69] R. Heales, S.E.C. Davies, T.E. Bates, J.B. Clark, Depletion of brain glutathione is accompanied by impaired mitochondrial function and decreased N-acetyl aspartate concentration, Neurochem Res 20 (1995) 31–38. https://doi.org/10.1007/BF00995149.

III. HIGH-THROUGHPUT MONITORING OF RESIDUAL SOLVENTS IN PHARMACEUTICAL PRODUCTS USING A PORTABLE ON-LINE PRE-CONCENTRATION GC-PID

Olajide Adetunji, Sargun Kaur, Nicole Wheeler, Victor Nam, Honglan Shi, Paul Nam *

Department of Chemistry, Center for Biomedical Research, Missouri University of Science and Technology, Rolla, MO, 65409, USA

ABSTRACT

Pharmaceutical manufacturing utilizes solvents at different stages of production. Some of the harmful solvent residuals may be retained in the final product; therefore, they need to be monitored for quality control and to meet the regulation requirement. Here, a novel method capable of rapidly analyzing residual solvents in pharmaceutical products was developed using a compact-portable gas chromatography with a photoionization detector (GC-PID). The system consists of modified Tedlar® bag sampling, online pre-concentration, separation of volatiles by miniaturized GC, and micro-PID detection. The limits of detections for the residual solvents in the method were in the range of 26.00 – 52.03 pg/mL which is much lower than the pharmaceutical compliance concentration limits. Limits of detection > 520 pg of analyte/g of drug was also determined for the over-the-counter drugs tested with this method. The method performance showed rapidity (3.8 mins total run time), good calibration linearity ($r^2 <$ 0.99), and reproducibility of retention time (RSD < 0.4%), which allowed direct analysis of residual solvents from solid samples without the need for complex sample preparation. The method was validated using over-the-counter pharmaceutical products. It yielded

good accuracy (recovery > 91.2%) and precision (RSD < 6.5%) for the selected residual solvents, including 1,4-dioxane, benzene, chlorobenzene, cyclohexane, o-, m-,p-xylene, and toluene. This method is expected to have broad applications in pharmaceutical production and quality control.

Keywords- volatile residual solvents, portable GC with photoionization detector, pharmaceutical products, on-line pre-concentration

GRAPHICAL ABSTRACT

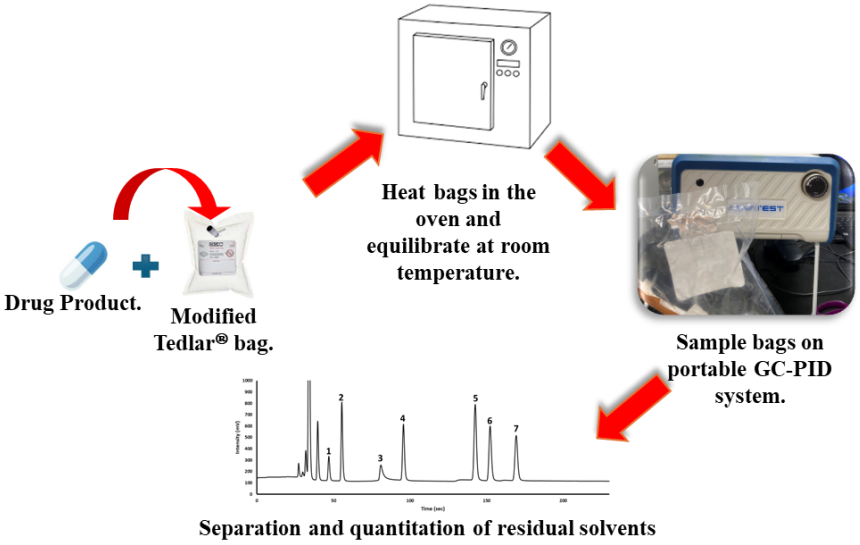

1. INTRODUCTION/ BACKGROUND

Residual solvents (RS) and volatile organic impurities in pharmaceutical products both represent the same class of compounds that are commonly used as catalysts or vehicles to carry out synthesis, purification, and formulation of bioactive molecules and

excipients used in the production process [1,2]. However, trace levels of these solvents may remain in the final product. Consequently, their use is critical and impacts product yield, the morphology of active pharmaceutical ingredient crystals, purity, and overall production efficiency of drug products [2–4]. Additionally, RS presence, as well as harmful RS-generated chemicals in the final drug product, may result in contamination during storage, packaging, and transportation, thereby changing the morphology, efficacy, bioavailability, odor, and taste of the final drug product [1,5], which is a concern for both producers and consumers of the drug [1,6,7]. Complete removal of these RS in the final product is necessary but can be arduous and near impossible [1,8–10]. Extensive efforts by manufacturers to minimize these RS can be pretty costly [1,2]. Some of the RS have been implicated as carcinogens and neurotoxins, which jeopardize the safe use of therapeutics. They also contribute to unfavorable environmental pollution [8–10]. Therefore, the drug manufacturing process is strictly controlled to ensure compliance with the set exposure limits deemed safe for patients to use within a certain period. These concentration limits have been set using risk-benefit assessment [10] to evaluate the impending risk of the use and presence of specific RS. The therapeutic benefits of the drug product are routinely assessed in comparison with the risks posed by the presence of unsafe RS. The concentration limits of undesirable RS during the manufacturing processes and in final products were set independently and generally agreed upon by many regulatory bodies [1]. They serve as the yardstick for set limits and methodologies of RS detection. RS are ranked in four categories based on toxicity [3], where the class 1 solvents are the most restricted for use due to their higher toxicity. Exposure limits are non-existent for class 1 because they should be avoided; however, their use is permitted if

a risk-benefit assessment shows excellent benefit in the therapeutic product. Their permissible limits are commonly in the ppm range. Although alternative solvents [1,11], like water, supercritical fluids, and ionic fluids, have been employed in drug manufacturing [1], the use of more common solvents and the presence of RS will likely continue. Although pharmacopeia-recommended analytical methods exist, there is still a pressing need to develop fast and efficient methods that are easily adaptable for monitoring RS in various pharmaceutical products [12].

Compliance with the pharmacopeia set limits by manufacturers is a criterion for drug products to move into the market. RS detection and control are the general precepts crucial for ensuring the safety, quality, and efficacy of pharmaceutical products for patients. However, the pharmaceutical industry considers the RS determination in drug substances with analytical processes complex and demanding [13]. Methodologies for RS evaluation range from a simple “loss-on-drying” method to more accurate chromatographic techniques [9]. The loss-on-drying method is accepted for class 3 RS with high limits [10,12]. Chromatographic methods are highly recommended for classes 1 and 2 RS because they provide necessary specificity, sensitivity, and eliminate the effect of external factors like humidity [12]. Due to most residual solvents' volatility and thermal stability, gas chromatographic (GC) analysis is the gold standard [1,14]. High-pressure liquid chromatography is also employed for analyzing the relatively non-volatile RS. Another factor to consider for RS analysis is sampling [14]. The solid phase micro-extraction (SPME) and headspace (HS) sampling methods are employed for the volatile analysis of solid and liquid pharmaceutical samples. GC analysis of RS is conducted with a detector that may be mass spectrometry (MS), Fourier transform infrared spectroscopy

(FTIR), and flame ionization detectors (FID). However, they are expensive, complex, and/or bulky instrumentations [9,15], which do not bode well for placement in fast-paced pharmaceutical manufacturing facilities. Static HS-GC-FID method is recommended by various pharmacopeias [3,8] for RS determination [3,8,9,12] but it has limited sensitivity and selectivity [16]. Photoionization detectors can be miniaturized and provide comparable sensitivity to RS. Combining PID detection with an easy-to-use portable GC system will benefit RS monitoring since it can satisfy the growing demand for convenience, versatility, and instrumentation portability [17].

Herein, we developed and validated an analytical method using a portable GC-PID system capable of simultaneously monitoring and quantifying selected RS in drug products from different ICH (The International Council for Harmonisation of Technical Requirements for Pharmaceuticals for Human Use) classifications. This study aims to simplify RS analysis by combining direct sampling of solid drug samples with an easy-to-use portable GC-PID system with online pre-concentration to provide a viable alternative to existing RS analysis methods.

2. MATERIALS AND METHODS

2.1. CHEMICALS AND REAGENTS

Reagent grade cyclohexane, toluene, and m-, o-, and p-xylene were purchased from Sigma Aldrich (St. Louis, MO, USA). 1,4-dioxane, benzene, chlorobenzene, and ethylbenzene were purchased from Acros Organics (Fairlawn, NJ, USA). Optima grade hexane used as a diluent was purchased from Fisher chemicals (Hampton, NH, USA). All standards had purities ranging from 98% to 100%. Tedlar® sampling bags (0.5 L) with

polypropylene fittings were purchased from SKC (Dorset, UK). High-purity 95 mL disposable helium gas canisters were acquired from Leland Gas Technologies (South Plainfield, NJ, USA). Excedrin®, Bayer® Plus aspirin, Bayer® low dose aspirin, and equate™ acetaminophen over the counter (OTC) drugs used as drug matrix were purchased from a local pharmacy.

2.2. STANDARD PREPARATION AND CALIBRATION

Individual stock solution of each solvent was prepared by dissolving 3mL of the pure reference standard in 5mL hexanes as the diluent. From the individual stock solution, a standard mixture was prepared by combining an equal volume of all stock solution standards in the same vial to make the working solution mixture at the concentration of 1 mg/mL of each standard. Calibration standard solutions were prepared in 0.5 L Tedlar® bags adequately filled with N2 gas by injecting 5 µL of working solutions into each Tedlar® bag. The final concentration in the Tedlar® bag corresponds to a 100,000-fold dilution, which yielded a final concentration in the Tedlar® bag of 10 ng/mL.

2.3. TEDLAR® BAG SAMPLING METHOD

Tedlar® bags (0.5 L) equipped with single propylene fitting were modified to accommodate solid matrix sampling by making a small slit diagonally at one of the bottom edges of the bag. The bag opening was resealed using a combination of tapes and clamps. The integrity of the tapes was tested by filling the modified bags with N_2 and checking for leaks before placing them in the oven. For calibration standards, resealed

bags were filled to volume with N_2, and 5 µL of the standard mixture was introduced through the polypropylene fitting on the 0.5 L bag. A similar procedure occurs for the drug matrix analysis; however, an extra step of inserting the drug matrix into the bag is done as well. Drug products were prepared by crushing the OTC tablet to a fine powder with a handheld mortar and pestle and transferring the appropriate weight amount into the bag via the slit made, and then resealing the bag. The bags were then placed in the oven at 60 oC for at least 20 mins for volatilization of RS and equilibrated at room temperature for at least 20 mins. The bags can be stored at constant room temperature after preparation for up to a day without any significant change. Nitrogen was used to fill the bags.

2.4. PORTABLE GC-PID

A compact NovaTest P100L – dimension, 36 x 30 x 15 cm, 7 kg in weight- GC (Nanova Environmental, Columbia, MO, USA) with a thermal desorption unit ideal for low concentration detections (ppb range) was used for analyzing the residual solvents. The P100L, with patented microfluidic and micro-electro-mechanical systems (MEMS) technology, uses helium in a portable, easily disposable canister as a carrier gas. A sampling unit pumps the sample into a volatile organic compound (VOC) trapping unit (pre-concentrator, desorption occurs at 300 ^{o}C in less than 0.5 sec). The trapping unit concentrates the sample before releasing it into a GC capillary column for separation and detection by the micro-PID (10.6 eV). The column temperature can go up to 200 ^{o}C, and sampling time can be adjusted as needed. An optional 11.7 eV Ultraviolet lamp detection unit is also available for the instrument. The online pre-concentrator is made up of

Carboxen 1018 beads packing as adsorbent material with insulated copper wire wrapping for thermal desorption and a thermocouple for temperature monitoring.

2.5. CHROMATOGRAPHY CONDITIONS

The system's sampling rate was 10 ml/min, and a pre-concentration sampling time of 1.5 mins was used with a system carrier gas pressure of 10 psi. Separation was achieved with a GC capillary column (RTX-VMSTM GC column., Restek Corp, Bellefonte, PA, USA.) 10 m in length (0.25 mm i.d. and 1.40 µm film thickness). The initial waiting time was 0 sec (time before sample collection to allow for system heat-up), and the waiting time (time after sampling but before sample injection into the system) was set to be 30 sec. The initial column oven temperature of 50 ^{o}C was maintained for 30 secs after sample introduction and then ramped up at a rate of 15 ^{o}C/min with no hold time to a final temperature (Temp 1) of 100 ^{o}C. Additionally, an optional secondary higher or equivalent temperature to heat the column and enhance analyte movement was set at no hold time, ramp rate of 30 ^{o}C and final temperature (Temp 2) of 100 ^{o}C. The total run time was 3.8 mins.

3. RESULTS AND DISCUSSION

The need for new, improved, and simplified analytical methodologies for accurate and precise quantitation of RS is never-ending. The choice of sampling method plays a vital role in achieving this. Advanced techniques like SPME and HS injection have been used successfully and have shown valuable utility. However, having a much easier, cheaper, and more rapid sampling method that can be carried out with little to no

extensive operator training would be of great benefit. Modification of Tedlar® bags allowed for solid sample introduction into the bags and resealing while still maintaining the structural integrity of the bags for analysis. The direct sampling of solid samples for RS analysis by simply heating the drug matrix in the Tedlar® bags filled with N2 to aid in the desorption of volatiles was found to be easier and more efficient than the addition of water/methanol to the sample for the removal of the volatile organic compounds [18]. Although different materials like polyethylene and polytetrafluoroethylene (PTFE) bags were explored, we observed Tedlar® bags as ideal and inert. The ability to withstand high temperatures up to 93 oC makes them suitable for residual solvent volatilization and pharmaceutical testing, indicating Tedlar® bags as viable alternatives to traditional HS and SPME sampling methods. Additionally, a sampling time of 1.5 mins was used as it was ideal for all analytes investigated to avoid pre-concentrator breakthrough of lower boiling point analytes.

Method performance characteristics of the GC-PID method were measured and determined as summarized in Table 1. The method displayed limits of detection (LOD) that were less than the set regulatory limits [8] with comparable and superior performance in some cases to other methods [15,19,20] previously used for the determination of the RS in drug products. Separation of all analytes was achieved in 230 secs (Figure 1). Additionally, the linearity and range of the calibration curve were displayed with R2 values > 0.99 except for that of 1,4-dioxane at $R^2 = 0.98$. A linear range of calibration was established as well. Furthermore, spike recovery studies were conducted in a drug matrix at three concentration levels (low, medium, and high) for method validation. We observed recovery levels (Table 2) of 100.2 - 178.6% for low

spike levels, 92.6 - 127.2% for medium spike levels, and 91.2 – 115.5% for high spike levels with %RSD < 6.5%. The concentration of the spike levels is shown in Table 2. The method also showed lower LOD than the recommended analytical methods [12]. Retention time and peak area repeatability were evaluated through the replicate sampling of standards, and they showed a %RSD of < 0.4% and < 5.3%, respectively. Retention time repeatability is pertinent since the identification of analytes using GC largely depends on consistent RT, which the method displayed. Notably, characteristic RS volatility makes GC the chromatographic method of choice due to the separating power shown by capillary columns [12,17]. However, using a GC system that does not involve complex method development and optimization parameters like the NovaTest P100 saved a significant amount of method development and run time. For the detection aspect of the analytical methods, PID has not found usage for RS analysis as much as FID and MS [12], even though it was found to be superior in simplicity, portability, low cost, lowering energy use, and shortening analysis time for analytes by the GC-PID[21] The use of PID detection would be a step in the right direction for RS analysis as we gear towards greener forms of analysis. One would argue that using a higher energy lamp like an 11.7 eV would help for the detection of a more extensive array of analytes with ionization energy that falls within the lamp’s capacity, which is, in fact, true and is the direction of the further development of the instrument; Nevertheless, the 10.6 eV PID lamp used in the NovaTest P100 is satisfactory for the panel of RS selected in this study with improved linearity and stability for volatile gas detection compared to regular PID systems.

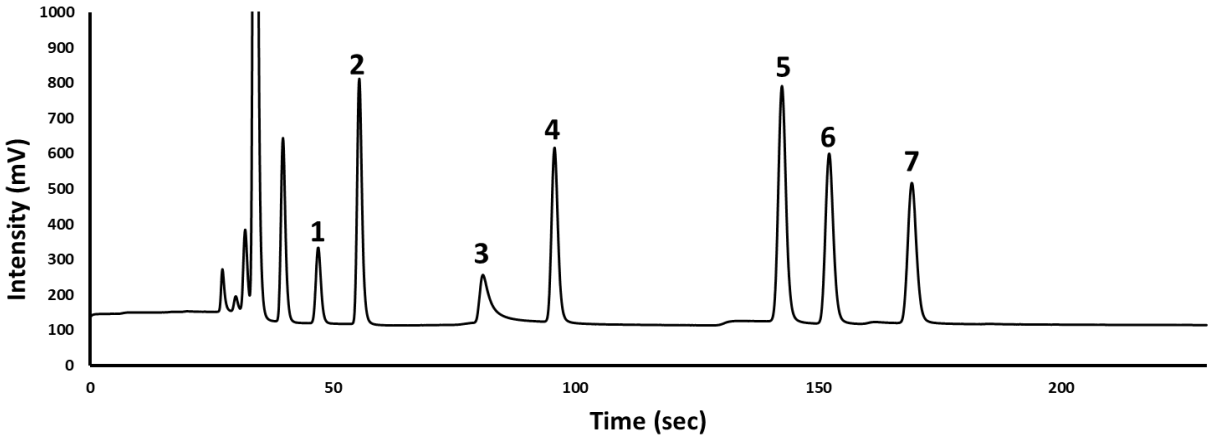

Figure 1. Chromatogram of a standard mixture containing the residual solvents. 1. Cyclohexane, 2. Benzene, 3. 1,4-dioxane 8, 4. Toluene, 5. Chlorobenzene, 6. m-, p-xylene, 7. o-xylene.

Furthermore, all analytes were completely resolved except for m and p-xylene, which could not be separated on the column; this is a common problem previously observed by others [15,19,21]. 1,4-dioxane peak was observed to tail on the column during separation, as shown in the chromatogram in Figure 1, which influenced 1,4-dioxane sensitivity over time. This led to the eventual exclusion of 1,4-dioxane in the spike recovery studies. Having a method with a LOD (pg/mL) way less than the toxicity limit (ppm) (Table 3) as set by pharmacopeias is of immense benefit to RS monitoring. As shown in Table 3, all the evaluated OTC drugs displayed RS levels less than the method LOD (> 520 pg/g of drug). Additionally, all analytes' method detection limits were lower than The United States Pharmacopeia (USP) prescribed RS limits, confirming the method's suitability for RS monitoring in pharmaceutical products.

Quality control samples were included to ensure system and analysis accuracy. Additionally, blank runs were carried out periodically during analysis to ensure that the

carryover response from the previous analysis was not influencing the current runs. The instrument also had an inbuilt cleaning procedure to remove possible residues in the system after every run to prepare it for the next run. The diluent choice of hexane in our study was influenced by the boiling point and solubility of all analytes of interest in hexane, even though the hexane peak was consistently intense in the chromatogram (Figure 1). However, the hexane peak does not interfere with the analysis of the analytes of interest because of its early elution in the method and low boiling point. Alternatively, methanol would have been a better choice due to its lack of detection on a 10.6eV lamp. However, methanol's solubility was not compatible with the selected analytes. Other advantages of PID detection are analysis simplicity, miniaturization, and low cost compared with the more complex MS and FID detection [21]. However, the operation of the PID lamp under high humidity conditions and water-based samples is not ideal [19].

Finally, the spike recovery studies were conducted by using commercial acetaminophen tablets as a drug matrix, and different drugs were crushed and added to the Tedlar® to test for the robustness of the method. It was observed that no notable peaks were spotted in the equate™ acetaminophen sample (Figure 2a), and one detected peak was found in Bayer® Plus aspirin (Figure 2b), which did not correlate with any of the investigated RS of interest; thus, it was not identified. Excedrin® and Bayer® low dose aspirin showed similar chromatograms from their sampling as equate™ acetaminophen and Bayer® Plus aspirin, respectively.

This high-throughput method will aid the manufacturing process tremendously by ensuring compliance with drug product guidelines and consequently improving drug product use safety [15].

Table 1. Calibration and method performance parameters of residual solvents.

Analyte	Linearity			Repeatability (%RSD)	
	Calibration range (ng/mL)	Correlation coefficient (r^2)	LOD* (pg/mL)	Peak Area n=4	T_r# n=4
1,4-dioxane	0.26 – 64.03	0.9786	26.00	4.26	0.08
Benzene	0.41 – 81.56	0.9979	40.78	3.94	0.39
Chlorobenzene	0.52 – 52.03	0.9918	52.03	5.32	0.32
Cyclohexane	0.36 — 72.66	0.9911	36.33	3.20	0.31
m-, p-xylene	0.41 – 40.78	0.9952	40.78	5.06	0.31
o-xylene	0.41 – 40.78	0.9962	40.78	4.72	0.30
Toluene	0.41 – 81.56	0.993	40.78	5.16	0.35

* LOD represents the DL of the RS analyzed in the bags.
\# Tr represents the retention time of the analytes.

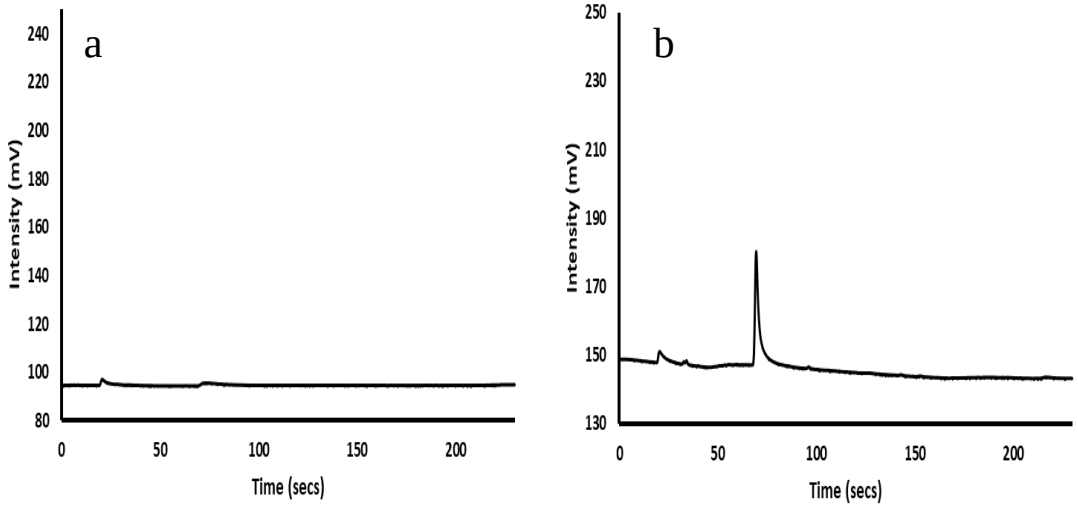

Figure 2. Chromatogram of OTC drug samples in Tedlar® bags a) acetaminophen, b) Bayer® Plus aspirin.

Table 2. Spike recovery results of the residual solvents at a) low, b) medium, and c) high levels using acetaminophen as a drug matrix.

Analyte	Spike Concentration [low, medium, high] (ng/mL)	Spike level					
		a) Low spike		b) Medium spike		c) High spike	
		%Recovery Avg (n = 3)	%RSD	%Recovery Avg (n = 3)	%RSD	%Recovery Avg (n = 3)	%RSD
Benzene	0.82, 2.04, 8.16	152.6	3.1	116.8	0.2	108.4	3.4
Chlorobenzene	1.04, 2.60, 10.41	100.3	4.1	94.1	0.5	97.9	4.0
Cyclohexane	0.73, 1.82, 7.27	178.6	4.7	127.2	3.0	115.5	1.9
m-, p-xylene	0.82, 2.04, 8.16	105.2	4.6	95.8	3.5	104.0	5.3
o-xylene	0.82, 2.04, 8.16	100.2	4.0	92.6	0.7	91.2	4.2
Toluene	0.82, 2.04, 8.16	109.9	6.5	99.7	1.2	103.50	4.8

Table 3. The concentration of residual solvents in over-the-counter drugs for method validation.

Analyte	Excedrin®		Bayer® Plus aspirin		Bayer® low dose aspirin		equate™ acetaminophen		USP* toxicity limit (ppm)
	(pg/mL)	pg/g of drug	(pg/mL)	pg/g of drug	(pg/mL)	pg/g of drug	(pg/mL)	pg/g of drug	
Benzene	< 40.78	< 611	< 40.78	< 611	< 40.78	< 611	< 40.78	< 584	2
Chlorobenzene	< 52.03	< 779	< 52.03	< 779	< 52.03	< 779	< 52.03	< 745	360
Cyclohexane	< 36.33	< 544	< 36.33	< 544	< 36.33	< 544	< 36.33	< 520	3880
m-, p-xylene	< 40.78	< 611	< 40.78	< 611	< 40.78	< 611	< 40.78	< 584	2170
o-xylene	< 40.78	< 611	< 40.78	< 611	< 40.78	< 611	< 40.78	< 584	2170
Toluene	< 40.78	< 611	< 40.78	< 611	< 40.78	< 611	< 40.78	< 584	890

*USP- United States Pharmacopeia.

However, the limitations of this system lie in its non-compatibility with the direct injection of water-based samples and the use of certain solvents. The method developed satisfied validation parameters- specificity, selectivity, linearity, accuracy, precision, limits of detection and quantitation, and most importantly, system suitability for RS analyses.

The instrument's portability can be used in various aspects of the manufacturing process, offering RS analysis at different stages of production due to the ease of moving the instrument to monitor RS concentrations [17]. Which we would refer to as in-manufacturing analysis. This would, in turn, eliminate the time needed for collection and transporting samples to the lab by giving instant results that can be acted upon quickly, thereby saving costs and preventing degradation that could affect analysis accuracy [21]. Additionally, calibration and sample Tedlar® bags could be kept at consistent room temperature and reanalyzed for up to a day without any significant change to the concentration. This will also address the pressing need for a robust, low-cost, and low-power demand portable device capable of reliable analyte-specific measurement at ppb and sub-ppb levels for VOC and RS analysis alike [15]. GC-PID has the advantage that it can be miniaturized over similar techniques for VOC detection [15] without affecting its robustness and is not limited to isothermal operation like some commercially available miniaturized GC instruments. Additionally, this GC-PID is even more compact than similar technology [19,21], and the instrument's ability to rapidly cool considerably shortens the waiting time after each run, consequently reducing overall analysis time.

4. CONCLUSION

The developed method showed less than 6.5% reproducibility and sub-ppb level detection for the RS evaluated. The method demonstrated qualitative and quantitative detection of the RS of interest. Air sampling of dry drug products using a Tedlar® bag is a viable alternative to conventional RS sampling methods like HS and SPME. We expected that this instrument and methodology could be deployed during the manufacturing processes of drug production to monitor RS generated at every stage of production to ensure an accurate determination of their presence and regulation. It is anticipated that the method can be modified with different columns and temperature programs to include more RS using this method on the GC-PID system, ultimately saving time and cost of analysis during the production process.

ACKNOWLEDGMENTS

This project was conducted with the support of Nanova Environmental, Inc. (Columbia, MO, USA).

Conflict of interest.

The authors have declared no conflict of interest.

Author contributions.

Olajide Adetunji- Experimental design, Investigation, Methodology, Data Curation, Validation, Formal analysis, and Writing- Original Draft.

Sargun Kaur- Methodology, Investigation, Writing- Review and Editing.

Nicole Wheeler- Investigation.

Victor Nam- Investigation.

Honglan Shi- Conceptualization, Funding acquisition, Writing- Review and Editing, and supervision.

Paul Nam- Conceptualization, Project administration, Funding acquisition, Writing- Review and Editing, and Supervision.

REFERENCES

[1] K. Grodowska, A. Parczewski, Organic solvents in the pharmaceutical industry, Acta Poloniae Pharmaceutica - Drug Research 67 (2010) 3–12.

[2] P. Kolář, J.W. Shen, A. Tsuboi, T. Ishikawa, Solvent selection for pharmaceuticals, Fluid Phase Equilib 194–197 (2002) 771–782. https://doi.org/10.1016/S0378-3812(01)00716-6.

[3] ICH Expert Working Group, Ich Harmonised Guideline - Impurities: Guideline for Residual Solvents Q3C(R8), International Council for Harmonisation of Technical Requirements for Pharmaceuticals for Human Use (ICH) (2021) 1–43.

[4] D.J.C. Constable, C. Jimenez-Gonzalez, R.K. Henderson, Perspective on solvent use in the pharmaceutical industry, Org Process Res Dev 11 (2007) 133–137. https://doi.org/10.1021/op060170h.

[5] C. Witschi, E. Doelker, Residual solvents in pharmaceutical products: Acceptable limits, influences on physicochemical properties, analytical methods and documented values, European Journal of Pharmaceutics and Biopharmaceutics 43 (1997) 215–242. https://doi.org/10.1016/S0939-6411(96)00037-9.

[6] H. Liu, Q. Tang, R.J. Markovich, A.M. Rustum, A general static-headspace gas chromatographic method for determination of residual benzene in oral liquid pharmaceutical products, J Pharm Biomed Anal 54 (2011) 417–421. https://doi.org/10.1016/j.jpba.2010.09.006.

[7] M. Hasznos-Nezdei, J. Kovács, S. Kováts, A.B. Shahroodi, P. Szabó-Révész, Correlation between the micromorphological parameters and residual solvent content of a crystalline steroid drug, Powder Technol 167 (2006) 104–107. https://doi.org/10.1016/j.powtec.2006.06.014.

[8] USP, Residual Solvents - Chapter 467, The United States Pharmacopeial Convention (2019) 22. https://www.uspnf.com/sites/default/files/usp_pdf/EN/USPNF/revisions/gc-467-residual-solvents-ira-20190927.pdf.

[9] M. Tankiewicz, J. Namieśnik, W. Sawicki, Analytical procedures for quality control of pharmaceuticals in terms of residual solvents content: Challenges and recent developments, TrAC - Trends in Analytical Chemistry 80 (2016) 328–344. https://doi.org/10.1016/j.trac.2015.09.008.

[10] USP 30, U.S. Pharmacopeia general chapter (467) current residual solvents, The United States Pharmacopeial Convention (2007).

[11] M. Tobiszewski, J. Namieśnik, Greener organic solvents in analytical chemistry, Curr Opin Green Sustain Chem 5 (2017) 1–4. https://doi.org/10.1016/j.cogsc.2017.03.002.

[12] K. Grodowska, A. Parczewski, Analytical methods for residual solvents determination in pharmaceutical products, Acta Poloniae Pharmaceutica - Drug Research 67 (2010) 13–26.

[13] C.C. Camarasu, M. Mezei-Szûts, G.B. Varga, Residual solvents determination in pharmaceutical products by GC-HS and GC-MS-SPME, J Pharm Belg 53 (1998) 165.

[14] S.K. Bhardwaja, K. Dwivedia, D.D. Agarwal, A Review: GC Method Development and validation Santosh, International Journal of Analytical and Bioanalytical Chemistry 6 (2016) 1–7.

[15] C.M. Wang, B.D. Esse, A.C. Lewis, Low-cost multispecies air quality sensor, WIT Transactions on Ecology and the Environment 198 (2015) 105–116. https://doi.org/10.2495/AIR150091.

[16] C.C. Camarasu, Unknown residual solvents identification in drug products by headspace solid phase microextraction gas chromatography-mass spectrometry, Chromatographia 56 (2002). https://doi.org/10.1007/bf02494126.

[17] C.M. Harris, GC to go, Anal Chem 74 (2002) 585–589.

[18] M. Ojala, M. Poutanen, I. Mattila, R.A. Ketola, T. Kotiaho, R. Kostiainen, Analysis of residual solvents in pharmaceuticals with purge-and-membrane mass spectrometry, Rapid Communications in Mass Spectrometry 14 (2000) 994–998. https://doi.org/10.1002/(SICI)1097-0231(20000615)14:11<994::AID-RCM977>3.0.CO;2-6.

[19] I. Frausto-Vicencio, A. Moreno, H. Goldsmith, Y.K. Hsu, F.M. Hopkins, Characterizing the performance of a compact btex gc-pid for near-real time analysis and field deployment, Sensors 21 (2021) 1–18. https://doi.org/10.3390/s21062095.

[20] R. Nasreddine, V. Person, C.A. Serra, S. Le Calvé, Development of a novel portable miniaturized GC for near real-time low-level detection of BTEX, Sens Actuators B Chem 224 (2016) 159–169. https://doi.org/10.1016/j.snb.2015.09.077.

[21] S.J. Edwards, A.C. Lewis, S.J. Andrews, R.T. Lidster, J.F. Hamilton, C.N. Rhodes, A compact comprehensive two-dimensional gas chromatography (GC×GC) approach for the analysis of biogenic VOCs, Analytical Methods 5 (2013) 141–150. https://doi.org/10.1039/c2ay25710f.

SECTION

2. CONCLUSIONS AND RECOMMENDATIONS

2.1. CONCLUSIONS

This dissertation demonstrates the utility of chromatography-based analytical methods coupled with mass spectrometry and photoionization detectors for analyzing biological metabolites and residual solvents in pharmaceutical products. The first two papers (I and II) discussed liquid chromatographic and tandem mass spectrometry methods for determining potential TBI biomarkers in different biomatrices derived from open-field blast animal models with mild TBI. Additionally, the second paper specifically evaluates antioxidant therapy efficacy for TBI treatment using biomarker changes and response to blast-induced mild-TBI and NACA treatment. The studies yielded results that indicate some of the biomarkers of interest (markers of neurotoxicity and oxidative stress), NAA, 5-HIAA, GSH, GSH-GSSG ratio responded to both open-field blast TBI disease state and NACA treatment in urine, plasma, and whole brain tissue matrices of rats. It further shows that NACA may be able to confer neuroprotection, maintain and restore redox health status, and ameliorate brain homeostasis perturbation from blast-induced TBI. Additionally, the study shows the utility and functionality of peripheral fluid biomarker investigations for TBI, which is typically a brain-centered disease. These first two studies involved innovative measures and optimization in simulating military-grade TBI with explosive devices using blast models, biological matrix collection, sample clean-up, and LC-MS/MS method developments. The instrumentation methods

and sample clean-up strategies were developed and optimized for analyte sensitivity, selectivity, robustness, precision, and accuracy to monitor the slight changes of analytes based on disease state or treatment strategy at sub-ppb levels. Having these methods for monitoring the selected biomarker panel will go a long way in understanding TBI pathophysiology and designing effective treatment strategies for combating TBI.

The third paper (Paper III) discusses the development and application of gas chromatography with photoionization detection (GC-PID) method for monitoring different USP classes of residual solvents in pharmaceutical products. It highlights using portable GC-PID instrumentation and modified Tedlar® bag sampling, a much easier, cheaper, smaller, and similarly efficient instrumentation for monitoring residual solvents in pharmaceutical products. The method developed was validated and applied to over-the-counter medications for residual solvent monitoring. Short analysis time, straightforward sample preparation, easy-to-use instrumentation, and compatibility make the overall method and instrumentation suitable for integration into the fast-paced stages of the pharmaceutical drug production process to save time and resources.

2.2. RECOMMENDATIONS

The revelation and observations made in the TBI studies corroborated the importance of peripheral fluid small molecule biomarkers. It will benefit our understanding of the various pathophysiologies of TBI to explore peripheral fluid biomarker changes, especially in urine, more than they are currently being studied. Future works can identify more secondary mechanisms and small molecule biomarkers that can be explored in the biomatrices used in this study and other biomatrices to understand

better TBI pathophysiology and the interconnection of TBI to other diseases. Additionally, multiple time point studies should be conducted to understand the temporal profile of small molecule biomarkers in response to TBI. For the antioxidant therapy efficacy of TBI using NACA to target oxidative stress characteristics of the disease, studies should be conducted to understand the effect of NACA dosage on various severities of TBI, especially mild TBI. Additionally, standalone and combined preexposure and postexposure prophylactic effects of NACA should be evaluated against TBI.

In the residual solvent analysis study, the GCPID method developed could include more residual solvents that can be used to analyze active pharmaceutical ingredients, excipients, and finished products. Integrating this instrumentation and method into residual solvent analysis in manufacturing may be a viable alternative to existing methods that require laboratory instrumentations, complex analysis processes, and resources. The portable GC-PID could be run with minimal training and resource expenses.

APPENDIX

EFFECTS OF BLAST AND NACA TREATMENT ON TBI BIOMARKERS IN ANIMAL MODELS ONE- AND FIVE-DAYS POST BLAST-INDUCED-TBI

1. OBJECTIVES

In this particular study, the aim was to understand better the temporal effect of TBI on the biomarkers studied. Additionally, NACA treatment was also conducted to see the efficacy of only preexposure treatment and the combination of preexposure and continuous post-exposure of the rats after blast-induced TBI. Animals were separated into two study groups that got blast-induced TBI and pre-exposure treatment of NACA on the same day. However, in one study group, Day 1 (D1-Collection), animals were euthanized the following day without any follow-up treatment. The second study group, Day 5 (D5-Collection), underwent intermittent NACA treatment for two days and euthanasia after five days post-blast.

2. ANIMAL CONDITIONS

The animal procedures used in this study were reviewed and approved by the Missouri S&T Animal Care and Use Committee in compliance with Federal regulations regarding the protection of animals used in research. Rats (Fischer CDF male rats {weight = 250-270 g;} Charles River, MA, USA) fifteen weeks old at the time of the experiment were used in this study. Animal housing was in a temperature and humidity-

controlled animal facility. Precisely one week of acclimatization was provided for the rats before studies were conducted. Food (Purina Lab Diet rat chow) and water (municipal tap) access were allowed for the animals *ad libitum*, and a 12-hour light-dark cycle was provided for the animals at the Missouri S&T Animal Research Facility.

3. EXPLOSIVE BLAST DETAILS

Twenty-four animals in two study groups (D1 and D5 Collections) containing 4 and 3 individual groups were used in this study. The first study group, D1-Collection, was divided into four groups: Sham (n = 3), D1-NACA (n=3), D1-b-TBI & NACA (n=4), and D1-b-TBI (n = 3). Also, the second study group, D5-Collection, was divided into three groups: D5-NACA (n=3), D5-b-TBI & NACA (n=5), and D5-b-TBI (n = 3). All animals were transported to the Missouri University of Science and Technology experimental mine facility. All animals were conscious prior to and after injury for both study groups. In the D1-Collection study group with four individual groups, no explosive device was detonated for control groups: 1. Sham, and 2. D1-NACA, however, the animals were kept in the same conditions as the blast-induced rats during the blast exercise for equilibration. The experimental (blast-induced) rat groups for the D1-Collection: 3. b-TBI & NACA and 4. b-TBI were suspended at a height of 60 cm in modified cages and subjected to an open-field explosive blast at 2.15 m from a 350 g charge of C4.

In the second study group, the D5-Collection study group with three individual groups, no explosive device was detonated for the control group: 5. D1-NACA, however, the D1-NACA rats were kept in the same conditions as the blast-induced rats during the

blast exercise for equilibration. The experimental (blast-induced) rat groups for the D5-Collection: 6. b-TBI & NACA and 7. b-TBI were suspended at a height of 60 cm in modified cages and subjected to an open-field explosive blast at 2.15 m from a 350 g charge of C4. The open-field blast model of TBI used in these animals was developed and validated previously in rodents. Table A1 shows a description of the groups and the blast-induced. The severity of the TBI from the blast-induced was considered mild.

Table A1 Study groups with blast simulation and NACA treatment description.

1st study group D1-Collection				
Group	**Blast Conducted**	**Injection**	**Injury**	**Number**
1. Sham	No Blast	PBS	Sham	3
2. D1-NACA	No Blast	NACA	Sham	3
3. D1-b-TBI & NACA	Blast at 2.15m	NACA	Blast	4
4. D1-b-TBI	Blast at 2.15m	PBS	Blast	3
2nd study group D5-Collection				
Group	**Blast Conducted**	**Injection**	**Injury**	**Number**
5. D5-NACA	No Blast	NACA	Sham	3
6. D5-b-TBI & NACA	Blast at 2.15m	NACA	Blast	5
7. D5-b-TBI	Blast at 2.15m	PBS	Blast	3

4. ANTIOXIDANT (NACA) TREATMENT

On the scheduled blast day, animals were treated with s.c. Injection of either PBS (1. Sham, 4. D1-b-TBI, and 7. D5-b-TBI) or 500 mg/kg NACA (2. D1-NACA, 3. D1-b-TBI & NACA, 5. D5-NACA, and 6. D5-b-TBI & NACA) 1 h prior to injury. Animals were transported to the Experimental Mine facility at Missouri University of Science and Technology and were subjected to open blast injury as described in the explosive blast details section. D1-Collection animals were euthanized one day after the blast and did not undergo subsequent treatment. D5-collection animals were treated with s.c injection of 500 mg/kg NACA or PBS for two more days after the blast exposure at intervals. Animals were fasted overnight before euthanasia. D1-collection animals were euthanized a day after the blast was induced, while D5-collection animals were euthanized five days after the blast was induced on the study rats. The collection of urine, blood, and whole brain tissue followed euthanasia. Table A1 shows a description of the treatment details of the groups.

5. SURGICAL PROCEDURE AND SAMPLE COLLECTION

Euthanasia, harvesting of tissues, and collections of biological fluids were conducted in the animal surgery theatre at the Missouri S&T Animal Research Facility one and five days after the blast for the D1-Collection and D5-Collection rats, respectively. Animals were deeply anesthetized via i.p injection of ketamine/xylazine. Animals were euthanized by exsanguination via cardiac puncture. Blood was collected into heparin-coated tubes and centrifuged (3000 g, 10 min; 4 °C) immediately to separate

plasma. Urine was drawn directly from the bladder. Each urine or plasma sample was divided into two aliquots. Upon collection, 10 mg/mL BHT was added to one aliquot of each urine or plasma sample to give a final 200 µg/mL BHT concentration. To the other aliquot of collected urine or plasma, 100 mM NEM was added (urine or plasma/NEM = 9:1, v/v), and the mixture was vortexed for a few seconds to form the stable GSH-NEM adduct. Whole brains were collected immediately following euthanasia. Stabilized urine, plasma, and brain samples were frozen immediately in liquid N2 and stored at -80 °C until analysis.

5.1. SAMPLE PREPARATION AND ANALYSIS

Samples were prepared and analyzed as described in Papers 1 and II, portrayed in the paper section of this dissertation.

5.2. DATA ANALYSIS

Data is represented as the mean ± SEM (standard error of the mean) of 3-5 animals. GraphPad Prism 6 (San Diego, California) was used to conduct One-way ANOVA to compare mean biomarker levels between all groups. Fisher LSD pair-wise test was used to compare two individual groups in the study. Values of $p \leq 0.05$ were considered statistically significant, and $p \leq 0.1$ were defined to approach statistical significance for analyses discussed here.

6. RESULTS AND DISCUSSION

6.1. EFFECT OF NACA ON BRAIN TISSUE FOR D1 AND D5 STUDY GROUPS

The exposure to blast overpressure (BOP) caused observable changes within and between collection days on the investigated metabolites in brain tissue. Brain tissue metabolites levels were recorded as ng(analyte)/mg(wet weight) of the tissue, and the one-way ANOVA results are as follows: NAA; ($F = 2.44$, $p = 0.0691$), 5-HIAA; ($F = 1.09$, $p = 0.4087$), GSH; ($F = 1.87$, $p = 0.1455$), GSSG; ($F = 1.50$, $p = 0.2371$), GSH/GSSG ratio; ($F = 3.178$, $p = 0.0280$). Further statistical post-hoc probing using Fisher LSD pair-wise comparison on brain tissue NAA showed a similar level between the sham and D1-b-TBI & NACA groups. With a p-value approaching statistical significance, there was a 7% reduced NAA level between D1-b-TBI & NACA vs. D1-b-TBI. This observation shows that NAA level changes may not be an accurate reflection of TBI one day after injury. However, in the D5 groups, the D5-NACA and D5-b-TBI & NACA groups showed similar NAA levels, while the D5-b-TBI group had slightly lower NAA levels compared to the other D5 groups. This result indicates that continuous NACA treatment may be able to increase and prevent the depletion of NAA levels in the brain for b-TBI-induced animals. The activity of 5-HIAA in the brain as a response to b-TBI and NACA treatment was unclear from our data. However, there were *p*-values of statistical significance ($p < 0.05$) and approaching statistical significance ($p < 0.1$) between the D1-b-TBI & NACA vs. D1-b-TBI and D1-b-TBI & NACA vs. D5-b-TBI respectively. However, GSH depletion was not observed in the D1 groups, possibly due to the delay of TBI effects to a later time point. This phenomenon was observed as there was a ~20% statistically significant ($p < 0.05$) decrease in GSH levels between the D5-b-

TBI & NACA vs. D5-b-TBI and a ~19% decrease approaching statistical significance ($p < 0.1$) between D5-NACA vs. D5-b-TBI. This shows that continuous NACA treatment can maintain GSH levels in b-TBI-induced animals, and b-TBI depletes GSH levels. This result agrees with our previous study. Additionally, the D1 study groups had relatively higher GSSG levels than the D5 study groups. Comparing the GSH/GSSG ratio of the animals in both study groups, it was observed that there were lower GSH/GSSG ratios in the D1 study groups than in the D5 study groups. The D5-NACA group had the highest GSH/GSSG ratio in the D5 study group; this was closely followed by the D5-b-TBI & NACA group, which was 12% lower than the D5-NACA group. However, the D5-b-TBI had the lowest GSH/GSSG ratio, which was 30% and 20 % lower than the D5-NACA and the D5-b-TBI & NACA groups, respectively. Additionally, significant differences in the GSH/GSSG ratio between the D1 and D5 study groups indicate that prolonged NACA treatment after initial pre-exposure treatment may better improve redox health outcomes. Results are represented in the boxplot in Figure A1, and the *p*-values of the one-way ANOVA and the Fisher LSD multiple pairwise comparisons are shown in Tables A2 and A3, respectively.

Table A2. One-way ANOVA *p*-values of the two study groups combined for different metabolites in the whole brain, urine, and plasma.

Analyte	**Biological matrix**		
	Brain	**Plasma**	**Urine**
NAA	**0.0691**	0.9386	**0.0084**
5-HIAA	0.4087	0.1742	0.7262
GSH	0.1455	0.1563	0.9709

Table A2. One-way ANOVA *p*-values of the two study groups combined for different metabolites in the whole brain, urine, and plasma. (Cont.)

Analyte	Biological matrix		
	Brain	**Plasma**	**Urine**
GSSG	0.2371	0.6187	0.5387
GSH/GSSG	**0.0280**	0.1465	**0.0452**

Table A3. Fisher LSD pairwise comparison of whole brain tissue metabolites between different groups in the study. Significant *p*-values and approaching statistical significance *p*-values are in bold font.

Day 1 and Day 5 study comparison *p*-value (Brain Tissue)					
Comparison	**NAA**	**5-HIAA**	**GSH**	**GSSG**	**GSH/GSSG**
Sham vs. D1 NACA	**0.0151**	0.587	0.2047	0.8428	0.5651
Sham vs. D1 b-TBI	0.2931	0.1607	**0.0713**	0.9096	0.2317
Sham vs. D1 b-TBI & NACA	0.5888	0.4879	0.1113	0.7556	0.2807
Sham vs. D5 NACA	0.1521	0.4367	0.1048	**0.0636**	**0.002**
Sham vs. D5 b-TBI	0.5664	0.2528	0.9543	0.1945	0.1599
Sham vs. D5 b-TBI & NACA	0.1182	0.587	**0.0644**	0.1768	**0.0149**
D1 NACA vs. D1 b-TBI	**0.089**	0.3939	0.6138	0.745	0.5479
D1 NACA vs. D1 b-TBI & NACA	**0.0047**	0.2237	0.7228	0.6113	0.6047
D1 NACA vs. D5 NACA	0.2456	0.811	0.6979	**0.0431**	**0.007**
D1 NACA vs. D5 b-TBI	**0.0261**	0.5797	0.1437	0.1335	0.427
D1 NACA vs. D5 b-TBI & NACA	0.3055	> 0.9999	0.519	0.1256	**0.0488**
D1 b-TBI vs. D1 b-TBI & NACA	0.1124	**0.0399**	0.8992	0.8262	0.9612
D1 b-TBI vs. D5 NACA	0.611	0.5465	0.9277	**0.061**	**0.0164**
D1 b-TBI vs. D5 b-TBI	0.5573	0.7077	**0.0377**	0.1982	0.8533
D1 b-TBI vs. D5 b-TBI &NACA	0.5091	0.3939	0.8516	0.182	0.116
D1 b-TBI & NACA vs. D5 NACA	**0.0561**	0.1505	0.9732	0.1136	**0.0212**
D1 b-TBI & NACA vs. D5 b-TBI	0.2463	**0.0646**	**0.0697**	0.3328	0.8254

Table A3. Fisher LSD pairwise comparison of whole brain tissue metabolites between different groups in the study. Significant *p*-values and approaching statistical significance *p*-values are in bold font. (Cont.)

Day 1 and Day 5 study comparison *p*-value (Brain Tissue)

Comparison	NAA	5-HIAA	GSH	GSSG	GSH/GSSG
D1 b-TBI & NACA vs. D5 b-TBI & NACA	**0.0422**	0.2237	0.7694	0.2896	0.129
D5 NACA vs. D5 b-TBI	0.2902	0.7729	**0.0649**	0.3973	**0.0182**
D5 NACA vs. D5 b-TBI & NACA	0.8855	0.811	0.7951	0.5727	0.359

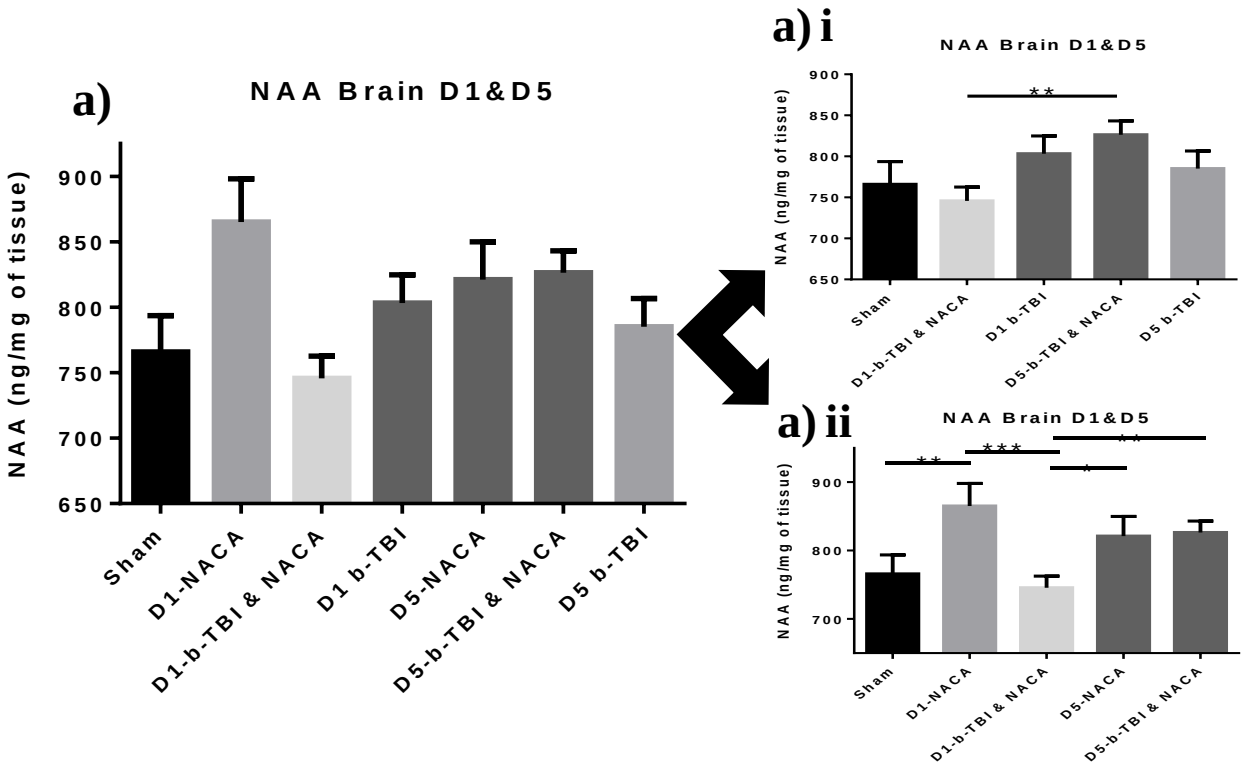

Figure A1. Whole brain tissue metabolite levels in Sham; D1-NACA; D1-b-TBI & NACA; D1-b-TBI; D5-NACA; D5-b-TBI & NACA; and D5-b-TBI groups for a) NAA, b) 5-HIAA, c) GSH, d) GSSG, e) GSH/GSSG ratio. (i) and (ii) are used to visualize the blast and treatment effects, respectively, for a, b, c, d, and e. Values are represented as mean ± SEM (n = 3-5). $p \leq 0.1$ (*), $p \leq 0.05$ (**), $p \leq 0.01$ (***), $p \leq 0.001$ (****). [D1 = Day 1 study group, D5= Day 5 study group, Sham = no blast + no treatment, NACA = no blast + NACA treatment, b-TBI & NACA = blast + NACA treatment, b-TBI = blast + no treatment]

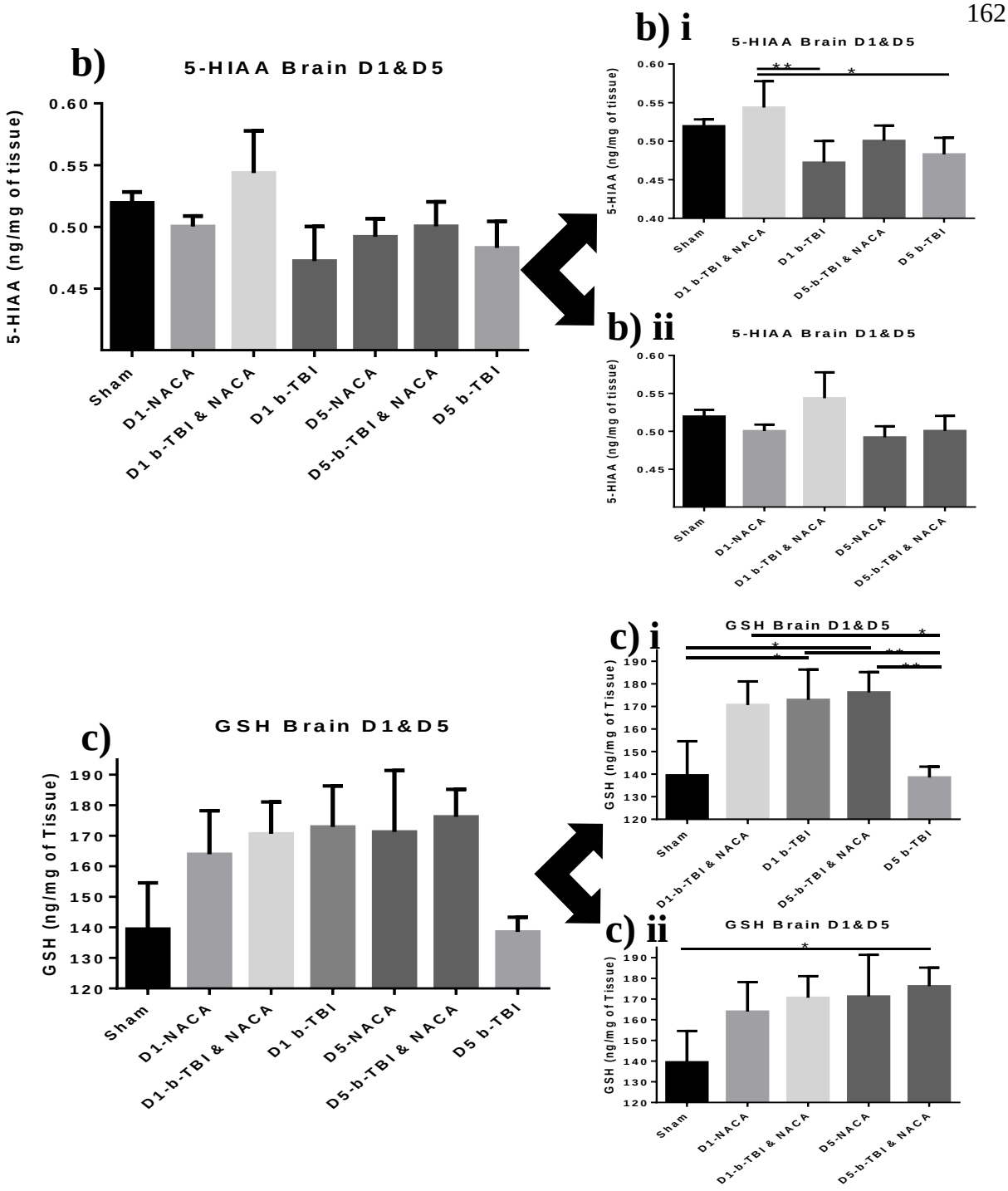

Figure A1. Whole brain tissue metabolite levels in Sham; D1-NACA; D1-b-TBI & NACA; D1-b-TBI; D5-NACA; D5-b-TBI & NACA; and D5-b-TBI groups for a) NAA, b) 5-HIAA, c) GSH, d) GSSG, e) GSH/GSSG ratio. (i) and (ii) are used to visualize the blast and treatment effects, respectively, for a, b, c, d, and e. Values are represented as mean ± SEM (n = 3-5). $p \leq 0.1$ (*), $p \leq 0.05$ (**), $p \leq 0.01$ (***), $p \leq 0.001$ (****). [D1 = Day 1 study group, D5= Day 5 study group, Sham = no blast + no treatment, NACA = no blast + NACA treatment, b-TBI & NACA = blast + NACA treatment, b-TBI = blast + no treatment] (Cont.)

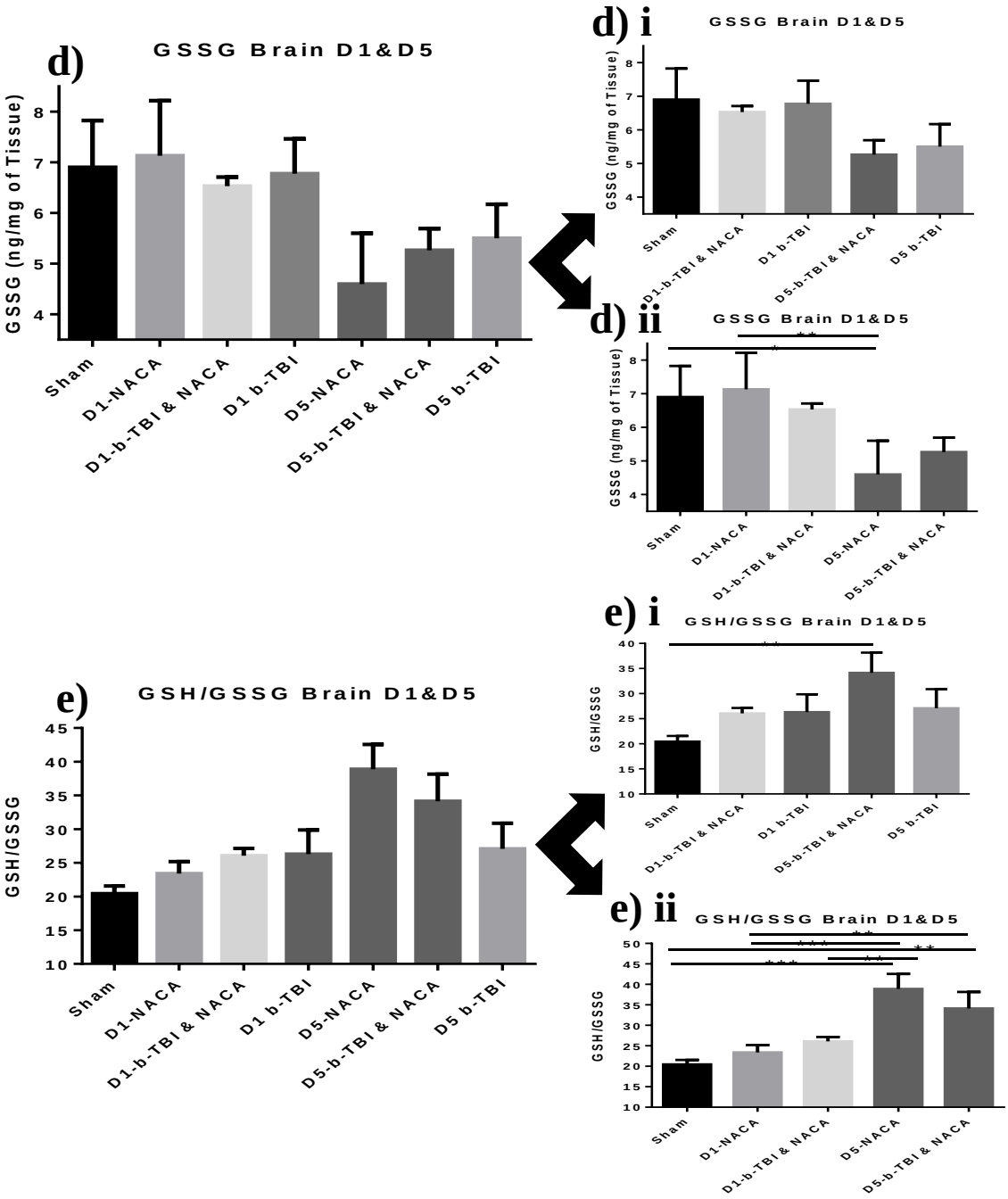

Figure A1. Whole brain tissue metabolite levels in Sham; D1-NACA; D1-b-TBI & NACA; D1-b-TBI; D5-NACA; D5-b-TBI & NACA; and D5-b-TBI groups for a) NAA, b) 5-HIAA, c) GSH, d) GSSG, e) GSH/GSSG ratio. (i) and (ii) are used to visualize the blast and treatment effects, respectively, for a, b, c, d, and e. Values are represented as mean ± SEM (n = 3-5). $p \leq 0.1$ (*), $p \leq 0.05$ (**), $p \leq 0.01$ (***), $p \leq 0.001$ (****). [D1 = Day 1 study group, D5= Day 5 study group, Sham = no blast + no treatment, NACA = no blast + NACA treatment, b-TBI & NACA = blast + NACA treatment, b-TBI = blast + no treatment] (Cont.)

6.2. EFFECT OF NACA IN PLASMA FOR D1 AND D5 STUDY GROUPS

Plasma metabolites levels were recorded as (Analyte)(ng/mL)/(CRT) (ug/mL) and the one-way ANOVA results are as follows: NAA; ($F = 0.28$, $p = 0.9386$), 5-HIAA; ($F = 1.73$, $p = 0.1742$), GSH; ($F = 1.81$, $p = 0.1563$), GSSG; ($F = 0.75$, $p = 0.6187$), GSH/GSSG ratio; ($F = 1.86$, $p = 0.1465$). No statistical significance was observed comparing the D1 and D5 study groups' mean; however, isolating the D5 study group shows a trend of increased NAA levels (~24-27%) that was approaching statistical significance for the D5-b-TBI group compared to D5-NACA and D5-b-TBI & NACA groups that were relatively similar. This indicates that days after the initial injury, b-TBI kept NAA levels elevated, and prolonged NACA treatment after an injury can keep NAA levels identical to that of the control group.

For 5-HIAA, comparing the D1 and D5 study group means with one another showed no outstanding statistical differences; however, by isolating the D5 groups, it is observed that there is an ~30% increase approaching statistical significance in D5-b-TBI 5-HIAA levels compared to D5-NACA and D5-b-TBI & NACA groups. This indicated that injury could elevate 5-HIAA levels days after injury, and prolonged NACA treatment after initial treatment can maintain 5-HIAA levels to control levels. This trend in plasma 5-HIAA was similar to that observed in plasma NAA and our previous blast study. The D1-b-TBI and D5-b-TBI levels remained relatively the same despite being in different treatment and study durations. No notable differences were observed between the GSH, GSSG, and GSH/GSSG ratio groups in plasma. Results are represented in the boxplot in Figure A2, and the p-values of the one-way ANOVA and the Fisher LSD multiple pairwise comparisons are shown in Tables A2 and A4, respectively.

Table A4. Fisher LSD pairwise comparison of plasma metabolites between different groups in the study. Significant *p*-values and approaching statistical significance *p*-values are in bold font.

Day 1 and Day 5 study comparison *p*-value (Plasma)					
Comparison	**NAA**	**5-HIAA**	**GSH**	**GSSG**	**GSH/GSSG**
Sham vs. D1 NACA	0.9858	0.1067	0.2283	0.3064	0.2466
Sham vs. D1 b-TBI & NACA	0.4781	0.4031	**0.0292**	0.2431	0.128
Sham vs. D1 b-TBI	0.7024	0.1737	**0.0437**	0.4853	0.1678
Sham vs. D5 NACA	0.8251	**0.0198**	**0.0685**	0.6134	0.4006
Sham vs. D5 b-TBI & NACA	0.8783	**0.0216**	**0.0089**	0.2058	**0.0427**
Sham vs. D5 b-TBI	0.5837	0.2517	**0.0311**	**0.081**	**0.0081**
D1 NACA vs. D1 b-TBI & NACA	0.4889	0.4094	0.2736	0.8787	0.6941
D1 NACA vs. D1 b-TBI	0.7165	0.6934	0.4109	0.684	0.8765
D1 NACA vs. D5 NACA	0.8113	0.3969	0.4963	0.5964	0.7396
D1 NACA vs. D5 b-TBI & NACA	0.8643	0.4205	0.1072	0.7971	0.3359
D1 NACA vs. D5 b-TBI	0.5972	0.4827	0.3538	0.508	0.1162
D1 b-TBI & NACA vs. D1 b-TBI	0.7036	0.6213	0.7186	0.5698	0.7905
D1 b-TBI & NACA vs. D5 NACA	0.3555	0.1045	0.6682	0.4966	0.4706
D1 b-TBI & NACA vs. D5 b-TBI & NACA	0.3907	0.1129	0.5766	0.9166	0.5627
D1 b-TBI & NACA vs. D5 b-TBI	0.8038	0.8224	0.7591	0.6214	0.2436
D1 b-TBI vs. D5 NACA	0.538	0.2011	0.9216	0.8724	0.6105
D1 b-TBI vs. D5 b-TBI & NACA	0.5863	0.2165	0.3432	0.4975	0.3802
D1 b-TBI vs. D5 b-TBI	0.8703	0.7493	0.9388	0.2437	0.1231
D5 NACA vs. D5 b-TBI & NACA	0.9458	0.9658	0.3287	0.4342	0.2017
D5 NACA vs. D5 b-TBI	0.4294	0.1094	0.8624	0.2178	**0.058**
D5 b-TBI & NACA vs. D5 b-TBI	0.4739	0.1192	0.3563	0.7055	0.5908

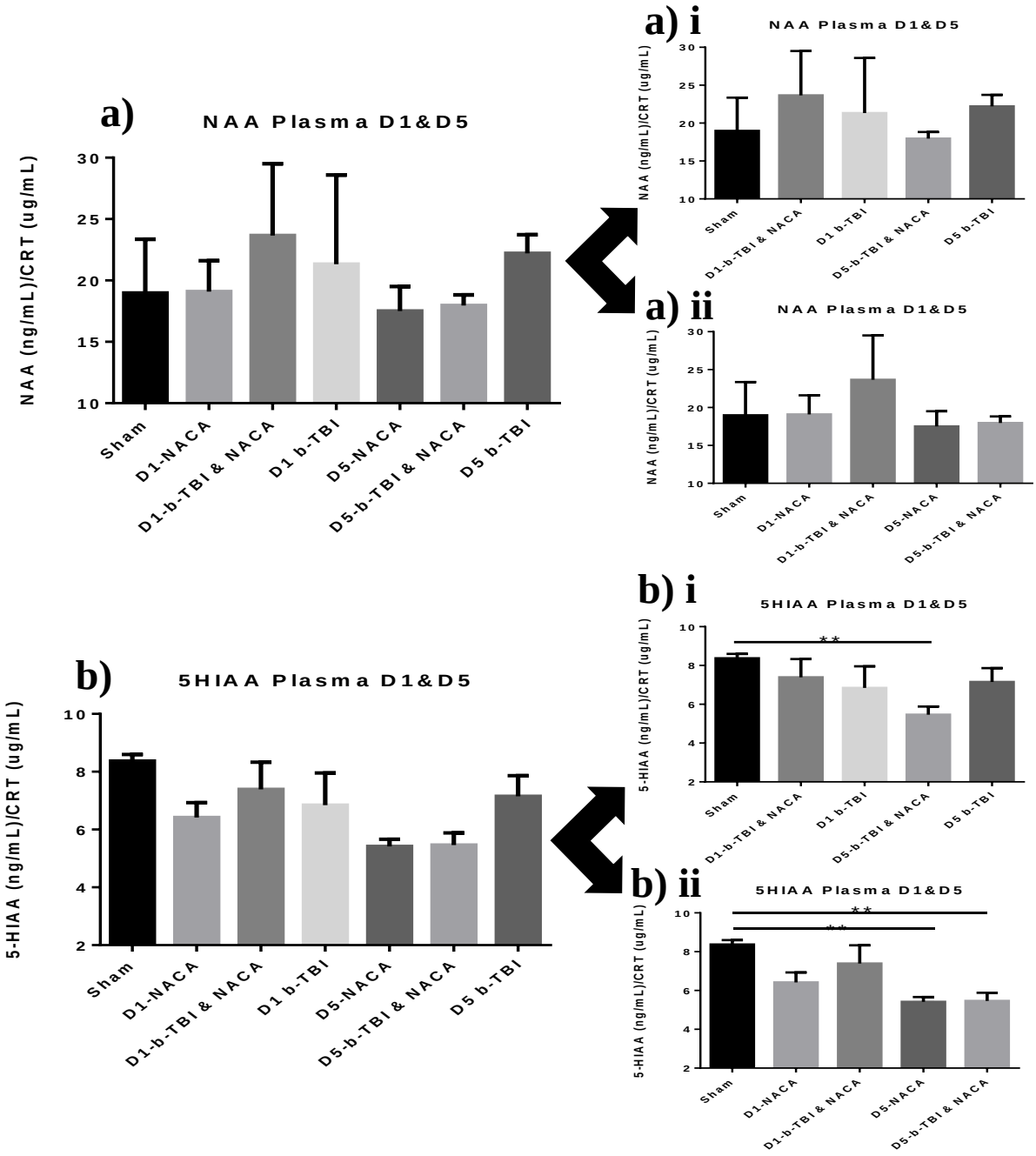

Figure A2. Plasma metabolite levels in Sham; D1-NACA; D1-b-TBI & NACA; D1-b-TBI; D5-NACA; D5-b-TBI & NACA; and D5-b-TBI groups for a) NAA, b) 5-HIAA, c) GSH, d) GSSG, e) GSH/GSSG ratio. (i) and (ii) are used to visualize the blast and treatment effects, respectively, for a, b, c, d, and e. Values are represented as mean ± SEM (n = 3-5). $p \leq 0.1$ (*), $p \leq 0.05$ (**), $p \leq 0.01$ (***), $p \leq 0.001$ (****). [D1 = Day 1 study group, D5= Day 5 study group, Sham = no blast + no treatment, NACA = no blast + NACA treatment, b-TBI & NACA = blast + NACA treatment, b-TBI = blast + no treatment]

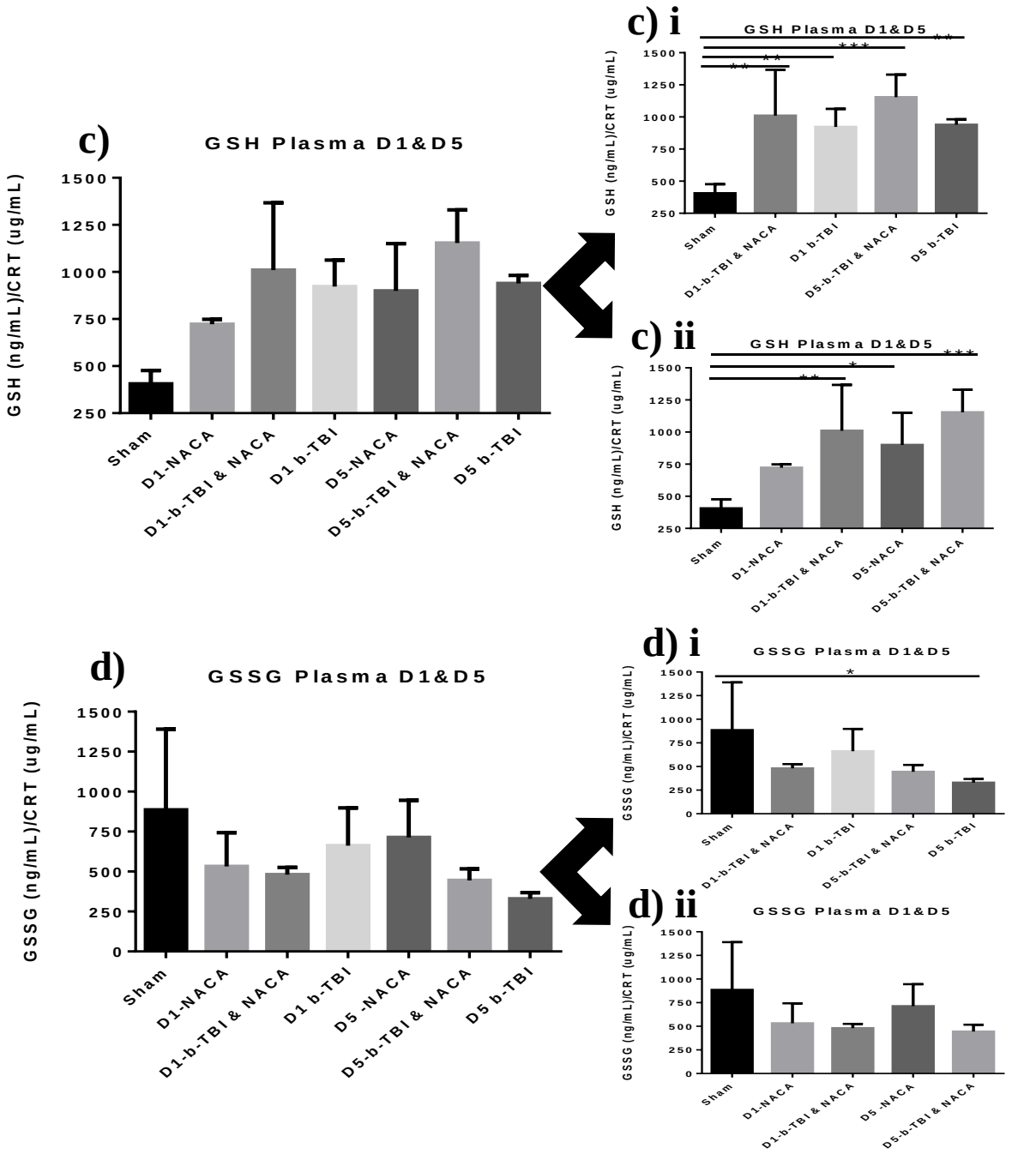

Figure A2. Plasma metabolite levels in Sham; D1-NACA; D1-b-TBI & NACA; D1-b-TBI; D5-NACA; D5-b-TBI & NACA; and D5-b-TBI groups for a) NAA, b) 5-HIAA, c) GSH, d) GSSG, e) GSH/GSSG ratio. (i) and (ii) are used to visualize the blast and treatment effects, respectively, for a, b, c, d, and e. Values are represented as mean ± SEM (n = 3-5). $p \leq 0.1$ (*), $p \leq 0.05$ (**), $p \leq 0.01$ (***), $p \leq 0.001$ (****). [D1 = Day 1 study group, D5= Day 5 study group, Sham = no blast + no treatment, NACA = no blast + NACA treatment, b-TBI & NACA = blast + NACA treatment, b-TBI = blast + no treatment] (Cont.)

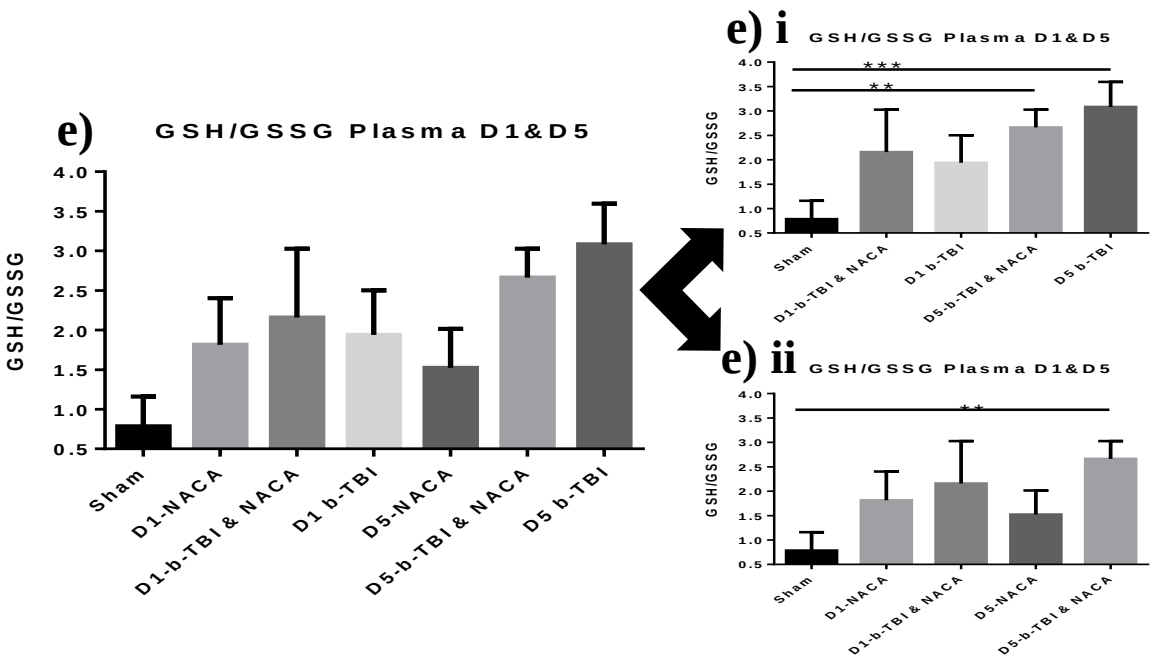

Figure A2. Plasma metabolite levels in Sham; D1-NACA; D1-b-TBI & NACA; D1-b-TBI; D5-NACA; D5-b-TBI & NACA; and D5-b-TBI groups for a) NAA, b) 5-HIAA, c) GSH, d) GSSG, e) GSH/GSSG ratio. (i) and (ii) are used to visualize the blast and treatment effects, respectively, for a, b, c, d, and e. Values are represented as mean ± SEM (n = 3-5). $p \leq 0.1$ (*), $p \leq 0.05$ (**), $p \leq 0.01$ (***), $p \leq 0.001$ (****). [D1 = Day 1 study group, D5= Day 5 study group, Sham = no blast + no treatment, NACA = no blast + NACA treatment, b-TBI & NACA = blast + NACA treatment, b-TBI = blast + no treatment] (Cont.)

6.3. EFFECT OF NACA IN URINE FOR D1 AND D5 STUDY GROUPS

Urinary metabolites levels were recorded as (Analyte)(ng/mL)/(CRT) (ug/mL), and the one-way ANOVA results are as follows: NAA; (F = 4.38, p = 0.0084), 5-HIAA; (F = 0.60, p = 0.7262), GSH; (F = 0.86, p = 0.5387), GSSG; (F = 0.20, p = 0.9709), and GSH/GSSG ratio; (F = 2.82, p = 0.0452). Post-hoc test using Fisher LSD for NAA showed multiple significant differences when comparing the group means for the D1 and D5 study groups. There was a general trend of increased NAA biomarker levels in the D5 study group compared to the D1 study group. TBI effect on urinary NAA was more

pronounced five days after injury than one day after injury, as shown by the significantly different ($p \leq 0.01$) increase of about 194 % in the D5-b-TBI group compared to the D1-b-TBI group. Subsequently, the effect of NACA in lowering urinary NAA levels in the injury animals was shown by the statistically significant ($p \leq 0.05$) 46% decrease observed when comparing the D5-b-TBI vs. D5-b-TBI & NACA groups. No statistically significant change was observed for the urinary 5-HIAA levels when comparing the means of the D1 and D5 study groups. However, isolating the D1 study group showed that there was a decreased level of urinary 5HIAA in the D1-b-TBI group compared with the D1- NACA and D1-b-TBI & NACA groups. Alternatively, isolating the D5 study group, it was observed that there was an increase (although not statistically significant) in urinary 5HIAA levels in the D1-b-TBI group compared with the D1- NACA and D1-b-TBI & NACA groups. The trend observed in both NAA and 5-HIAA was similar to previously observed urinary biomarker trends in our previous study. Urinary GSH and GSSG levels did not show any statistically significant differences comparing group means. However, the trend observed shows a generally reduced GSH level for the D5 study groups compared to the D1 study groups, with the GSSG levels staying relatively the same in both study groups. To evaluate the redox health status in urine, the GSH/GSSG ratio was determined, and it showed a generally higher GSH/GSSG ratio for the D1 study group compared to the D5 study group. Results are graphically depicted in the boxplot in Figure A3, and the *p*-values of the one-way ANOVA and the Fisher LSD multiple pairwise comparisons are shown in Tables A2 and A5, respectively.

Table A5 Fisher LSD pairwise comparison of urinary metabolites between different groups in the study. Significant *p*-values and approaching statistical significance *p*-values are in bold font.

Day 1 and Day 5 study comparison *p*-value (Urine)					
Comparison	**NAA**	**5-HIAA**	**GSH**	**GSSG**	**GSH/GSSG**
Sham vs. D1 NACA	0.3475	0.567	0.5954	0.3973	0.6875
Sham vs. D1 b-TBI & NACA	0.6291	0.4706	0.8164	0.4339	0.1187
Sham vs. D1 b-TBI	0.6777	0.1679	0.7148	0.6345	0.6488
Sham vs. D5 NACA	0.2061	0.151	0.1439	0.4809	0.1325
Sham vs. D5 b-TBI & NACA	0.5845	0.196	0.1207	0.4352	0.1246
Sham vs. D5 b-TBI	**0.0075**	0.4244	0.2219	0.6298	0.3008
D1 NACA vs. D1 b-TBI & NACA	0.7138	0.8315	0.8069	0.9805	0.2179
D1 NACA vs. D1 b-TBI	0.5495	0.4244	0.8385	0.6622	0.9794
D1 NACA vs. D5 NACA	**0.0362**	0.3694	0.3346	0.8842	**0.0634**
D1 NACA vs. D5 b-TBI & NACA	0.1465	0.4554	0.2886	0.9455	**0.0593**
D1 NACA vs. D5 b-TBI	**0.0008**	0.8701	0.5154	0.637	0.1462
D1 b-TBI & NACA vs. D1 b-TBI	0.886	0.6273	0.9378	0.681	0.2026
D1 b-TBI & NACA vs. D5 NACA	0.1141	0.5505	0.2717	0.877	**0.0074**
D1 b-TBI & NACA vs. D5 b-TBI & NACA	0.3362	0.6461	0.2364	0.9318	**0.0069**
D1 b-TBI & NACA vs. D5 b-TBI	**0.0055**	0.9287	0.4069	0.6609	**0.0148**
D1 b-TBI vs. D5 NACA	**0.0856**	0.8688	0.222	0.7779	**0.0464**
D1 b-TBI vs. D5 b-TBI & NACA	0.323	0.9985	0.1864	0.7156	**0.0431**
D1 b-TBI vs. D5 b-TBI	**0.0015**	0.4628	0.3513	0.9867	0.1099
D5 NACA vs. D5 b-TBI & NACA	0.4584	0.8758	0.9194	0.9383	0.972
D5 NACA vs. D5 b-TBI	0.1326	0.399	0.6609	0.7565	0.4922
D5 b-TBI & NACA vs. D5 b-TBI	**0.027**	0.5007	0.582	0.692	0.4684

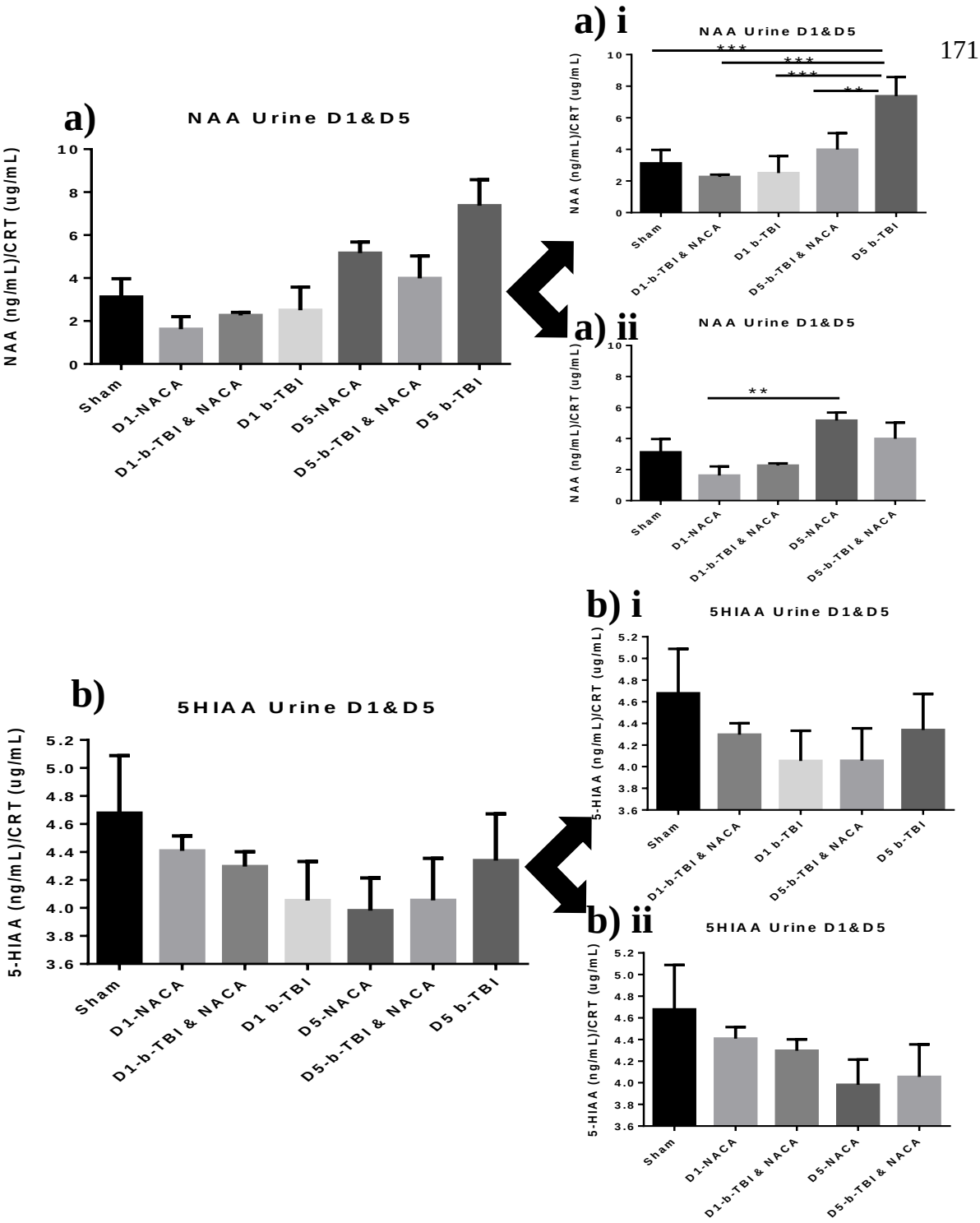

Figure A3. Urinary metabolite levels in Sham; D1-NACA; D1-b-TBI & NACA; D1-b-TBI; D5-NACA; D5-b-TBI & NACA; and D5-b-TBI groups for a) NAA, b) 5-HIAA, c) GSH, d) GSSG, e) GSH/GSSG ratio. (i) and (ii) are used to visualize the blast and treatment effects, respectively, for a, b, c, d, and e. Values are represented as mean ± SEM (n = 3-5). $p \leq 0.1$ (*), $p \leq 0.05$ (**), $p \leq 0.01$ (***), $p \leq 0.001$ (****). [D1 = Day 1 study group, D5= Day 5 study group, Sham = no blast + no treatment, NACA = no blast + NACA treatment, b-TBI & NACA = blast + NACA treatment, b-TBI = blast + no treatment]

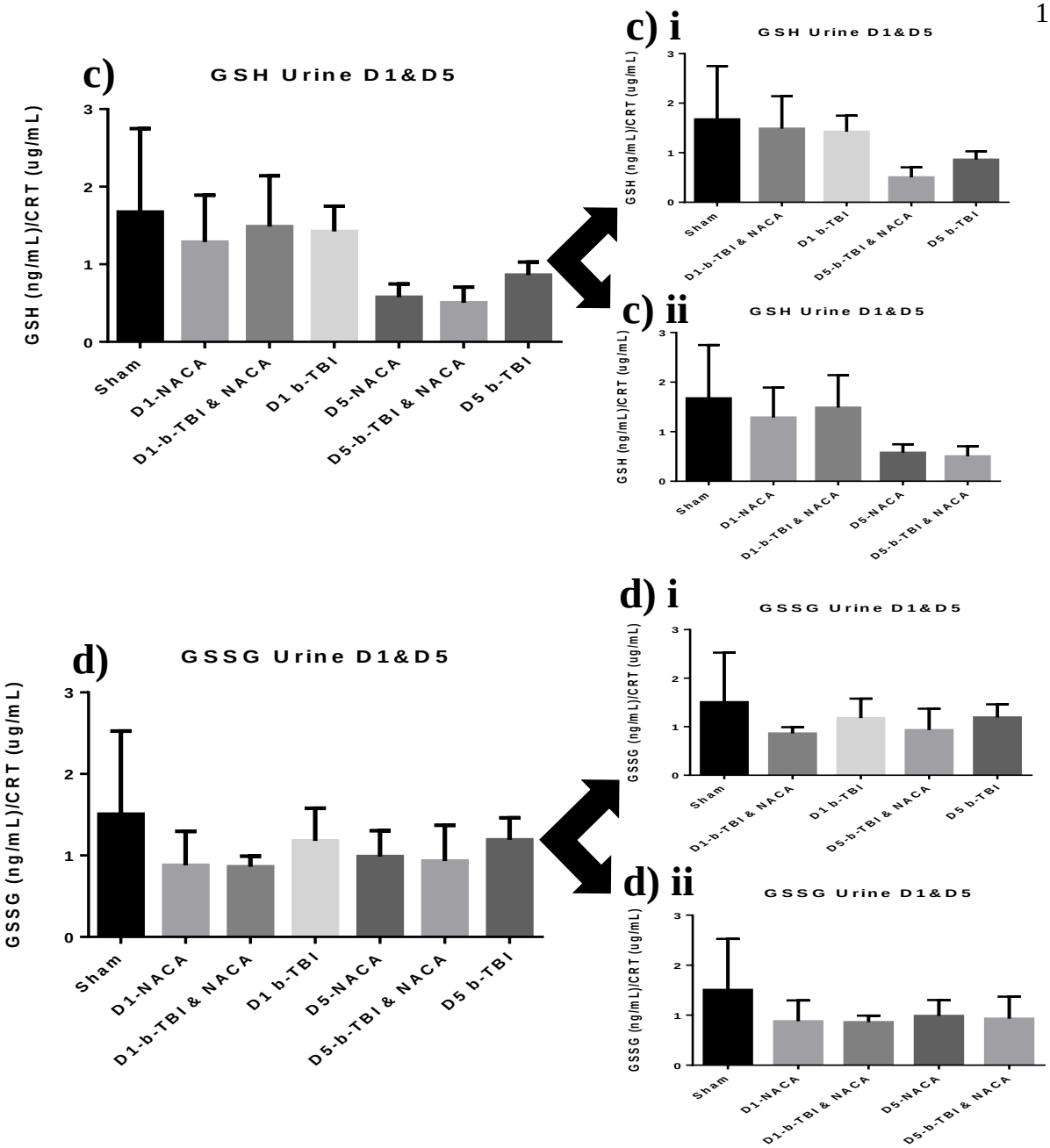

Figure A3. Urinary metabolite levels in Sham; D1-NACA; D1-b-TBI & NACA; D1-b-TBI; D5-NACA; D5-b-TBI & NACA; and D5-b-TBI groups for a) NAA, b) 5-HIAA, c) GSH, d) GSSG, e) GSH/GSSG ratio. (i) and (ii) are used to visualize the blast and treatment effects, respectively, for a, b, c, d, and e. Values are represented as mean ± SEM (n = 3-5). $p \leq 0.1$ (*), $p \leq 0.05$ (**), $p \leq 0.01$ (***), $p \leq 0.001$ (****). [D1 = Day 1 study group, D5= Day 5 study group, Sham = no blast + no treatment, NACA = no blast + NACA treatment, b-TBI & NACA = blast + NACA treatment, b-TBI = blast + no treatment] (Cont.)

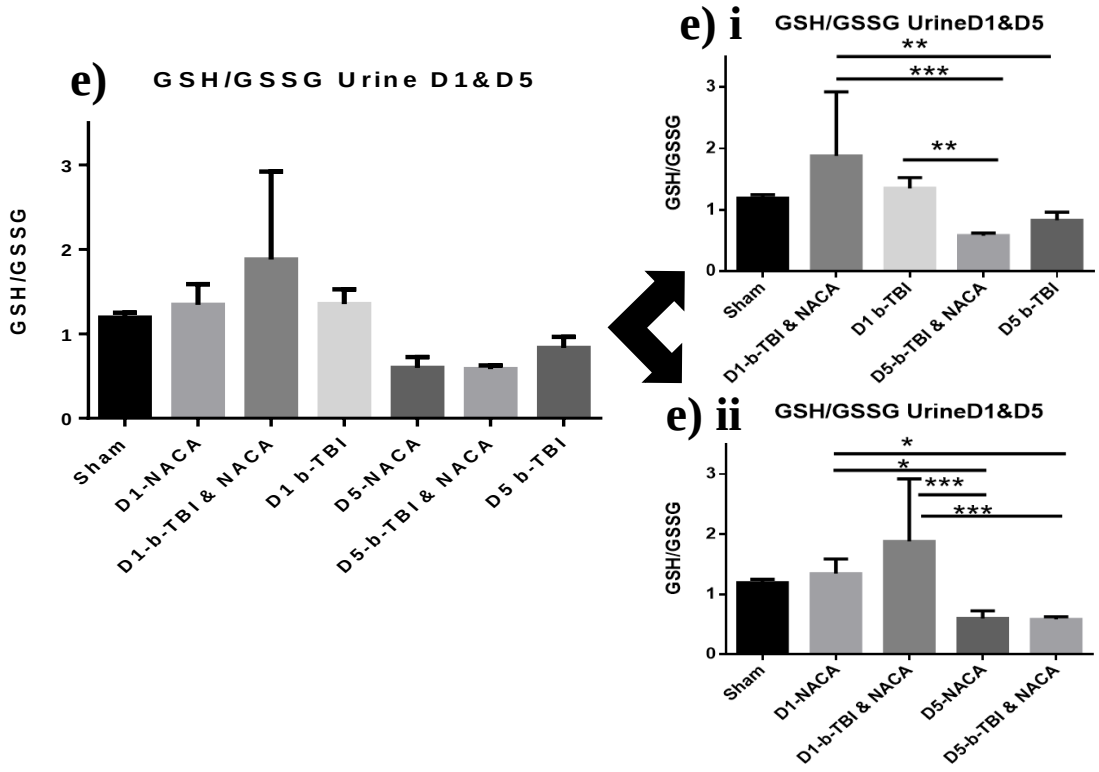

Figure A3. Urinary metabolite levels in Sham; D1-NACA; D1-b-TBI & NACA; D1-b-TBI; D5-NACA; D5-b-TBI & NACA; and D5-b-TBI groups for a) NAA, b) 5-HIAA, c) GSH, d) GSSG, e) GSH/GSSG ratio. (i) and (ii) are used to visualize the blast and treatment effects, respectively, for a, b, c, d, and e. Values are represented as mean ± SEM (n = 3-5). $p \leq 0.1$ (*), $p \leq 0.05$ (**), $p \leq 0.01$ (***), $p \leq 0.001$ (****). [D1 = Day 1 study group, D5= Day 5 study group, Sham = no blast + no treatment, NACA = no blast + NACA treatment, b-TBI & NACA = blast + NACA treatment, b-TBI = blast + no treatment] (Cont.)

7. CONCLUSION

From the data observations made from our results and as previously determined in our earlier studies, NAA and 5-HIAA biomarkers were influenced more in the peripheral fluid than in the brain where the initial insults occur. This evidence points to biochemical changes relating to blood-brain barrier changes that result in the movement of specific molecules that would otherwise not be transported in normal conditions. The effect of TBI on GSH, GSSG, and GSH/GSSG ratio was more visible in the brain tissue analysis,

and we observed depleting GSH levels in the injury rats in the D5 study group. Also, the GSH/GSSG ratio displayed better redox health status in the NACA-treated groups than in the D5 study group's injury group. Incidentally, follow-up treatment with NACA was more effective than a one-point initial pretreatment, and the manifestation of TBI on the selected small molecule biomarkers is more pronounced in the D5 study group than in the D1 study group. In order words, a combination of NACA pretreatment after injury followed up with post-injury may be the appropriate approach to getting the desired effect in TBI treatment. Overall, this result partially agreed with our previous study that involved the treatment of rats for four days straight after initial injury rather than for alternating days in this study. Also, additional evidence of time point changes to biomarkers was shown in this present study.

BIBLIOGRAPHY

[1] E. Ignowski, A.N. Winter, N. Duval, H. Fleming, T. Wallace, E. Manning, L. Koza, K. Huber, N.J. Serkova, D.A. Linseman, The cysteine-rich whey protein supplement, Immunocal®, preserves brain glutathione and improves cognitive, motor, and histopathological indices of traumatic brain injury in a mouse model of controlled cortical impact, Free Radic Biol Med 124 (2018) 328–341. https://doi.org/10.1016/j.freeradbiomed.2018.06.026.

[2] H. Ling, J. Hardy, H. Zetterberg, Neurological consequences of traumatic brain injuries in sports, Molecular and Cellular Neuroscience 66 (2015) 114–122. https://doi.org/10.1016/j.mcn.2015.03.012.

[3] R. Vorn, R. Naunheim, C. Lai, C. Wagner, J.M. Gill, W.B. Hubbard, R.G. Gatto, Elevated Axonal Protein Markers Following Repetitive Blast Exposure in Military Personnel, 16 (2022) 1–6. https://doi.org/10.3389/fnins.2022.853616.

[4] K.K.W. Wang, A. Moghieb, Z. Yang, Z. Zhang, Systems biomarkers as acute diagnostics and chronic monitoring tools for traumatic brain injury, Sensing Technologies for Global Health, Military Medicine, and Environmental Monitoring III 8723 (2013) 87230O. https://doi.org/10.1117/12.2020030.

[5] D. Laskowitz, G. Grant, Translational research in traumatic brain injury, Translational Research in Traumatic Brain Injury 3 (2016) 1–394. https://doi.org/10.1201/b18959.

[6] A.I.R. Maas, D.K. Menon, A. David et al., Traumatic brain injury: Integrated approaches to improve prevention, clinical care, and research, Lancet Neurol 16 (2017) 987–1048. https://doi.org/10.1016/S1474-4422(17)30371-X.

[7] D. V. Agoston, A. Shutes-David, E.R. Peskind, Biofluid biomarkers of traumatic brain injury, Brain Inj 31 (2017) 1195–1203. https://doi.org/10.1080/02699052.2017.1357836.

[8] L. Price, C. Wilson, G. Grant, Blood–Brain Barrier Pathophysiology following Traumatic Brain Injury. In: Laskowitz D, Grant G, editors. Translational Research in Traumatic Brain Injury. Boca Raton (FL): CRC Press/Taylor and Francis Group; 2016. Chapter 4. Available from:, (n.d.). https://www.ncbi.nlm.nih.gov/books/NBK326726/.

[9] N. Khatri, M. Thakur, V. Pareek, S. Kumar, S. Sharma, A.K. Datusalia, Oxidative Stress: Major Threat in Traumatic Brain Injury, CNS Neurol Disord Drug Targets 17 (2018) 689–695. https://doi.org/10.2174/1871527317666180627120501.

[10] S.Y. Ng, A.Y.W. Lee, Traumatic Brain Injuries: Pathophysiology and Potential Therapeutic Targets, Front Cell Neurosci 13 (2019) 1–23. https://doi.org/10.3389/fncel.2019.00528.

[11] U. Uknowledge, J.R. Kulbe, Neuroprotective Strategies Following Experimental Neuroprotective Strategies Following Experimental Traumatic Brain Injury: Lipid Peroxidation-Derived Traumatic Brain Injury: Lipid Peroxidation-Derived Aldehyde Scavenging and Inhibition of Mitochondrial A, (2019). https://doi.org/10.13023/etd.2019.228.

[12] H. Adrian, K. Mårten, N. Salla, V. Lasse, Disorders of the Nervous System Biomarkers of Traumatic Brain Injury: Temporal Changes in Body Fluids, ENeuro 3 (2016) 1–13. https://www.ncbi.nlm.nih.gov/pmc/articles/PMC5175263/pdf/ENEURO.0294-16.2016.pdf.

[13] A.J. Sorby-Adams, A.M. Marcoionni, E.R. Dempsey, J.A. Woenig, R.J. Turner, The role of neurogenic inflammation in blood-brain barrier disruption and development of cerebral oedema following acute central nervous system (CNS) injury, Int J Mol Sci 18 (2017) 1–24. https://doi.org/10.3390/ijms18081788.

[14] D. Shlosberg, M. Benifla, D. Kaufer, A. Friedman, Blood–brain barrier breakdown as a therapeutic target in traumatic brain injury, Nat Rev Neurol 6 (2010) 393–403. https://doi.org/10.1038/nrneurol.2010.74.

[15] Y. Sophie Su, A. Veeravagu, G. Grant, Neuroplasticity after Traumatic Brain Injury. In: Laskowitz D, Grant G, editors. Translational Research in Traumatic Brain Injury. Boca Raton (FL): CRC Press/Taylor and Francis Group; 2016. Chapter 8. Available from: https://www.ncbi.nlm.nih.gov/books/NBK, (n.d.).

[16] P. Kaur, S. Sharma, Recent Advances in Pathophysiology of Traumatic Brain Injury, Curr Neuropharmacol 16 (2017) 1224–1238. https://doi.org/10.2174/1570159x15666170613083606.

[17] P.R. McCrory, S.F. Berkovic, The history of clinical and pathophysiological concepts and misconceptions, Neurology 57 (2001) 2283–2289. https://doi.org/10.1212/WNL.57.12.2283.

[18] J. Bhatti, B. Nascimento, U. Akhtar, S.G. Rhind, H. Tien, A. Nathens, L.T. da Luz, Systematic review of human and animal studies examining the efficacy and safety of N-acetylcysteine (NAC) and N-Acetylcysteine Amide (NACA) in traumatic brain injury: Impact on neurofunctional outcome and biomarkers of oxidative stress and inflammation, Front Neurol 8 (2018). https://doi.org/10.3389/fneur.2017.00744.

[19] R. Tomaiuolo, M. Zibetti, C. Di Resta, G. Banfi, Challenges of the Effectiveness of Traumatic Brain Injuries Biomarkers in the Sports-Related Context, J Clin Med 12 (2023). https://doi.org/10.3390/jcm12072563.

[20] J.K. Yue, H. Deng, Traumatic Brain Injury: Contemporary Challenges and the Path to Progress, J Clin Med 12 (2023). https://doi.org/10.3390/jcm12093283.

[21] A.I.R. Maas, D.K. Menon, G.T. Manley et al., Traumatic brain injury: progress and challenges in prevention, clinical care, and research, Lancet Neurol 21 (2022) 1004–1060. https://doi.org/10.1016/S1474-4422(22)00309-X.

[22] H. Song, J. Cui, A. Simonyi, C.E. Johnson, G.K. Hubler, R.G. DePalma, Z. Gu, Linking blast physics to biological outcomes in mild traumatic brain injury: Narrative review and preliminary report of an open-field blast model, Behavioural Brain Research 340 (2018) 147–158. https://doi.org/10.1016/j.bbr.2016.08.037.

[23] F. Mesfin, N. Gupta, H. et al. Shapshak A, Diffuse Axonal Injury. [Updated 2023 Jun 12]. In: StatPearls [Internet]. Treasure Island (FL): StatPearls Publishing; 2024 Jan-. Available from: https://www.ncbi.nlm.nih.gov/books/NBK448102/, (n.d.).

[24] J.D. Cassidy, L.J. Carroll, P.M. Peloso, J. Borg, H. von Holst, L. Holm, J. Kraus, V.G. Coronado, Incidence, risk factors and prevention of mild traumatic brain injury: Results of the WHO Collaborating Centre Task Force on Mild Traumatic Brain Injury, J Rehabil Med Suppl (2004) 28–60. https://doi.org/10.1080/16501960410023732.

[25] G. Ling, F. Bandak, R. Armonda, G. Grant, J. Ecklund, Explosive blast neurotrauma, J Neurotrauma 26 (2009) 815–825. https://doi.org/10.1089/neu.2007.0484.

[26] A. Burton, Geoffrey Manley: TBI guy, Lancet Neurol 21 (2022) 967. https://doi.org/10.1016/S1474-4422(22)00401-X.

[27] N.E. Lopez, L. Gaston, K.R. Lopez, R.C. Coimbra, A. Hageny, J. Putnam, B. Eliceiri, R. Coimbra, V. Bansal, Early ghrelin treatment attenuates disruption of the blood brain barrier and apoptosis after traumatic brain injury through a UCP-2 mechanism, Brain Res 1489 (2012) 140–148. https://doi.org/10.1016/j.brainres.2012.10.031.

[28] U. Kawoos, R.M. McCarron, M. Chavko, Protective effect of N-acetylcysteine amide on blast-induced increase in intracranial pressure in rats, Front Neurol 8 (2017) 1–8. https://doi.org/10.3389/fneur.2017.00219.

[29] M.E. Hoffer, C. Balaban, M.D. Slade, J.W. Tsao, B. Hoffer, Amelioration of Acute Sequelae of Blast Induced Mild Traumatic Brain Injury by N-Acetyl Cysteine: A Double-Blind, Placebo Controlled Study, PLoS One 8 (2013) 1–10. https://doi.org/10.1371/journal.pone.0054163.

[30] D.W. Bryden, J.I. Tilghman, S.R. Hinds, Blast-Related Traumatic Brain Injury: Current Concepts and Research Considerations, J Exp Neurosci 13 (2019) 7–10. https://doi.org/10.1177/1179069519872213.

[31] A. Frati, D. Cerretani, A.I. Fiaschi, P. Frati, V. Gatto, R. La Russa, A. Pesce, E. Pinchi, A. Santurro, F. Fraschetti, V. Fineschi, Diffuse axonal injury and oxidative stress: A comprehensive review, Int J Mol Sci 18 (2017) 1–20. https://doi.org/10.3390/ijms18122600.

[32] H.M. Bramlett, W.D. Dietrich, Synuclein aggregation: possible role in traumatic brain injury, Exp Neurol 184 (2003) 27–30. https://doi.org/10.1016/S0014-4886(03)00401-1.

[33] B.Michael. Su Eric, Diffuse Axonal Injury. In: Laskowitz D, Grant G, editors. Translational Research in Traumatic Brain Injury. Boca Raton (FL): CRC Press/Taylor and Francis Group; 2016. Chapter 3. Available from: https://www.ncbi.nlm.nih.gov/books/NBK326722/, (n.d.).

[34] J. Li, X.Y. Li, D.F. Feng, D.C. Pan, Biomarkers associated with diffuse traumatic axonal injury: Exploring pathogenesis, early diagnosis, and prognosis, Journal of Trauma - Injury, Infection and Critical Care 69 (2010) 1610–1618. https://doi.org/10.1097/TA.0b013e3181f5a9ed.

[35] L. Young, G.T. Rule, R.T. Bocchieri, T.J. Walilko, J.M. Burns, G. Ling, When physics meets biology: Low and high-velocity penetration, blunt impact, and blast injuries to the brain, Front Neurol 6 (2015) 1–13. https://doi.org/10.3389/fneur.2015.00089.

[36] F. Friedlander, Propagation of a Pulse in an Inhomogeneous Medium. New York: Institute of Mathematical Sciences, New York University; 1955., n.d.

[37] J.M. Dewey, The shape of the blast wave: studies of the Friedlander equation. In Proceedings of the 21st international symposium on military aspects of blast and shock (pp. 1-9)., (n.d.).

[38] G.I. Taylor, The formation of a blast wave by a very intense explosion. - II. The atomic explosion of 1945, Proc R Soc Lond A Math Phys Sci 201 (1950) 175–186.

[39] H.R. Champion, J.B. Holcomb, L.A. Young, Injuries from explosions: Physics, biophysics, pathology, and required research focus, Journal of Trauma - Injury, Infection and Critical Care 66 (2009) 1468–1477. https://doi.org/10.1097/TA.0b013e3181a27e7f.

[40] I. Cullis, Blast Waves and How They Interact With Structures, J R Army Med Corps 147 (2001) 16–26. https://doi.org/10.1136/jramc-147-01-02.

[41] C.J. CLEMEDSON, H. PETTERSSON, Propagation of a high explosive air shock wave through different parts of an animal body., Am J Physiol 184 (1956) 119–126. https://doi.org/10.1152/ajplegacy.1955.184.1.119.

[42] I. Cernak, L.J. Noble-Haeusslein, Traumatic brain injury: An overview of pathobiology with emphasis on military populations, Journal of Cerebral Blood Flow and Metabolism 30 (2010) 255–266. https://doi.org/10.1038/jcbfm.2009.203.

[43] A.C. Courtney, M.W. Courtney, A thoracic mechanism of mild traumatic brain injury due to blast pressure waves, Med Hypotheses 72 (2009) 76–83. https://doi.org/10.1016/j.mehy.2008.08.015.

[44] K.N. Corps, T.L. Roth, D.B. McGavern, Inflammation and neuroprotection in traumatic brain injury, JAMA Neurol 72 (2015) 355–362. https://doi.org/10.1001/jamaneurol.2014.3558.

[45] J.B. Hiebert, Q. Shen, A.R. Thimmesch, J.D. Pierce, Traumatic Brain Injury and Mitochondrial Dysfunction, American Journal of the Medical Sciences 350 (2015) 132–138. https://doi.org/10.1097/MAJ.0000000000000506.

[46] J.C. LaManna, L.M. Vendel, R.M. Farrell, Brain adaptation to chronic hypobaric hypoxia in rats, J Appl Physiol 72 (1992) 2238–2243. https://doi.org/10.1152/jappl.1992.72.6.2238.

[47] T. V. Veenith, E.L. Carter, T. Geeraerts, J. Grossac, V.F.J. Newcombe, J. Outtrim, G.S. Gee, V. Lupson, R. Smith, F.I. Aigbirhio, T.D. Fryer, Y.T. Hong, D.K. Menon, J.P. Coles, Pathophysiologic mechanisms of cerebral ischemia and diffusion hypoxia in traumatic brain injury, JAMA Neurol 73 (2016) 542–550. https://doi.org/10.1001/jamaneurol.2016.0091.

[48] A. Nguyen, A.B. Patel, I.P. Kioutchoukova, M.J. Diaz, B. Lucke-Wold, Mechanisms of Mitochondrial Oxidative Stress in Brain Injury: From Pathophysiology to Therapeutics, Oxygen 3 (2023) 163–178. https://doi.org/10.3390/oxygen3020012.

[49] H. Ismail, Z. Shakkour, M. Tabet, S. Abdelhady, A. Kobaisi, R. Abedi, L. Nasrallah, G. Pintus, Y. Al-Dhaheri, S. Mondello, R. El-Khoury, A.H. Eid, F. Kobeissy, J. Salameh, Traumatic brain injury: Oxidative stress and novel anti-oxidants such as mitoquinone and edaravone, Antioxidants 9 (2020) 1–18. https://doi.org/10.3390/antiox9100943.

[50] E.D. Hall, R.A. Vaishnav, A.G. Mustafa, Antioxidant Therapies for Traumatic Brain Injury, Neurotherapeutics 7 (2010) 51–61. https://doi.org/10.1016/j.nurt.2009.10.021.

[51] M.T. Lin, M.F. Beal, Mitochondrial dysfunction and oxidative stress in neurodegenerative diseases, Nature 443 (2006) 787–795. https://doi.org/10.1038/nature05292.

[52] D.H. Smith, D.F. Meaney, W.H. Shull, Diffuse axonal injury in head trauma, Journal of Head Trauma Rehabilitation 18 (2003) 307–316. https://doi.org/10.1097/00001199-200307000-00003.

[53] A. Ozcan, M. Ogun, Biochemistry of Reactive Oxygen and Nitrogen Species, in: Basic Principles and Clinical Significance of Oxidative Stress, InTech, 2015: p. 13. https://doi.org/10.5772/61193.

[54] R. Patel, L. Rinker, J. Peng, W.M. Chilian, Reactive Oxygen Species: The Good and the Bad, in: Reactive Oxygen Species (ROS) in Living Cells, InTech, 2018: p. 13. https://doi.org/10.5772/intechopen.71547.

[55] B. Halliwell, Redox biology is a fundamental theme of aerobic life, Plant Physiol 141 (2006) 312–322. https://doi.org/10.1104/pp.106.077073.312.

[56] H.J. Forman, H. Zhang, Targeting oxidative stress in disease: promise and limitations of antioxidant therapy, Nat Rev Drug Discov 20 (2021) 689–709. https://doi.org/10.1038/s41573-021-00233-1.

[57] S. Tobwala, N. Ercal, N-acetylcysteine amide (NACA), a novel GSH prodrug: Its metabolism and implications in health, 2013.

[58] K.A. Salman, S. Ashraf, Reactive oxygen species: A link between chronic inflammation and cancer., Asia-Pacific J. Mol. Biol. Biotechnol 21 (2013) 41–49.

[59] G.Y. Liou, P. Storz, Reactive oxygen species in cancer, 2010. https://doi.org/10.3109/10715761003667554.

[60] A.A. Alfadda, R.M. Sallam, Reactive oxygen species in health and disease, J Biomed Biotechnol 2012 (2012). https://doi.org/10.1155/2012/936486.

[61] Y. Liu, G. Fiskum, D. Schubert, Generation of reactive oxygen species by the mitochondrial electron transport chain, J Neurochem 80 (2002) 780–787. https://doi.org/10.1046/j.0022-3042.2002.00744.x.

[62] A.A. Starkov, G. Fiskum, C. Chinopoulos, B.J. Lorenzo, S.E. Browne, M.S. Patel, M.F. Beal, Mitochondrial α-ketoglutarate dehydrogenase complex generates reactive oxygen species, Journal of Neuroscience 24 (2004) 7779–7788. https://doi.org/10.1523/JNEUROSCI.1899-04.2004.

[63] H. Bayir, Reactive oxygen species, Crit Care Med 33 (2005) S498–S501. https://doi.org/10.1097/01.CCM.0000186787.64500.12.

[64] C.M. Curieses Andrés, J.M. Pérez de la Lastra, C. Andrés Juan, F.J. Plou, E. Pérez-Lebeña, From reactive species to disease development: Effect of oxidants and antioxidants on the cellular biomarkers, J Biochem Mol Toxicol 37 (2023). https://doi.org/10.1002/jbt.23455.

[65] S.J. Forrester, D.S. Kikuchi, M.S. Hernandes, Q. Xu, K.K. Griendling, Reactive oxygen species in metabolic and inflammatory signaling, Circ Res 122 (2018) 877–902. https://doi.org/10.1161/CIRCRESAHA.117.311401.

[66] A. Salminen, J. Ojala, K. Kaarniranta, A. Kauppinen, Mitochondrial dysfunction and oxidative stress activate inflammasomes: Impact on the aging process and age-related diseases, Cellular and Molecular Life Sciences 69 (2012) 2999–3013. https://doi.org/10.1007/s00018-012-0962-0.

[67] B.K. Siesjö, P. Siesjö, Mechanisms of secondary brain injury, Eur J Anaesthesiol 13 (1996) 247–268. https://doi.org/10.1097/00003643-199605000-00004.

[68] G. Pizzino, N. Irrera, M. Cucinotta, G. Pallio, F. Mannino, V. Arcoraci, F. Squadrito, D. Altavilla, A. Bitto, Oxidative Stress: Harms and Benefits for Human Health, Oxid Med Cell Longev 2017 (2017). https://doi.org/10.1155/2017/8416763.

[69] U. Sherin, M. Devaskar, The Role of Oxygen in Health and Disease - A Series of Reviews, Pediatr Research 66 (2009) 121–127.

[70] E. Birben, U.M. Sahiner, C. Sackesen, S. Erzurum, O. Kalayci, Oxidative stress and antioxidant defense, World Allergy Organization Journal 5 (2012) 9–19. https://doi.org/10.1097/WOX.0b013e3182439613.

[71] B. Hakiminia, B. Alikiaii, F. Khorvash, S. Mousavi, Oxidative stress and mitochondrial dysfunction following traumatic brain injury: From mechanistic view to targeted therapeutic opportunities, Fundam Clin Pharmacol 36 (2022) 612–662. https://doi.org/10.1111/fcp.12767.

[72] T.I. Peng, M.J. Jou, Oxidative stress caused by mitochondrial calcium overload, Ann N Y Acad Sci 1201 (2010) 183–188. https://doi.org/10.1111/j.1749-6632.2010.05634.x.

[73] M. Stefani, Protein aggregation diseases: Toxicity of soluble prefibrillar aggregates and their clinical significance, 2010. https://doi.org/10.1007/978-1-60761-756-3_2.

[74] K. Funai, S.A. Summers, J. Rutter, Reign in the membrane: How common lipids govern mitochondrial function, Curr Opin Cell Biol 63 (2020) 162–173. https://doi.org/10.1016/j.ceb.2020.01.006.

[75] K.D. Bruce, A. Zsombok, R.H. Eckel, Lipid processing in the brain: A key regulator of systemic metabolism, Front Endocrinol (Lausanne) 8 (2017) 1–11. https://doi.org/10.3389/fendo.2017.00060.

[76] M. Bains, E.D. Hall, Antioxidant therapies in traumatic brain and spinal cord injury, Biochimica et Biophysica Acta (BBA) - Molecular Basis of Disease 1822 (2012) 675–684. https://doi.org/10.1016/j.bbadis.2011.10.017.

[77] J.R. Muñoz-Castañeda, P. Montilla, F.J. Padillo, I. Bujalance, M.C. Muñoz, J. Muntané, I. Túnez, Role of serotonin in cerebral oxidative stress in rats, Acta Neurobiol Exp (Wars) 66 (2006) 1–6.

[78] A.R. Pfaff, J. Beltz, E. King, N. Ercal, Medicinal Thiols: Current Status and New Perspectives, Mini-Reviews in Medicinal Chemistry 20 (2019) 513–529. https://doi.org/10.2174/1389557519666191119144100.

[79] G.H. Danton, W.D. Dietrich, Neuroprotection: Where Are We Going?, in: From Neuroscience To Neurology, Elsevier, 2005: pp. 237–265. https://doi.org/10.1016/B978-012738903-5/50015-1.

[80] B.E. Masel, D.S. DeWitt, Traumatic brain injury: A disease process, not an event, J Neurotrauma 27 (2010) 1529–1540. https://doi.org/10.1089/neu.2010.1358.

[81] P.K. Crane, L.E. Gibbons, K. Dams-O'Connor, E. Trittschuh, J.B. Leverenz, C. Dirk Keene, J. Sonnen, T.J. Montine, D.A. Bennett, S. Leurgans, J.A. Schneider, E.B. Larson, Association of traumatic brain injury with late-life neurodegenerative conditions and Neuropathologic findings, JAMA Neurol 73 (2016) 1062–1069. https://doi.org/10.1001/jamaneurol.2016.1948.

[82] M. Cruz-Haces, J. Tang, G. Acosta, J. Fernandez, R. Shi, Pathological correlations between traumatic brain injury and chronic neurodegenerative diseases, Transl Neurodegener 6 (2017) 1–10. https://doi.org/10.1186/s40035-017-0088-2.

[83] D.C. Perry, V.E. Sturm, M.J. Peterson, C.F. Pieper, T. Bullock, B.F. Boeve, B.L. Miller, K.M. Guskiewicz, M.S. Berger, J.H. Kramer, K.A. Welsh-Bohmer, Association of traumatic brain injury with subsequent neurological and psychiatric disease: a meta-analysis, J Neurosurg 124 (2016) 511–526. https://doi.org/10.3171/2015.2.JNS14503.

[84] L. Wilson, W. Stewart, K. Dams-O'Connor, R. Diaz-Arrastia, L. Horton, D.K. Menon, S. Polinder, The chronic and evolving neurological consequences of traumatic brain injury, Lancet Neurol 16 (2017) 813–825. https://doi.org/10.1016/S1474-4422(17)30279-X.

[85] P. Ciurli, R. Formisano, U. Bivona, A. Cantagallo, P. Angelelli, Neuropsychiatric disorders in persons with severe traumatic brain injury: Prevalence, phenomenology, and relationship with demographic, clinical, and functional features, Journal of Head Trauma Rehabilitation 26 (2011) 116–126. https://doi.org/10.1097/HTR.0b013e3181dedd0e.

[86] R.E. Jorge, R.G. Robinson, D. Moser, A. Tateno, B. Crespo-Facorro, S. Arndt, Major Depression Following Traumatic Brain Injury, Arch Gen Psychiatry 61 (2004) 42–50. https://doi.org/10.1001/archpsyc.61.1.42.

[87] C.C. Liao, Y.C. Chou, C.C. Yeh, C.J. Hu, W.T. Chiu, T.L. Chen, Stroke risk and outcomes in patients with traumatic brain injury: 2 Nationwide studies, Mayo Clin Proc 89 (2014) 163–172. https://doi.org/10.1016/j.mayocp.2013.09.019.

[88] G. Mooney, J. Speed, The association between mild traumatic brain injury and psychiatric conditions, Brain Inj 15 (2001) 865–877. https://doi.org/10.1080/02699050110065286.

[89] A.H. Bell, S.L. Miller, M. Castillo-Melendez, A. Malhotra, The Neurovascular Unit: Effects of Brain Insults During the Perinatal Period, Front Neurosci 13 (2020) 1–19. https://doi.org/10.3389/fnins.2019.01452.

[90] C. Iadecola, M. Nedergaard, Glial regulation of the cerebral microvasculature, Nat Neurosci 10 (2007) 1369–1376. https://doi.org/10.1038/nn2003.

[91] J. Lok, X.S. Wang, C.H. Xing, T.K. Maki, L.M. Wu, S.Z. Guo, N. Noviski, K. Arai, M.J. Whalen, E.H. Lo, X.Y. Wang, Targeting the Neurovascular Unit in Brain Trauma, CNS Neurosci Ther 21 (2015) 304–308. https://doi.org/10.1111/cns.12359.

[92] P. Barzó, A. Marmarou, P. Fatouros, F. Corwin, J. Dunbar, Magnetic resonance imaging-monitored acute blood-brain barrier changes in experimental traumatic brain injury, J Neurosurg 85 (1996) 1113–1121. https://doi.org/10.3171/jns.1996.85.6.1113.

[93] M.M. Banoei, C. Casault, S.M. Metwaly, B.W. Winston, Metabolomics and Biomarker Discovery in Traumatic Brain Injury, J Neurotrauma 35 (2018) 1831–1848. https://doi.org/10.1089/neu.2017.5326.

[94] P.M. Rees, Contemporary Issues in Mild Traumatic Brain Injury, Arch Phys Med Rehabil 84 (2003) 1885–1894. https://doi.org/10.1016/j.apmr.2003.03.001.

[95] C. Eierud, R.C. Craddock, S. Fletcher, M. Aulakh, B. King-Casas, D. Kuehl, S.M. Laconte, Neuroimaging after mild traumatic brain injury: Review and meta-analysis, Neuroimage Clin 4 (2014) 283–294. https://doi.org/10.1016/j.nicl.2013.12.009.

[96] C.B. Jeter, G.W. Hergenroeder, N.H. Ward, A.N. Moore, P.K. Dash, Human mild traumatic brain injury decreases circulating branched-chain amino acids and their metabolite levels, J Neurotrauma 30 (2013) 671–679. https://doi.org/10.1089/neu.2012.2491.

[97] J.H. Wang, J. Byun, S. Pennathur, Analytical approaches to metabolomics and applications to systems biology, Semin Nephrol 30 (2010) 500–511. https://doi.org/10.1016/j.semnephrol.2010.07.007.

[98] C.B. Jeter, G.W. Hergenroeder, M.J. Hylin, J.B. Redell, A.N. Moore, P.K. Dash, Biomarkers for the diagnosis and prognosis of mild traumatic brain injury/concussion, J Neurotrauma 30 (2013) 657–670. https://doi.org/10.1089/neu.2012.2439.

[99] P.K. Dash, J. Zhao, G. Hergenroeder, A.N. Moore, Biomarkers for the Diagnosis, Prognosis, and Evaluation of Treatment Efficacy for Traumatic Brain Injury, Neurotherapeutics 7 (2010) 100–114. https://doi.org/10.1016/j.nurt.2009.10.019.

[100] K.K. Wang, Z. Yang, T. Zhu, Y. Shi, R. Rubenstein, J.A. Tyndall, G.T. Manley, An update on diagnostic and prognostic biomarkers for traumatic brain injury, Expert Rev Mol Diagn 18 (2018) 165–180. https://doi.org/10.1080/14737159.2018.1428089.

[101] B.A. Plog, M.L. Dashnaw, E. Hitomi, W. Peng, Y. Liao, N. Lou, R. Deane, M. Nedergaard, Biomarkers of traumatic injury are transported from brain to blood via the glymphatic system, Journal of Neuroscience 35 (2015) 518–526. https://doi.org/10.1523/JNEUROSCI.3742-14.2015.

[102] A. Chodobski, B.J. Zink, J. Szmydynger-Chodobska, Blood-Brain Barrier Pathophysiology in Traumatic Brain Injury, Transl Stroke Res 2 (2011) 492–516. https://doi.org/10.1007/s12975-011-0125-x.

[103] P.S. Upadhyayula, J.K. Yue, J. Yang, H.S. Birk, J.D. Ciacci, The current state of rural neurosurgical practice: An international perspective, J Neurosci Rural Pract 9 (2018) 123–131. https://doi.org/10.4103/jnrp.jnrp_273_17.

[104] J.K. Yue, P.S. Upadhyayula, L.N. Avalos, R.R.L. Phelps, C.G. Suen, T.A. Cage, Concussion and Mild-Traumatic Brain Injury in Rural Settings: Epidemiology and Specific Health Care Considerations, J Neurosci Rural Pract 11 (2020) 23–33. https://doi.org/10.1055/s-0039-3402581.

[105] A.L. Walker, S.Z. Imam, R.A. Roberts, Drug discovery and development: Biomarkers of neurotoxicity and neurodegeneration, Exp Biol Med 243 (2018) 1037–1045. https://doi.org/10.1177/1535370218801309.

[106] B.J. Blyth, A. Farahvar, H. He, A. Nayak, C. Yang, G. Shaw, J.J. Bazarian, Elevated Serum Ubiquitin Carboxy-Terminal Hydrolase L1 Is Associated with Abnormal Blood–Brain Barrier Function after Traumatic Brain Injury, J Neurotrauma 28 (2011) 2453–2462. https://doi.org/10.1089/neu.2010.1653.

[107] N. Pham, V. Fazio, L. Cucullo, Q. Teng, P. Biberthaler, J.J. Bazarian, D. Janigro, Extracranial sources of S100B do not affect serum levels, PLoS One 5 (2010) 1–9. https://doi.org/10.1371/journal.pone.0012691.

[108] J.R. Kulbe, J.W. Geddes, Current status of fluid biomarkers in mild traumatic brain injury, Exp Neurol 275 (2016) 334–352. https://doi.org/10.1016/j.expneurol.2015.05.004.

[109] M.D. Habgood, N. Bye, K.M. Dziegielewska, C.J. Ek, M.A. Lane, A. Potter, C. Morganti-Kossmann, N.R. Saunders, Changes in blood-brain barrier permeability to large and small molecules following traumatic brain injury in mice, European Journal of Neuroscience 25 (2007) 231–238. https://doi.org/10.1111/j.1460-9568.2006.05275.x.

[110] A. Fesharaki-Zadeh, Oxidative Stress in Traumatic Brain Injury, Int J Mol Sci 23 (2022). https://doi.org/10.3390/ijms232113000.

[111] R. Busto, W.D. Dietrich, M.Y.T. Globus, O. Alonso, M.D. Ginsberg, Extracellular release of serotonin following fluid-percussion brain injury in rats, J Neurotrauma 14 (1997) 35–42. https://doi.org/10.1089/neu.1997.14.35.

[112] M.Y. -T. Globus, O. Alonso, W.D. Dietrich, R. Busto, M.D. Ginsberg, Glutamate Release and Free Radical Production Following Brain Injury: Effects of Posttraumatic Hypothermia, J Neurochem 65 (1995) 1704–1711. https://doi.org/10.1046/j.1471-4159.1995.65041704.x.

[113] R. Heales, S.E.C. Davies, T.E. Bates, J.B. Clark, Depletion of brain glutathione is accompanied by impaired mitochondrial function and decreased N-acetyl aspartate concentration, Neurochem Res 20 (1995) 31–38. https://doi.org/10.1007/BF00995149.

[114] H.S. Lee, S.M. Kim, J.H. Jang, H.D. Park, S.Y. Lee, Serum 5-hydroxyindoleacetic acid and ratio of 5-hydroxyindoleacetic acid to serotonin as metabolomics indicators for acute oxidative stress and inflammation in vancomycin-associated acute kidney injury, Antioxidants 10 (2021). https://doi.org/10.3390/antiox10060895.

[115] R.J. Shannon, S. Van Der Heide, E.L. Carter, I. Jalloh, D.K. Menon, P.J. Hutchinson, K.L.H. Carpenter, Extracellular N-Acetylaspartate in Human Traumatic Brain Injury, J Neurotrauma 33 (2016) 319–329. https://doi.org/10.1089/neu.2015.3950.

[116] J.R. Moffett, P. Arun, P.S. Ariyannur, A.M.A. Namboodiri, N-Acetylaspartate reductions in brain injury: Impact on post-injury neuroenergetics, lipid synthesis, and protein acetylation, Front Neuroenergetics 5 (2013) 1–19. https://doi.org/10.3389/fnene.2013.00011.

[117] J. Xuan, G. Pan, Y. Qiu, L. Yang, M. Su, Y. Liu, J. Chen, G. Feng, Y. Fang, W. Jia, Q. Xing, L. He, Metabolomic profiling to identify potential serum biomarkers for schizophrenia and risperidone action, J Proteome Res 10 (2011) 5433–5443. https://doi.org/10.1021/pr2006796.

[118] R.H. Al-Samsam, B. Alessandri, R. Bullock, Extracellular N-acetyl-aspartate as a biochemical marker of the severity of neuronal damage following experimental acute traumatic brain injury, J Neurotrauma 17 (2000) 31–39. https://doi.org/10.1089/neu.2000.17.31.

[119] J.R. Lenchner, C. Santos, Biochemistry, 5 Hydroxyindoleacetic Acid. [Updated 2023 May 1]. In: StatPearls [Internet]. Treasure Island (FL): StatPearls Publishing; 2024 Jan-. Available from: https://www.ncbi.nlm.nih.gov/books/NBK551684/, (n.d.).

[120] F. Bai, D.C. Jones, S.S. Lau, T.J. Monks, Serotonergic neurotoxicity of 3,4-(±)-methylenedioxyamphetamine and 3,4-(±)-methylendioxymethamphetamine (ecstasy) is potentiated by inhibition of γ-glutamyl transpeptidase, Chem Res Toxicol 14 (2001) 863–870. https://doi.org/10.1021/tx010011l.

[121] H. Jayamohananan, M.K. Manoj Kumar, A. T P, 5-HIAA as a Potential Biological Marker for Neurological and Psychiatric Disorders, Adv Pharm Bull 9 (2019) 374–381. https://doi.org/10.15171/apb.2019.044.

[122] S. Bolandparvaz, M. Vasei, A.A. Owji, N. Ata-Ee, A. Amin, Y. Daneshbod, S.V. Hosseini, Urinary 5-hydroxy indole acetic acid as a test for early diagnosis of acute appendicitis, Clin Biochem 37 (2004) 985–989. https://doi.org/10.1016/j.clinbiochem.2004.07.003.

[123] X.M. Han, Y.J. Qin, Y. Zhu, X.L. Zhang, N.X. Wang, Y. Rang, X.J. Zhai, Y.N. Lu, Development of an underivatized LC-MS/MS method for quantitation of 14 neurotransmitters in rat hippocampus, plasma and urine: Application to CUMS induced depression rats, J Pharm Biomed Anal 174 (2019) 683–695. https://doi.org/10.1016/j.jpba.2019.06.043.

[124] N. Ballatori, S.M. Krance, S. Notenboom, S. Shi, K. Tieu, C.L. Hammond, Glutathione dysregulation and the etiology and progression of human diseases, Biol Chem 390 (2009) 191–214. https://doi.org/10.1515/BC.2009.033.

[125] S.C. Lu, Glutathione synthesis, Biochim Biophys Acta Gen Subj 1830 (2013) 3143–3153. https://doi.org/10.1016/j.bbagen.2012.09.008.

[126] A. Mendes Arent, L.F. De Souza, R. Walz, A.L. Dafre, Perspectives on molecular biomarkers of oxidative stress and antioxidant strategies in traumatic brain injury, Biomed Res Int 2014 (2014). https://doi.org/10.1155/2014/723060.

[127] D. Janigro, D.M. Bailey, S. Lehmann, J. Badaut, R. O'Flynn, C. Hirtz, N. Marchi, Peripheral Blood and Salivary Biomarkers of Blood–Brain Barrier Permeability and Neuronal Damage: Clinical and Applied Concepts, Front Neurol 11 (2021). https://doi.org/10.3389/fneur.2020.577312.

[128] F.K. Pearl Chung, Traumatic Brain Injury (TBI): Overview of Diagnosis and Treatment, J Neurol Neurophysiol 05 (2013) 1–10. https://doi.org/10.4172/2155-9562.1000182.

[129] A. Jarrahi, M. Braun, M. Ahluwalia, R. V. Gupta, M. Wilson, S. Munie, P. Ahluwalia, J.R. Vender, F.L. Vale, K.M. Dhandapani, K. Vaibhav, Revisiting traumatic brain injury: From molecular mechanisms to therapeutic interventions, Biomedicines 8 (2020) 1–42. https://doi.org/10.3390/biomedicines8100389.

[130] R. Shi, C.C. Huang, R.S. Aronstam, N. Ercal, A. Martin, Y.W. Huang, N-acetylcysteine amide decreases oxidative stress but not cell death induced by doxorubicin in H9c2 cardiomyocytes, BMC Pharmacol 9 (2009) 1–9. https://doi.org/10.1186/1471-2210-9-7.

[131] Y. Xiong, P.L. Peterson, C.P. Lee, Effect of N-acetylcysteine on mitochondrial function following traumatic brain injury in rats, J Neurotrauma 16 (1999) 1067–1082. https://doi.org/10.1089/neu.1999.16.1067.

[132] U. Kawoos, R. Abutarboush, S. Zarriello, A. Qadri, S.T. Ahlers, R.M. McCarron, M. Chavko, N-acetylcysteine amide ameliorates blast-induced changes in blood-brain barrier integrity in rats, Front Neurol 10 (2019) 1–7. https://doi.org/10.3389/fneur.2019.00650.

[133] S. Tobwala, A. Khayyat, W. Fan, N. Ercal, Comparative evaluation of N-acetylcysteine and N-acetylcysteineamide in acetaminophen-induced hepatotoxicity in human hepatoma HepaRG cells, Exp Biol Med 240 (2015) 261–272. https://doi.org/10.1177/1535370214549520.

[134] J.R. Martin, T.A., Causey, D.H., Sheffner, A.L., Wheeler, A.G., Corrigan, Amides of N-Acylcysteines as mucolytic agents., J. Med. Chem. 10, 1172–1176 (1967) 89. http://www.nber.org/papers/w16019.

[135] R. He, W. Zheng, T. Ginman, H. Ottosson, S. Norgren, Y. Zhao, M. Hassan, Pharmacokinetic profile of N-acetylcysteine amide and its main metabolite in mice using new analytical method, European Journal of Pharmaceutical Sciences 143 (2020) 105158. https://doi.org/10.1016/j.ejps.2019.105158.

[136] C.K. Sen, L. Packer, Thiol homeostasis and supplements in physical exercise, American Journal of Clinical Nutrition 72 (2000). https://doi.org/10.1093/ajcn/72.2.653s.

[137] S. Tobwala, S.K.Y. Maddirala, N. Ercal, Effect of a novel thiol antioxidant, N-acetylcysteine Amide (NACA), on reversing sodium selenite-induced cataracts in wistar rats. (Unpublished poster), in: n.d.

[138] M. Reza Khorramizadeh, F. Saadat, Animal models for human disease, in: Anim Biotechnol, Elsevier, 2020: pp. 153–171. https://doi.org/10.1016/B978-0-12-811710-1.00008-2.

[139] A. Loewa, J.J. Feng, S. Hedtrich, Human disease models in drug development, Nature Reviews Bioengineering 1 (2023) 545–559. https://doi.org/10.1038/s44222-023-00063-3.

[140] K.A. Smith, Louis Pasteur, the father of immunology?, Front Immunol 3 (2012) 1–10. https://doi.org/10.3389/fimmu.2012.00068.

[141] S.H.E. Kaufmann, Remembering emil von behring: From tetanus treatment to antibody cooperation with phagocytes, MBio 8 (2017) 1–6. https://doi.org/10.1128/mBio.00117-17.

[142] D. V Agoston, A. Kamnaksh, Modeling the Neurobehavioral Consequences of Blast-Induced Traumatic Brain Injury Spectrum Disorder and Identifying Related Biomarkers. In: Kobeissy FH, editor. Brain Neurotrauma: Molecular, Neuropsychological, and Rehabilitation Aspects. Boca Raton (FL):, (n.d.).

[143] W.T. O'Connor, A. Smyth, M.D. Gilchrist, Animal models of traumatic brain injury: A critical evaluation, Pharmacol Ther 130 (2011) 106–113. https://doi.org/10.1016/j.pharmthera.2011.01.001.

[144] E.C. Bryda, The Mighty Mouse: the impact of rodents on advances in biomedical research., Mo Med. 110(3):207 (2013) PMID: 23829104; PMCID: PMC3987984. https://www.ncbi.nlm.nih.gov/pmc/articles/PMC3987984/.

[145] J.M. Meythaler, J.D. Peduzzi, E. Eleftheriou, T.A. Novack, Current concepts: Diffuse axonal injury–associated traumatic brain injury, Arch Phys Med Rehabil 82 (2001) 1461–1471. https://doi.org/10.1053/apmr.2001.25137.

[146] J.K. Nicholson, I.D. Wilson, Understanding "global" systems biology: Metabonomics and the continuum of metabolism, Nat Rev Drug Discov 2 (2003) 668–676. https://doi.org/10.1038/nrd1157.

[147] Z. Pan, D. Raftery, Comparing and combining NMR spectroscopy and mass spectrometry in metabolomics, Anal Bioanal Chem 387 (2007) 525–527. https://doi.org/10.1007/s00216-006-0687-8.

[148] K. Dettmer, P.A. Aronov, B.D. Hammock, Mass spectrometry-based metabolomics, Mass Spectrom Rev 26 (2007) 51–78. https://doi.org/10.1002/mas.20108.

[149] J.R. Bain, R.D. Stevens, B.R. Wenner, O. Ilkayeva, D.M. Muoio, C.B. Newgard, Metabolomics applied to diabetes research: Moving from information to knowledge, Diabetes 58 (2009) 2429–2443. https://doi.org/10.2337/db09-0580.

[150] R. Grandori, C. Santambrogio, S. Brocca, G. Invernizzi, M. Lotti, Electrospray-ionization mass spectrometry as a tool for fast screening of protein structural properties, Biotechnol J 4 (2009) 73–87. https://doi.org/10.1002/biot.200800250.

[151] S. Banerjee, S. Mazumdar, Electrospray Ionization Mass Spectrometry: A Technique to Access the Information beyond the Molecular Weight of the Analyte, Int J Anal Chem 2012 (2012) 1–40. https://doi.org/10.1155/2012/282574.

[152] R.K. Azad, V. Shulaev, Metabolomics technology and bioinformatics for precision medicine, Brief Bioinform 20 (2019) 1957–1971. https://doi.org/10.1093/bib/bbx170.

[153] USP, Residual Solvents - Chapter 467, The United States Pharmacopeial Convention (2019) 22. https://www.uspnf.com/sites/default/files/usp_pdf/EN/USPNF/revisions/gc-467-residual-solvents-ira-20190927.pdf.

[154] ICH Expert Working Group, Ich Harmonised Guideline - Impurities: Guideline for Residual Solvents Q3C(R8), International Council for Harmonisation of Technical Requirements for Pharmaceuticals for Human Use (ICH) (2021) 1–43.

[155] C. Witschi, E. Doelker, Residual solvents in pharmaceutical products: Acceptable limits, influences on physicochemical properties, analytical methods and documented values, European Journal of Pharmaceutics and Biopharmaceutics 43 (1997) 215–242. https://doi.org/10.1016/S0939-6411(96)00037-9.

[156] M. Ojala, M. Poutanen, I. Mattila, R.A. Ketola, T. Kotiaho, R. Kostiainen, Analysis of residual solvents in pharmaceuticals with purge-and-membrane mass spectrometry, Rapid Communications in Mass Spectrometry 14 (2000) 994–998. https://doi.org/10.1002/(SICI)1097-0231(20000615)14:11<994::AID-RCM977>3.0.CO;2-6.

[157] C.C. Camarasu, Unknown residual solvents identification in drug products by headspace solid phase microextraction gas chromatography-mass spectrometry, Chromatographia 56 (2002). https://doi.org/10.1007/bf02494126.

[158] C.C. Camarasu, M. Mezei-Szûts, G.B. Varga, Residual solvents determination in pharmaceutical products by GC-HS and GC-MS-SPME, J Pharm Belg 53 (1998) 165.

[159] Y. Liu, C.Q. Hu, Establishment of a knowledge base for identification of residual solvents in pharmaceuticals, Anal Chim Acta 575 (2006) 246–254. https://doi.org/10.1016/j.aca.2006.05.098.

[160] K. Grodowska, A. Parczewski, Analytical methods for residual solvents determination in pharmaceutical products, Acta Poloniae Pharmaceutica - Drug Research 67 (2010) 13–26.

[161] M. Tankiewicz, J. Namieśnik, W. Sawicki, Analytical procedures for quality control of pharmaceuticals in terms of residual solvents content: Challenges and recent developments, TrAC - Trends in Analytical Chemistry 80 (2016) 328–344. https://doi.org/10.1016/j.trac.2015.09.008.

[162] C.M. Wang, B.D. Esse, A.C. Lewis, Low-cost multispecies air quality sensor, WIT Transactions on Ecology and the Environment 198 (2015) 105–116. https://doi.org/10.2495/AIR150091.

[163] C.M. Harris, GC to go, Anal Chem 74 (2002) 585–589.

[164] J. Batts, L. Elson, Thinking Small: The Benefits and Challenges of Miniaturization, The Column (n.d.).

[165] G. Coelho Rezende, S. Le Calvé, J.J. Brandner, D. Newport, Micro photoionization detectors, Sens Actuators B Chem 287 (2019) 86–94. https://doi.org/10.1016/j.snb.2019.01.072.

[166] R. Nasreddine, V. Person, C.A. Serra, S. Le Calvé, Development of a novel portable miniaturized GC for near real-time low level detection of BTEX, Sens Actuators B Chem 224 (2016) 159–169. https://doi.org/10.1016/j.snb.2015.09.077.

[167] J.H. Sun, F.Y. Guan, X.F. Zhu, Z.W. Ning, T.J. Ma, The Integrated Mini GC-PID System for Monitoring Air Pollution, in: Current Air Quality Issues, InTech, 2015: p. 13. https://doi.org/10.5772/59725.

[168] M. Xu, Z. Tang, Y. Duan, Y. Liu, GC-Based Techniques for Breath Analysis: Current Status, Challenges, and Prospects, Crit Rev Anal Chem 46 (2016) 291–304. https://doi.org/10.1080/10408347.2015.1055550.

[169] P. Atkins, Looking with Light: Understanding Gas Chromatography, Part II: Sample Introduction and Inlets, Cannabis Science and Technology (2022) Pages: 20-26.

[170] Shimadzu Corporation, A Guide to GCMS Sample Introduction Systems: Choosing the best system for your analysis, (2021).

[171] GL sciences, Sample Introduction in Capillary Gas Chromatography, (2016) 29. https://www.glsciences.eu/optic/gc-injections-manual.pdf.

[172] A. Stolarczyk, T. Jarosz, Micropreconcentrators: Recent Progress in Designs and Applications, Sensors 22 (2022) 1–14. https://doi.org/10.3390/s22041327.

[173] A.R. Chowdhury, T.A. Lee, C. Day, T. Hutter, A Review of Preconcentrator Materials, Flow Regimes and Detection Technologies for Gas Adsorption and Sensing, Adv Mater Interfaces 9 (2022) 1–17. https://doi.org/10.1002/admi.202200632.

[174] User Manual- NovaTest P100 Portable VOC Analyzer, Nanova Environmental, Inc., (2020).

[175] Infinita Lab. Advantages of Gas Chromatography Analysis. http://tinyurl.com/bdfytj9c Accessed on February 25, 2024., (n.d.).

VITA

Olajide Philip Adetunji was born in Lagos, Nigeria. He was awarded a Bachelor of Science degree in Industrial Chemistry (First-Class Honors) from Kwara State University, Malete, Kwara State, Nigeria in June 2017. In August of 2019, he resumed his studies at Missouri University of Science and Technology for a PhD in Chemistry. Subsequently, he joined Dr. Nam's research group to focus on Analytical Chemistry research. His research under the guidance of Dr. Nam focused on using analytical instrumentation for monitoring TBI biomarkers and evaluating antioxidant therapy, residual solvents in pharmaceutical products, and oxygen sensing medical device for detecting pressure ulcers. During his program, he was awarded the Claypool fellowship for Medical Research (Spring 2023), presentation awards at the Centre for Biomedical Research (MAR 2022) and the Mid-American Environmental Engineering Conference (NOV 2023), and the Chemistry department Outstanding Graduate Service Assistant Award (APR 2023). He also presented his research works at American Chemical Society (ACS) Midwest regional meeting, Iowa city, IA, USA (OCT 2022) and Pittcon Conference and Expo, Philadelphia, PA, USA (MAR 2023). He was an active member of the ACS and National Organization for the Professional Advancement of Black Chemists and Chemical Engineers (NOBCChE). He received a Doctor of Philosophy in Chemistry from Missouri University of Science and Technology in May 2024.